5-20-2011

Patterns of protein expression in tissues of the killifish, Fundulus heteroclitus and Fundulus grandis

Naga Vijayalaxmi Abbaraju
University of New Orleans

Patterns of protein expression in tissues of the killifish, *Fundulus heteroclitus* and *Fundulus grandis*

A Dissertation

Submitted to the Graduate Faculty of the
University of New Orleans
in partial fulfillment of the
requirements for the degree of

Doctor of Philosophy
in
Chemistry

by

Naga Vijayalaxmi Abbaraju

Bachelor of Science. Osmania University, India, 2001
Master of Science. Pune University, India, 2003

May, 2011

Dedication

I would like to dedicate this dissertation to my beloved parents Jogeswara Prasad Abbaraju, Hemalatha Abbaraju, my husband Venkata Ramana Kethineedi, and my daughter Shriya Kethineedi.

Acknowledgments

It is a pleasure to thank many people who made this thesis possible. Foremost, I would like to express my sincere gratitude to my research advisor Dr. Bernard B. Rees for his support, guidance, and encouragement during graduate school. Working in Dr. Rees lab had been a wonderful learning experience; I could not have imagined having a better advisor and mentor for my PhD study. He has always been my inspiration for hardwork and perfection in whatever he does. I thank him for his patience, motivation, lots of research ideas, and good teaching throughout my tenure as a graduate student as well as in writing my thesis.

I would like to thank Dr. Richard B. Cole who made by Chapter 4 possible. I thank him for all the knowledge I gained about mass spectrometry and database searching. I also thank Dr. Yang Cai for all the LC-MS/MS analysis and help with database search. I would like to express my gratitude to my other advisory committee members Dr. Zhengchang Liu, and Dr. Edwin Stevens for their comments and suggestions throughout my graduate research.

I also would like to thank Dr. Guangdi Wang from Xavier University for use of the spotcutter and digester and Qiang Zhang for his help with the instruments. I greatly appreciate Kan Chen and Nazim Boutaghou for the training and help with the mass spectrometer and sample analysis. I thank my past and present research group members for their advice and help. I give special thanks to all the faculty and staff in the Departments of Chemistry and Biological Sciences for their support.

I would like to greatly thank my family for their undying support and encouragement. I could not have made it this far without them. I thank my brother Sainath Abbaraju, my sister Srivalli Abbaraju, my father-in-law Narasimha Rao Kethineedi, and my mother-in-law, late Samanthakamani Kethineedi.

Table of Contents

List of Figures

List of Tables

Abstract

Fundulus is a diverse and widespread genus of small teleost fish of North America. Due to its high tolerance for physiochemical variation (e.g. temperature, oxygen, salinity), *Fundulus* is a model organism to study physiological and molecular adaptations to environmental stress. The thesis focuses on patterns of protein expression in *Fundulus heteroclitus and F. grandis.*The patterns of protein expression were investigated using traditional methods of enzyme activity measurements and recent proteomic approaches. The findings of the study can be used to guide future studies on the proteomic responses of vertebrates to environmental stress.

Chapter 2 focuses on measurement of the temporal effects of oxygen treatments on the maximal specific activities of nine glycolytic enzymes in liver and skeletal muscle during chronic exposure (28d) of *Fundulus heteroclitus*. The fish was exposed to four different oxygen treatments: hyperoxia, normoxia, moderate hypoxia, and severe hypoxia. The time course of changes in maximal glycolytic enzyme specific activities was assessed at 0, 8, 14 and 28 d. The results demonstrate that chronic hypoxia alters the capacity for carbohydrate metabolism in *F. heteroclitus*, with the important observation that the responses are both tissue- and enzyme-specific.

Chapter 3 studies the effect of tissue storage on protein profile of tissues of *F. grandis*. The technique of one dimensional gel electrophoresis (1D-SDS-PAGE) was used to assess the effects of tissue sampling, flash frozen in liquid nitrogen versus immersion of fresh tissue in RNA later®, for five tissues, liver, skeletal muscle, brain, gill, and heart, followed by LC-MS/MS to identify protein bands that were differentially stabilized in gill and liver. The study shows that, in *F. grandis*, the preferred method of preservation was tissue specific.

Chapter 4 focuses on the use of advanced 2DE-MS/MS to characterize the proteome of multiple tissues in *F. grandis.* Database searching resulted in the identification of 253 non-redundant proteins in five tissues: liver, muscle, brain, gill, and heart. Identifications include enzymes of energy metabolism, heat shock proteins, and structural proteins. The protein identification rate was approximately 50 % of the protein spots analyzed. This identification rate for a species without a sequenced genome demonstrates the utility of *F. grandis* as a model organism for environmental proteomic studies in vertebrates.

Key words: *Fundulus heteroclitus*, *Fundulus grandis,* Hypoxia, Glycolytic enzyme specific activities, Protein expression, tissue storage, Proteomics, Fish, Mass Spectrometry, Liquid Chromatography, Two dimensional Polyacrylamide Gel Electrophoresis, Gene Ontology.

Chapter 1

Introduction

Proteomics is defined as the direct qualitative and quantitative analysis of the full complement of proteins present in an organism, tissue, or cell under a given set of physiological or environmental conditions. In molecular biology, after genome sequencing, the focus of considerable attention has turned towards proteomics. New improvements in instrumentation, advances in bioinformatics and and development of robust, reliable and reproducible analytical techniques have led to applications of proteomics to address several biological questions [1]. However, proteomics presents greater technological challenges than genomics because of the complex nature of the proteome due to variable post translational modifications that occur from mRNA to protein [2, 3]. Moreover, unlike nucleic acids, proteins cannot be amplified; therefore, techniques must operate at small sample sizes. Proteomics provides a powerful tool to investigate global changes of genes and proteins in biological systems. The techniques not only operate with minimum sample but also offer the advantages of simultaneous analysis of thousands of proteins [4]. Proteomics have also been used for protein characterization, to study protein modifications and interaction of proteins in complexes [1]. Thus, proteomic approaches have been extended in the recent years to address different questions related to environmental biology. In fish, proteomics have been used to understand physiological processes, development processes, and effect of pollutants [5].

Fish are an interesting study group of vertebrates for investigating the organism-environment interface because of their close physiological relationship with the environment. They account for large group of vertebrates groups with more than 25,000 species occupying a

variety of habitats [6]. Fish share several developmental pathways, physiological mechanisms, and organ systems with other veretebrates, including humans. However, because their bodies are completely immersed in water, fish may be more susceptible to variations in environmental conditions. They are extraordinarily diverse in terms of body forms, lifestyles, physiologies, and environmental conditions they experience [7]. Thus, the diversity of fish provides the material to answer questions in ecological physiology and provide insight into responses from individual cells to whole organisms.

Fundulus belongs to largest fish group, the teleost fish.The genus *Fundulus* is diverse and widespread with many related species inhabiting a wide range of aquatic habitats of North America. They are abundant, small in size, adapted to various environments, and many species are easy to maintain in lab. These fish are exposed to fluctuations in various environmental variables, including salinity, temperature, pH and oxygen, that occur on a regular basis in their habitats. *Fundulus heteroclitus* and *Fundulus grandis* are closely related species that are found in salt marshes of the Atlantic coast and the Gulf of Mexico, respectively [8]. *F. heteroclitus* has widely been used to understand the mechanisms by which fish adapt to fluctuations in environment such as, variation in oxygen levels [9], changes in salinity [10], and temperature [11]. In addition, they have also been used to study reproduction, development, toxicology, ecology, and evolutionary biology [8, 12-14]. The broad range of research in *F. heteroclitus* thus provides insight into physiology, toxicology, ecology, and gene-expression in the teleost fish. Among the various species belonging to this genus, *F. heteroclitus* thus has been developed as a potential model for the study of physiological processes, disease processes, toxicological mechanisms, and ecological processes in aquatic vertebrates. Although the genome of *F. heteroclitus* has not been sequenced, there is a variety of molecular tools available in this species

including many nuclear markers, such as microsatellites, amplified fragment length polymorphisms, and approximately 55,000 nucleotide sequences [15-17] listed on The National Center for Biotechnology Information (NCBI).

Oxygen is one of the environmental variables that fluctuate greatly in areas inhabited by *F. heteroclitus* and *F. grandis*. Compared to other estuarine fishes, *F. heteroclitus* exhibits high tolerance to low oxygen (hypoxia) with little or no mortality occurring until dissolved oxygen drops below 1 mg L^{-1} [9]. *Fundulus grandis,* sister species of *F. heteroclitus* found in same type of habitats, is also shown to exhibit high hypoxia tolerance [18]. *Fundulus* species living in these habitats compensate for extreme environments through physiological, behavioral, and biochemical adjustments to hypoxia. At the molecular level, they alter the levels of expression for enzymes that affect metabolism or show changes in gene expression [19, 20]. Several studies have demonstrated changes in glycolytic enzyme activities in *F. heteroclitus* and *F. grandis*, under reduced oxygen levels. The studies measured maximal enzyme activities under chronic hypoxia and demonstrated tissue- and enzyme-specific responses in *F. heteroclitus* and *F. grandis* for the enzymes involved in carbohydrate metabolism [21, 22].

1.1 Enzyme Activity versus Proteomics

The traditional approach of measuring maximal enzyme activities is to perform an enzymatic assay. In a typical enzyme assay, maximal enzyme activities (V_{max}) are measured. The maximal initial velocity (V_{max}) can be described as,

$$V_{max} = [E]\, k_{cat} ,$$

where [E] is the enzyme concentration and k_{cat} is the catalytic rate constant. At saturating conditions, the maximal initial velocity is a function of enzyme concentration and the catalytic rate constant. Assuming catalytic rate k_{cat} to be constant, the differences in maximal activities are

due to changes in enzyme concentration [23, 24]. Under these conditions V_{max} is an index of enzyme concentration [E] and maximal enzyme activity reflects protein expression.

Proteomics provides a powerful tool to study large scale patterns of protein expression. One main objective of proteomic research is the systematic identification and quantification of proteins expressed in a biological system. The standard approaches to achieve the goal are one- or two-dimensional gel electrophoresis or liquid chromatography followed by mass spectrometry (Figure 1.1). Proteomic analysis includes two essential components; protein fractionation and protein identification. Protein fractionation is necessary to reduce the protein complexity, and is typically done by column chromatography or gel electrophoresis. Protein identification is accomplished by mass spectrometry (MS). In a typical proteomics work flow, for the gel based methods, proteins are separated by iso-electric point (pI) and molecular weights, detected by staining, and quantified according to staining intensities [25]. Proteins are then cut out of the gel, trypsin digested, and identified by mass spectrometry. For the liquid chromatography (LC) based methods, the complex protein mixture is first trypsin digested and the peptides are separated by LC columns, and then detected, identified, and quantified by mass spectrometry [26]. The spectra are then matched against publicly available protein sequence databases for protein identifications [27]. Finally the relationship between protein sequences and their biological functions is depicted using web-based gene ontology tools [28].

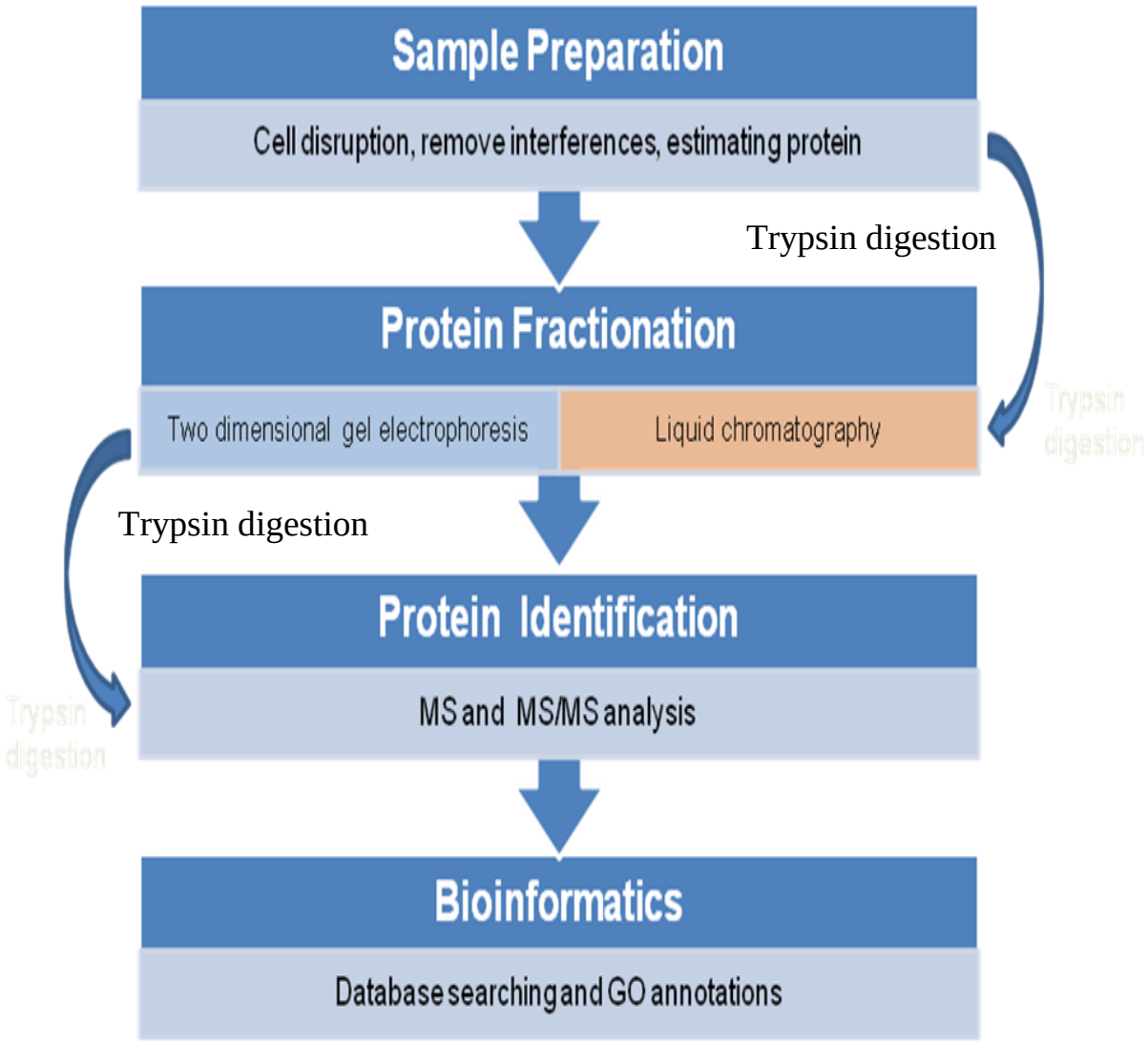

Figure 1.1 Proteomics work flow.

1.2 Protein Fractionation

1.2.1 Two dimensional gel electrophoresis

Originally introduced by O'Farell in 1975, two dimensional gel electrophoresis (2DE) is a widely used fractionation method for separation of proteins [29]. The technique of 2DE performs isoelectric focusing (IEF) in first dimension followed by sodium dodecyl polyacrylamide gel electrophoresis (SDS-PAGE) in second dimension. Thus, proteins are separated first according to their isoelectric point (pI) followed by separation according to their molecular weight. In high resolution 2DE, proteins are denatured completely, reduced and solubilized, to disrupt molecular interactions. Sample solubilization is carried out using a buffer containing chaotropes (urea and/or thiourea), nonionic (Triton X-100) or zwitterionic detergents (CHAPS), reducing agents (DTT), carrier ampholytes and sometimes protease and phosphatase inhibitors [30, 31].

The original method of first-dimension IEF depended on carrier-ampholyte-generated pH gradients in cylindrical polyacrylamide gels cast in glass rods or tubes. Due to number of limitations and problems associated with carrier ampholyte pH gradients, immobilized pH gradients (IPG) were developed [32]. An immobilized pH gradient is created by covalently incorporating a gradient of acidic and basic buffering groups (immobilines) into a polyacrylamide gel at the time it is cast. Immobilines of various pKa can create an immobilized pH gradient inside the acrylamide gel. Precast drystrip gels are rehydrated in a solution containing the necessary additives and, sometimes with the sample protein depending on type of loading employed (active, passive, or cuploading). After IEF, the Immobiline drystrip gels are equilibrated in equilibration solution. The equilibration solution contains buffer, urea and glycerol along with DTT, to maintain a reducing environment followed by iodoacetamide to

alkylate reduced thiol groups, preventing their re-oxidation during electrophoresis. The equilibration with DTT and iodoacetamide is performed one after the other. The equilibrated IPG strips are applied onto vertical or flatbed SDS-PAGE gels for the second-dimension separation.

In SDS-PAGE, migration is determined by the molecular weight of the polypeptides. The SDS-denatured and reduced proteins are separated according to an apparent molecular weight. There is a linear relationship between the logarithm of the molecular weight and the migration distance that depends on the percentage of polyacrylamide [33]. Gels are then visualized using one of several staining techniques. Conventional visible dyes are comassie blue, colloidal comassie blue and silver nitrate, which have sensitivities of 50, 10 and 0.5 ng of detectable protein per spot, respectively [34]. Fluorescent dyes are SYPRO dyes, cyanine dyes (Cydyes), and cysteine specific fluorescent dyes, FlaSH dyes [35]. Stained gels are scanned on a visible or fluorescent scanner that depends on type of stain used for visualization. The images are imported to software for spot detection and analysis. Software, such as Image Master, Progenesis, PDQuest, and Samespots, can be used to detect spots and to compare the spot intensity between samples [36, 37]. Spots of interest are selected for further mass spectrometric analysis.

1.2.2 Liquid chromatography

A major difference between traditional high performance liquid chromatography (HPLC) and the chromatography used in liquid chromatography coupled to mass spectrometry (LC-MS) is miniaturization of column size to improve the sensitivity and reduce sample consumption. Also LC-MS offers other advantages like increased chromatographic resolving power and faster analysis by utilizing low volumes of chemically modified stationary phase to reduce column bleeding that primarily produces background noise. A high resolution LC (or LC/LC) separation coupled on-line with MS is the central component of many proteomics platforms. Over the past

decade, there have been significant advances in LC separations as well as in MS instrumentation. Protein mixtures are typically digested by trypsin (or other proteases) into polypeptides, which are then separated by capillary LC and analyzed by MS on-line via an ESI interface. Although most popular reports of LC-MS use the ESI source interface, off-line MALDI-TOF/TOF coupled with HPLC is another important technique in proteomics work [38].

1.3 Mass Spectrometry

Mass spectrometry in conjunction with software and automation techniques has become an important tool to identify and analyze proteins. Most common applications of mass spectrometry are the identification of proteins derived from 2D gels or multi-dimensional liquid chromatography. Mass spectrometry (MS) is an analytical technique used for determining masses of particles, elemental composition of a sample or molecule, and for elucidating the chemical structures of molecules such as peptides. The MS principle consists of ionizing chemical compounds to generate charged molecules or molecule fragments which are then characterized by their mass to charge ratios *(m/z)* and relative abundances [39]. A typical, mass spectrometer consists of an ion source, a mass analyzer that measures the mass-to-charge ratio (m/z) of the ionized analytes, and a detector that records the number of ions at each m/z value.

The method of sample introduction to the ionization source often depends on the ionization method being used, as well as the type and complexity of the sample under investigation. The ionization methods used for the majority of biochemical analyses are Electro Spray Ionization (ESI) and Matrix Assisted Laser Desorption Ionization (MALDI). ESI is one of the Atmospheric Pressure Ionization (API) techniques and is well-suited to the analysis of polar molecules ranging from less than 100 Da to more than 1,000,000 Da in molecular mass. ESI ionizes the analytes out of a solution and is therefore readily coupled to liquid-based separation

tools like liquid chromatography and capillary electrophoresis. MALDI is laser-based soft ionization technique that sublimates and ionizes the samples out of a dry, crystalline matrix after bombardment of the sample with laser light. MALDI-MS is used for analysis of simple peptide mixtures, whereas integrated liquid-chromatography ESI-MS systems (LC-MS) for analysis of complex samples [40, 41].

The main function of the mass analyzer is to separate the ions formed in the ionization source of the mass spectrometer according to their mass-to-charge (*m/z*) ratios under electromagnetic field. These mass analyzers have different features, including mass accuracy, the *m/z* range that can be covered, resolution, and sensitivity [42]. There are a number of mass analyzers currently available; four basic types of mass analyzers used in proteomics research include quadrupoles, time-of-flight (TOF) analyzers, and both Fourier transform (FT-MS) and quadrupole ion traps. They are very different in design and performance, each with its own advantages and limitations. The compatibility of different analyzers with different ionization methods varies. The analyzers can be stand alone or put together in tandem to take advantage of the strengths of each. A tandem mass spectrometer consists of more than one mass analyser, generally two mass analysers. The mass analyser can be of same type or different. More popular tandem mass spectrometers are quadrupole-quadrupole, magnetic sector-quadrupole, and the quadrupole-time-of-flight [43]. MALDI is usually coupled to TOF analyzers that measure the mass of intact peptides, whereas ESI has mostly been coupled to ion traps and triple quadrupole instruments. In addition, new combinations of mass analyzers and ion sources are being used in various applications. For example, MALDI ion sources have recently been coupled to quadrupole ion-trap mass spectrometers and to two types of TOF instruments (MALDI-TOF/TOF) [44]. In tandem mass spectrometers fragmentation of specific sample ion is achieved

by any of the following methods: collision induced dissociation (CID), photon induced and surface induced dissociation. In each of these methods the peptide ion to be analyzed is isolated and fragmented in a collision cell, and the fragment ion spectrum is recorded [43].

1.4 Protein Identification

In the first step of the MS analysis, the masses of the peptides provide a unique peptide mass fingerprint (PMF) specific to the compound under investigation (Figure 1.2). MALDI-TOF is the preferred method to identify proteins by PMF due to its simplicity, mass accuracy, high resolution, insensitivity to contaminants, and sensitivity to analyte. The principle behind protein identification by mass mapping is quite simple; after proteolysis with a specific protease, protein of different amino acid sequences produce groups of peptides, the masses of which are unique for a specific protein [45]. Tandem mass spectra are generated by the fragmentation of peptide ions in the gas phase at low collision energy.

After collision with the inert gas, the peptide can break apart at any point along its amino acid backbone or on its side chains. There are three different types of bonds that can fragment along the amino acid backbone: the NH-CH, CH-CO, and CO-NH bonds. Each bond breakage gives rise to two species, one neutral and the other one charged, and only the charged species is monitored by the mass spectrometer. The charge can stay on either of the two fragments depending on the relative proton affinity of the two species. Hence, there are six possible fragment ions for each amino acid residue (labeled in the diagram), with the a, b, and c ions having the charge retained on the N-terminal fragment, and the x, y, and z ions having the charge

A)

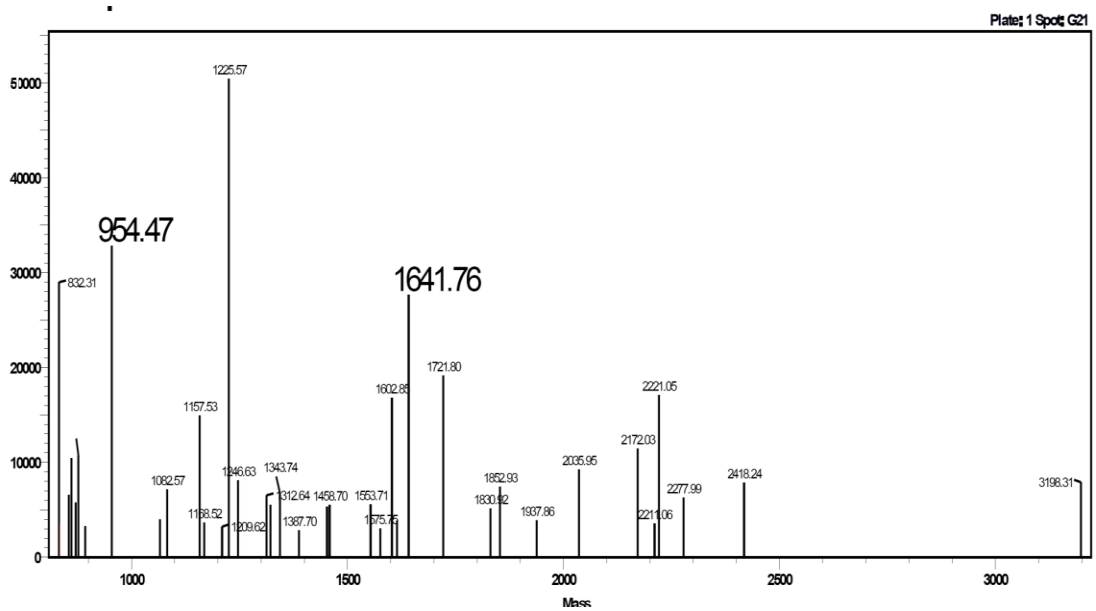

B)

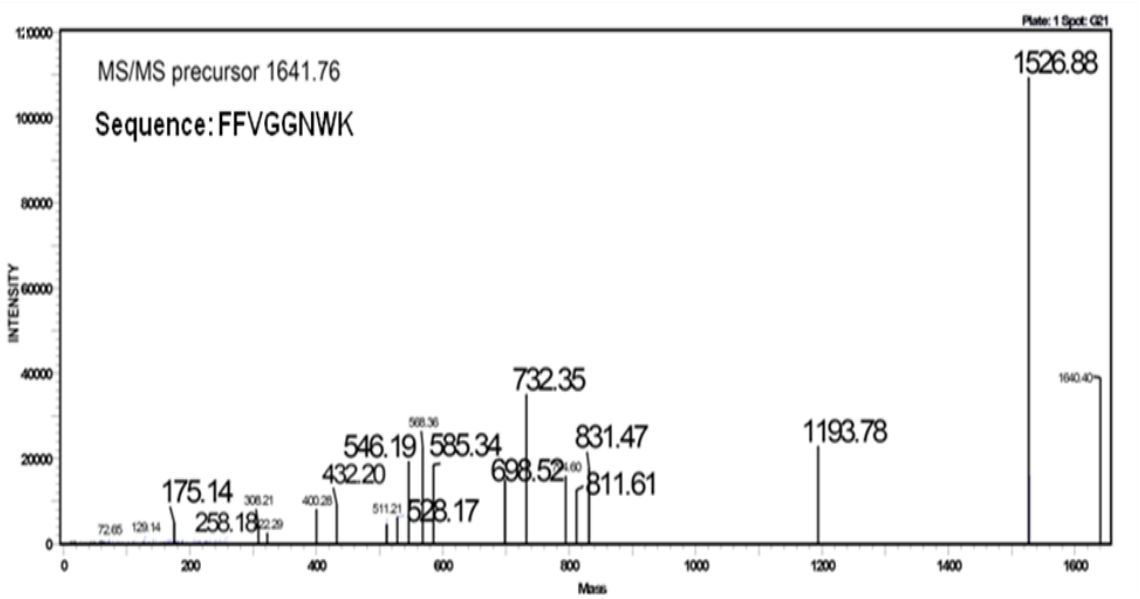

Figure 1.2 Representative peptide mass fingerprinting (PMF) and MS/MS spectra of the identified liver tissue proteins of *Fundulus grandis* (spot 8306) discussed in chapter 4. The matched peptides are labeled on PMF spectrum (A), and the matched fragment series are represented as shown for precursor 1641.76 MS/MS spectra (B).

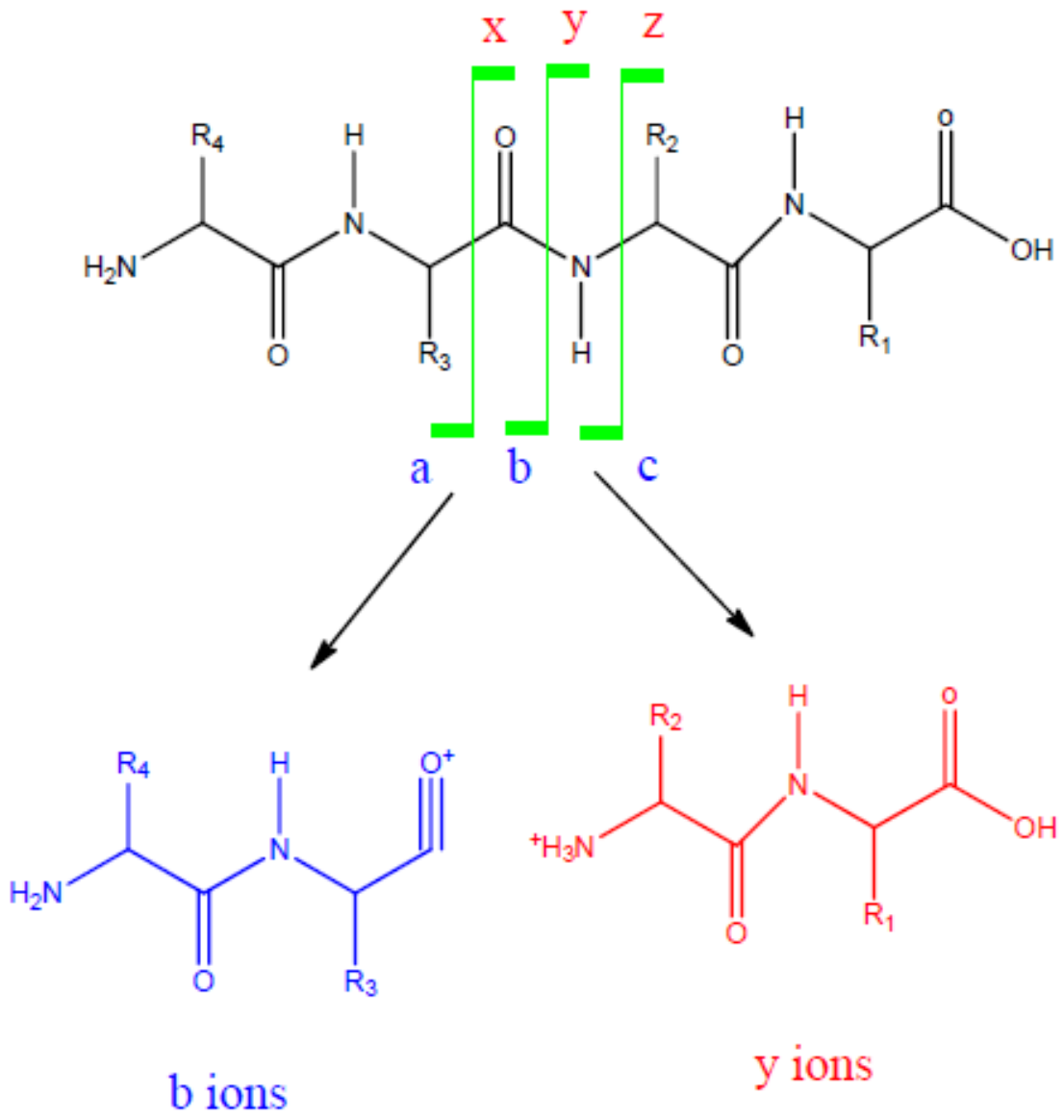

Figure 1.3 Peptide fragmentation pattern.

retained on the C-terminal fragment (Figure 1.3). The most common cleavage sites are at the CO-NH bonds which give rise to the b and the y ions. The mass difference between two adjacent b ions, or y ions, is indicative of a particular amino acid residue [43]. Each peptide tandem mass spectrum will contain *b* and *y* ions as well as other fragment ions that can be used to interpret the amino acid sequence (Figure 1.2). The MS/MS spectra of peptides thus generated not only contain sufficient amount of information for unambiguous identification of a protein and are also high quality, sequence specific, and are relatively simple to interpret. Protein identifications using MS/MS spectra are clearer than those achieved by peptide mass fingerprint because, in addition to the peptide mass, the peak pattern in the MS/MS spectrum also provides information about peptide sequence [46]. Thus, a typical proteomics experiment generates thousands of mass spectra that require several computational approaches and software tools for automated assignment of peptide sequences to MS/MS spectra.

Several computational and software tools are developed that compare the set of measured peptide masses against the predicted masses for each protein in the database and assign a score to each match that ranks the quality of the matches. Therefore, if a database containing the specific protein sequence is searched using selected masses (i.e., the observed peptide mass fingerprint), then the protein can be correctly identified. For a protein to be identified, its sequence or a closely related sequence has to exist in the sequence database being used for comparison. Both protein and DNA sequence databases can be used. If DNA sequence databases are being used, the DNA sequences are first translated into protein sequences prior to digestion. The approach is, therefore, best suited for genetically well-characterized organisms where either the entire genome is known or extensive protein or cDNA sequence is available. PMF is not suited for searches of EST databases or for identification of proteins in complex mixtures if unseparated

mixtures are proteolyzed. The reason being that protein identifications by peptide mass mapping depends on the correlation of several peptide masses derived from the same protein with corresponding data calculated from the database. Digests of unseparated protein mixtures present a problem for mass mapping because it is not apparent if peptides in the complex peptide mixture originated from the same protein. Thus, PMF is most popular for the identification of proteins from species for which complete genome sequences have been determined and for use after protein fractionation by 2DE where ancillary information on protein molecular weight and isoelectric point information can be used to aid identification. It is often combined with tandem MS of peptides [47]. Tandem mass spectrometry has proven to be excellent tool for the identification of proteins from species with large and incompletely sequenced genomes. Unlike PMF, MS/MS does not require a purified target protein, and composition of even relatively complex protein mixtures can be ascertained without purification of individual proteins using two-dimensional chromatography methods coupled to ESI-MS/MS [48].

Statistical testing of protein identifications requires advanced computational approaches. In the cross-correlation method, peptide sequences in the database are used to construct theoretical mass spectra and the overlap or crosscorrelation of these predicted spectra with the measured mass spectra determines the best match. In probability based matching, the calculated fragments from peptide sequences in the database are compared with observed peaks. From this comparison, a database search score is generated according to some scoring function that measures the degree of similarity between the experimental spectrum and theoretical fragmentation patterns of the candidate peptides which reflects the statistical significance of the match between the spectrum and the sequences contained in a database [49]. Different database search tools use different scoring schemes and some tools calculate more than one score. A

variety of scoring schemes have been described in literature including those based in spectral correlation functions, shared fragment counts, spectral alignment, or based on empirically derived tools. In each of these methods, the identified peptides are compiled into a protein hit list, which is the output of a typical proteomic experiment. SEQUEST is the first MS/MS database search tool that became commercially available and most commonly used programs. For each experimental spectrum, SEQUEST calculates cross correlation score (Xcorr) for all candidate peptides queried from the database [50]. Another widely used database search tool, Mascot, computes probablility based score called the Mascot score. Mascot estimates the probablility of the number of matches occurring by chance given the number of peaks in the searched spectrum and the distribution of *m/z* values of predicted ions for all candidate peptides in the database [51]. In addition, several other algorithms, like Spectrum mill [52], phenyx [53, 54], are available which perform database search to look for matched peptides. Because protein identifications rely on matches with sequence databases, high-throughput proteomics is currently restricted largely to those species for which comprehensive sequence databases are available.

De novo sequencing strategy has been used for species with unsequenced genomes in which protein identifications could not be obtained. The method is based on manual or computer aided interpretation of mass spectra. After sequencing of individual peptides, the sequence information is assembled to reconstruct the protein sequence. The MS-based methods attempt to derive sequence information without tandem MS. They are based on the generation of peptide ladders that differ in length by one amino acid. Therefore, three or more different proteases like trypsin, chymotrypsin etc are often used independently to generate overlapping peptides. The peptides are then put together to obtain the protein sequence. In the MS/MS-based approaches a number of chemical modification procedures have been introduced to identify the *b* and *y* ion

series and the peptide sequence [55]. With the development of computer algorithms and large-scale databases, utilization of *de novo* sequencing of peptides is declining. However, for the sequence analysis of the many proteins from species for which no genomic or expressed sequence tag database is available, interpreting amino acid sequences from MS/MS spectra will help in identification of protein with increased confidence [56].

1.5 Annotations

The next challenge is to understand the relationship between protein sequences and their biological functions; this is achieved by Gene ontology annotations (GO). Traditionally, the functional annotation of genes was done by experienced individuals with the help of literature and advanced searching tools. Nowadays, several automated web-based software tools are available that perform the function of gene annotation. The function of a query protein can be deduced from these web-based programs and if the GO annotation is not available then homologous proteins of known functions are obtained from database searches. These tools typically involve a search of homologous proteins in GO mapped databases including Genbank and Swiss-Prot [57, 58]. The assumption used by these approaches is that similar sequences infer similar biological functions [59-61]. The Gene ontology project provides a vocabulary to describe gene and gene product attributes in any organism. GO includes three ontological categories or vocabularies: molecular function, biological process, and cellular component. A molecular function GO term represents a biological activity involving one or more gene products. A biological process GO term represents a series of biological activities. And a cellular component GO term represents a component of a cell. According to the Gene ontology website, over 87,000 species have GO annotation, comprising over 6.8 million annotations [62]. However GO ontology project is not complete yet, and work is in progress to update the databases.

1.6 Fish Proteomics

Proteomic techniques have been employed in model, as well as nonmodel, species to understand fish biology. Due to lack of available genetic information on most fish, very few studies have attempted to integrate proteomics with other levels of biological organization for 'non-model' organisms [63]. For organisms without sequenced genomes, the identifications were based on homologies with sequences from other organisms, thus resulting in identifications of only conserved proteins [64, 65]. The *de novo* strategy has been demonstrated to be an interesting and helpful method for those fish species with little available genomic information [66]. The fresh water teleost zebrafish has been chosen as the most common model species. In 45 studies cited in a review article, around 40 different fish species were analyzed using different proteomic approaches, with zebrafish and salmonids (rainbow trout and Atlantic salmon) being the species most frequently investigated. Proteomics in zebrafish were mainly focused to study development biology [67-70], but there are also studies in adult fish [71]. Zebrafish was used to test the effects of pollutants on the proteome of embryos [72], adult liver, and brain [73, 74]. Proteomics in non-model fish species have been reported in fish that were commercially important in aquaculture and in fish that serve as environmental reporters. The Salmonids, especially Atlantic salmon and rainbow trout (*Oncorhynchus mykiss*), are commercially important cultured fish. The effects of X-ray exposure in rainbow trout [75], viral infection and stress in Atlantic salmon [76, 77], and anoxia in crucian carp (*Carassius carassius*) were studied using proteomic approaches [78]. Human melanoma was studied using green swordtail (*Xiphophorus hellerii*), a freshwater fish species of the family Poecilidae (Cyprinodontiformes) [79]. The proteome of *Xiphophorus sp.* has also been analyzed in the search for proteins involved in the malignancy of tumors produced in this fish [80].

Over the past decade, most of the published proteome projects use two dimensional gel electrophoresis (2DE) as the method of choice to separate protein in fish tissue [5]. At the molecular level, 2D gel electrophoresis and mass spectrometry-based proteomics techniques were applied to understand the adjustments made in fish tissues to physiological challenges [81-83]. The choice of technique in most studies was 2DE-MS/MS mainly using ESI-IT or MALDI-TOF/TOF [5]. There are examples in literature where by using similar proteomic tools, the protein identification rates are very similar for zebrafish [71], Atlantic salmon [84] or rainbow trout [85]. The current alternative to 2DE for quantitative proteomics is the LC-MS/MS technology. Both 2DE and LC-MS/MS approaches were used to address the same biological questions, but LC-MS/MS presents several advantages over 2DE in terms of automation, reproducibility, proteome coverage, and quantization [86]. For the first time Desouza et al have established large-scale proteome profile of a zebrafish gill tissue using a shotgun method based two-dimensional liquid chromatography–electrospray ionization tandem mass spectrometry [87]. A similar approach was used to establish proteome profile of the zebrafish brain at normal conditions [88].

1.7 References

1] Gromov, P., Celis, J., From genomics to proteomics. *Molecular Biology* 2000, 34, 508-520.

2] Gygi, S. P., Rochon, Y., Franza, B. R., Aebersold, R., Correlation between protein and mRNA abundance in yeast. *Mol. Cell. Biol.* 1999, 19, 1720-1730.

3] Gooley, A., and Packer, N. (Ed.), The importance of co- and post-translational modifications in proteome projects, in Proteome Research, *Springer-Verlag.* 1997.

4] Vercauteren, F. G. G., Arckens, L., Quirion, R., Applications and current challenges of proteomic approaches, focusing on two-dimensional electrophoresis. *Amino Acids* 2007, 33, 405-414.

5] Forné, I., Abián, J., Cerdà, J., Fish proteome analysis: Model organisms and non-sequenced species. *Proteomics* 2010, 10, 858-872.

6] Venkatesh, B., Evolution and diversity of fish genomes. *Curr Opin Genet Dev.* 2003, 13, 588–592.

7] Cossins, A. R., Crawford, D. L., Fish as models for environmental genomics. *Nat Rev Genet.* 2005, 6, 324-333.

8] Burnett, K. G., Bain, L. J., Baldwin, W. S., Callard, G. V., *et al.*, *Fundulus* as the premier teleost model in environmental biology: Opportunities for new insights using genomics. *Comparative Biochemistry and Physiology Part D: Genomics and Proteomics* 2007, 2, 257-286.

9] Smith, K. J., Able, K. W., Dissolved oxygen dynamics in saltmarsh pools and its potential impacts on fish assemblages. *Mar. Ecol. Prog. Ser.* 2003, 258, 223–232.

10] Griffith, R.W., Environment and salinity tolerance in the genus *Fundulus*. *Copeia* 1974, 2, 319–331.

11] Crawford, D.L., Powers, D.A., Evolutionary adaptation to different thermal environments via transcriptional regulation. *Mol. Biol. Evol.* 1992, 9, 806–813.

12] Greytak, S.R., Champlin, D., Callard, G.V., 2005. Isolation and characterization of two cytochrome P450 aromatase forms in killifish (*Fundulus heteroclitus*): differential expression in fish from polluted and unpolluted environments. *Aquat. Toxicol.* 71, 371–389.

13] Oleksiak, M.F., Roach, J.L., Crawford, D.L., Natural variation in cardiac metabolism and gene expression in *Fundulus heteroclitus*. *Nat. Genet.* 37, 2005, 67–72.

14] Whitehead, A., Crawford, D.L., Variation within and among species in gene expression: raw material for evolution. *Mol. Ecol.* 2006, 15, 1197–1211.

15] Paschall, J. E., Oleksiak, M. F., VanWye, J. D., Roach, J. L., Whitehead, J. A., Wyckoff, G. J., Kolell, K. J., Crawford, D. L., FunnyBase: a systems level functional annotation of *Fundulus* ESTs for the analysis of gene expression. *BMC Genomics* 2004, 5, 96.

16] Adams, S. M., Lindmeier, J. B., Duvernell, D. D., Microsatellite analysis of the phylogeography, pleistocene history and secondary contact hypotheses for the killifish, *Fundulus heteroclitus*. *Mol. Ecol.* 2006, 15, 1109–1123.

17] McMillan, A. M., Bagley, M. J., Jackson, S. A., Nacci, D. E., Genetic diversity and structure of an estuarine fish (*Fundulus heteroclitus*) indigenous to sites associated with a highly contaminated urban harbor. *Ecotoxicology* 2006, 15, 539–548.

18] Love, J. W., Rees, B. B., Seasonal differences in hypoxia tolerance in gulf killifish, *Fundulus grandis (Fundulidae). Environ. Biol. Fish.* 2002, 63, 103–115.

19] Wu, R., S. S., Hypoxia: from molecular responses to ecosystem responses. *Marine Pollution Bulletin* 2002, *45*, 35-45.

20] Nikinmaa, M., Rees, B. B., Oxygen-dependent gene expression in fishes. *American Journal of Physiology Regulatory, Integrative and Comparative Physiology* 2005, 288, R1079-R1090.

21] Martinez, M. L., Landry, C. A., Boehm, R., Manning, S., Cheek, A. O., Rees, B. B., Effects of long-term hypoxia on enzymes of carbohydrate metabolism in the gulf killifish, *Fundulus grandis. J. Exp. Biol.* 2006, 209, 3851–3861.

22] Kraemer, L. D., Schulte, P. M., Prior PCB exposure suppresses hypoxia induced up-regulation of glycolytic enzymes in *Fundulus heteroclitus*. *Comp. Biochem. Physiol. C, Comp. Pharmacol. Toxicol*. 2004, 139, 23–29.

23] Pierce, V. A., Crawford, D. L., Rapid enzyme assays investigating the variation in the glycolytic pathway in field-caught populations of *Fundulus heteroclitus*. *Biochem. Genet.* 1994, 32, 315–330.

24] Pierce, V. A., Crawford, D. L., Variation in the glycolytic pathway: the role of evolutionary and physiological processes. *Physiol. Zool*. 1996, 69, 489–508.

25] Görg, A., Weiss, W., Dunn, M. J., Current two-dimensional electrophoresis technology for proteomics. *Proteomics* 2004, 4, 3665-3685.

26] Davis, M. T., Beierle, J., Bures, E. T., McGinley, M. D., *et al.*, Automated LC-LC-MS-MS platform using binary ion-exchange and gradient reversed-phase chromatography for improved proteomic analyses. *Journal of Chromatography B: Biomedical Sciences and Applications* 2001, 752, 281-291.

27] Nesvizhskii, A., I., Protein identification by tandem mass spectrometry and sequence database searching. *Methods Mol Biol.* 2007, 367, 87-119.

28] Duan, Z. H., Hughes, B., Reichel, L., Dianne, M., Perez, D. M., Shi, T., The relationship between protein sequences and their gene ontology functions. *BMC Bioinformatics* 2006, 7, S11.

29] O'Farell, P. H., High resolution two-dimensional electrophoresis of proteins. *J. Biol. Chem.* 1975, 250, 4007–4021.

30] Musante, L., Candiano, G., Ghiggeri, G. M., Resolution of fibronectin and other uncharacterized proteins by two-dimensional polyacrylamide electrophoresis with thiourea. *Journal of Chromatography B: Biomedical Sciences and Applications* 1998, 705, 351-356.

31] Perdew, G. H., Schaup, H. W., Selivonchick, D. P., The use of a zwitterionic detergent in two-dimensional gel electrophoresis of trout liver microsomes. *Analytical Biochemistry* 1983, 135, 453-455.

32] Görg, A., Obermaier, C., Boguth, G., Harder, A., *et al.*, The current state of two-dimensional electrophoresis with immobilized pH gradients. *Electrophoresis* 2000, 21, 1037-1053.

33] Weber, K., Osborn, M., The reliability of molecular weight determinations by dodecyl sulfate-polyacrylamide gel electrophoresis. *Journal of Biological Chemistry* 1969, 244, 4406-4412.

34] Chevalier F, R. V., Rossignol M, Visible and fluorescent staining of two-dimensional gels. *Methods in Molecular Biology* 2007, 355, 145-156.

35] Miller, I., Crawford, J., Gianazza, E., Protein stains for proteomic applications: Which, when, why? *Proteomics* 2006, 6, 5385-5408.

36] Maurer, M. H., Software analysis of two-dimensional electrophoretic gels in proteomic experiments. *Current Bioinformatics* 2006, 1, 255-262.

37] Panchaud, A., Affolter, M., Moreillon, P., Kussmann, M., Experimental and computational approaches to quantitative proteomics: Status quo and outlook. *Journal of Proteomics* 2008, 71, 19-33.

38] Qian, W. J., Jacobs, J. M., Liu, T., Camp, D. G., Smith, R. D., Advances and challenges in liquid chromatography-mass spectrometry-based proteomics profiling for clinical applications. *Molecular & Cellular Proteomics* 2006, 5, 1727-1744.

39] Aebersold, R., Mann, M., Mass spectrometry-based proteomics. *Nature* 2003, 422, 198-207.

40] Fenn, J. B., Mann, M., Meng, C. K., Wong, S. F., Whitehouse, C. M., Electrospray ionization for the mass spectrometry of large biomolecules. *Science* 1989, 246, 64–71.

41] Karas, M., Hillenkamp, F., Laser desorption ionization of proteins with molecular mass exceeding 10000 daltons. *Anal. Chem.* 1988, 60, 2299–2301.

42] Ong, S. E., Mann, M., Mass spectrometry-based proteomics turns quantitative. *Nat. Chem. Biol.* 2005, 1, 252-262.

43] Aebersold, R., Goodlett, D. R.., Mass spectrometry in proteomics. *Chem. Rev.* 2001, 101 269-295.

44] Loboda, A. V., Krutchinsky, A. N., Bromirski, M., Ens, W., Standing, K. G. , A tandem quadrupole/time-of-flight mass spectrometer with a matrix-assisted laser desorption/ionization source: design and performance. *Rapid Commun. Mass Spectrom.* 2000, 14, 1047–1057.

45] James, P., Quadroni, M., Carafoli, E., Gonnet, G., Protein identification by mass profile fingerprinting. *Biochemical and Biophysical Research Communications* 1993, 195, 58-64.

46] Medzihradszky, K. F., The characteristics of peptide collision-induced dissociation using a high performance MALDI-TOF/TOF tandem mass spectrometer. *Anal. Chem.* 2000, 72, 552–558.

47] Henzel, W. J., Billeci, T. M., Stults, J. T., Wong, S. C., *et al.*, Identifying proteins from two-dimensional gels by molecular mass searching of peptide fragments in protein sequence databases. *Proceedings of the National Academy of Sciences of the United States of America* 1993, 90, 5011-5015.

48] Mann, M., Hendrickson, R. C., Pandey, A., Analysis of proteins and proteomes by mass spectrometry. *Annu. Rev. Biochem.* 2001, 70, 437–473.

49] Clauser, K. R., Baker, P., Burlingame, A. L., Role of accurate mass measurement (±10 ppm) in protein identification strategies employing MS or MS/MS and database searching. *Analytical Chemistry* 1999, 71, 2871-2882.

50] Eng, J. K., McCormack, A. L., Yates Iii, J. R., An approach to correlate tandem mass spectral data of peptides with amino acid sequences in a protein database. *Journal of the American Society for Mass Spectrometry* 1994, 5, 976-989.

51] Perkins, D. N., Pappin, D. J. C., Creasy, D. M., Cottrell, J. S., Probability-based protein identification by searching sequence databases using mass spectrometry data. *Electrophoresis* 1999, 20, 3551-3567.

52] Zhang, N., Aebersold, R., Schwikowski, B., ProbID: A probabilistic algorithm to identify peptides through sequence database searching using tandem mass spectral data. *Proteomics* 2002, 2, 1406-1412.

53] Allet, N., Barrillat, N., Baussant, T., Boiteau, C., *et al.*, In vitro and in silico processes to identify differentially expressed proteins. *Proteomics* 2004, 4, 2333-2351.

54] Sadygov, R. G., Yates, J. R., A hypergeometric probability model for protein identification and validation using tandem mass spectral data and protein sequence databases. *Analytical Chemistry* 2003, 75, 3792-3798.

55] Gu, S., Pan, S., Bradbury, E. M., Chen, X., Use of deuterium-labeled lysine for efficient protein identification and peptide *de novo* sequencing. *Analytical Chemistry* 2002, 74, 5774-5785.

56] Yates, J. R., III. , Mass spectrometry from genomics to proteomics. *Trends. Genet.* 2000, 16, 5-8.

57] Hennig, S., Groth, D., Lehrach, H., Automated Gene Ontology annotation for anonymous sequence data. *Nucleic Acids Research* 2003, 31, 3712-3715.

58] Zehetner, G., OntoBlast function: from sequence similarities directly to potential functional annotations by ontology terms. *Nucleic Acids Research* 2003, 31, 3799-3803.

59] Gerlt, J., Babbitt, P., Can sequence determine function? *Genome Biology* 2000, 1, reviews0005.0001 - reviews0005.0010.

60] Ouzounis, C., Karp, P., The past, present and future of genome-wide re-annotation. *Genome Biology* 2002, 3, comment2001.2001 - comment2001.2006.

61] Sali, A., Genomics: Functional links between proteins. *Nature* 1999, 402, 23-26.

62] Ashburner, M, C., Blake, A., Botstein, D., Butler, H., Cherry, J. M., Davis, A. P., Dolinski, K., Dwight, S. S., Eppig, J. T., Harris, M. A., Hill, D. P., Issel-Tarver, L., Kasarskis, A., Lewis, S., Matese, J. C., Richardson, J. E., Ringwald, M., Rubin, G. M, Sherlock, G., Gene ontology: tool for the unification of biology. The Gene Ontology Consortium. *Nat Genet.* 2000, 25, 25-29.

63] Tomanek, L., Environmental Proteomics: Changes in the proteome of marine organisms in response to environmental stress, pollutants, infection, symbiosis, and development. *Annu. Rev. Mar. Sci.* 2011, 3, 373–399.

64] Zhu, J. Y., Huang, H. Q., Bao, X. D., Lin, Q. M., Cai, Z., Acute toxicity profile of cadmium revealed by proteomics in brain tissue of *Paralichthys olivaceus*: Potential role of transferrin in cadmium toxicity. *Aquatic Toxicology* 2006, 78, 127-135.

65] Junqueira, M., Spirin, V., Balbuena, T. S., Thomas, H. *et al*., Protein identification pipeline for the homology-driven proteomics. *J. Proteomics* 2008, 71, 346–356.

66] Seidler, J., Zinn, N., Boehm, M. E., Lehmann, W. D., *De novo* sequencing of peptides by MS/MS. *Proteomics* 2010, 10, 634-649.

67] Lemeer, S., Jopling, C., Gouw, J., Mohammed, S. *et al*, Comparative phosphorproteomics of zebrafish fyn/yes morpholino knockdown embryos. *Mol. Cell. Proteomics* 2008, 7, 2176–2187.

68] Lemeer, S., Pinkse, M. W. H., Mohammed, S., van Breukelen, B. *et al.*, Online automated *in vivo* zebrafish phosphoproteomics: from large-scale analysis down to a single embryo. *J. Proteome Res.* 2008, 7, 1555–1564.

69] Ziv, T., Gattegno, T., Chapovetsky, V., Wolf, H. *et al.*, Comparative proteomics of the developing fish (zebrafish and gilthead seabream) oocytes. *Comp. Biochem. Physiol. D Genomics Proteomics* 2008, 3, 12–35.

70] Lucitt, M. B., Price, T. S., Pizarro, A., Wu, W., *et al.*, Analysis of the zebrafish proteome during embryonic development. *Molecular & Cellular Proteomics* 2008, 7, 981-994.

71] Bosworth, C. A., Chou, C. W., Cole, R. B., Rees, B. B., Protein expression patterns in zebrafish skeletal muscle: initial characterization and the effects of hypoxic exposure. *Proteomics* 2005, 5, 1362-1371.

72] Gündel, U., Benndorf, D., von Bergen, M., Altenburger, R., Küster, E., Vitellogenin cleavage products as indicators for toxic stress in zebra fish embryos: A proteomic approach. *Proteomics* 2007, 7, 4541-4554.

73] De Wit, M., Keil, D., Remmerie, N., van der Ven, K. *et al*., Molecular targets of TBBPA in zebrafish analyzed through integration of genomic and proteomic approaches. *Chemosphere* 2008, 74, 96–105.

74] Damodaran, S., Dlugos, C. A., Wood, T. D., Rabin, R. A., Effects of chronic ethanol administration on brain protein levels: a proteomic investigation using 2-D DIGE system. *Eur. J. Pharmacol.* 2006, 547, 75–82.

75] Smith, R. W., Wood, C. M., Cash, P., Diao, L. *et al.*, Apolipoprotein AI could be a significant determinant of epithelial integrity in rainbow trout gill cell cultures: a study in functional proteomics. *Biochim. Biophys*. *Acta* 2005, 1749, 81–93.

76] Booy, A. T., Haddow, J. D., Ohlund, L. B., Hardie, D. B.*et al.*, Application of isotope coded affinity tag (ICAT)analysis for the identification of differentially expressed proteins following infection of atlantic salmon (Salmo salar) with infectious hematopoietic necrosis virus (IHNV) or Renibacterium salmoninarum (BKD). *J. Proteome Res.*2005, 4, 325–334.

77] Martin, S. A. M., Mohanty, B. P., Cash, P., Houlihan, D. F. *et al.*, Proteome analysis of the Atlantic salmon (Salmo salar) cell line SHK-1 following recombinant IFN-gamma stimulation. *Proteomics* 2007, 7, 2275–2286.

78] Smith, R. W., Cash, P., Ellefsen, S., Nilsson, G. E., Proteomic changes in the crucian carp brain during exposure to anoxia. *Proteomics* 2009, 9, 2217–2229.

79] Lokaj, K., Meierjohann, S., Schultz, C., Teutschbein, J., *et al.*, Quantitative differential proteome analysis in an animal model for human melanoma. *Journal of Proteome Research* 2009, *8*, 1818-1827.

80] Meierjohann, S., Schartl, M., Volff, J.-N., Genetic, biochemical and evolutionary facets of Xmrk-induced melanoma formation in the fish Xiphophorus. *Comparative Biochemistry and Physiology Part C: Toxicology & Pharmacology* 2004, *138*, 281-289.

81] Dowd, W. W., Harris, B. N., Cech, J. J., Kultz, D., Proteomic and physiological responses of leopard sharks (*Triakis semifasciata*) to salinity change. *J Exp Biol.* 2010, 213, 210-224.

82] Dowd, W. W., Wood, C. M., Kajimura, M., Walsh, P. J. and Kültz, D. Natural feeding influences protein expression in the dogfish shark rectal gland: a proteomic analysis. *Comp. Biochem. Physiol.* 2008, 3D, 118-127.

83] Kültz, D., Fiol, D., Valkova, N., Gomez-Jimenez, S., Chan, S. Y. and Lee, J., Functional genomics and proteomics of the cellular osmotic stress response in 'nonmodel' organisms. *J. Exp. Biol.* 2007, 210, 1593-1601.

84] Zupanc, M. M., Wellbrock, U. M., Zupanc, G. K. H., Proteome analysis identifies novel protein candidates involved in regeneration of the cerebellum of teleost fish. *Proteomics* 2006, 6, 677–696.

85] Wulff, T., Jessen, F., Roepstorff, P., Hoffmann, E.S., Long term anoxia in rainbow trout investigated by 2-DE and MS/MS. *Proteomics* 2008, 8, 1009–1018.

86] Delahunty, C., Yates Iii, J. R., Protein identification using 2D-LC-MS/MS. *Methods* 2005, 35, 248-255.

87] De Souza, A. G., MacCormack, T. J., Wang, N., Li, L., Goss, G. G., Large-scale proteome profile of the zebrafish (Danio rerio) gill for physiological and biomarker discovery studies. *Zebrafish* 2009, 6, 229-238.

88] Singh, S. K., Sundaram, C. S., Shanbhag, S., Idris, M. M., proteomic profile of zebrafish brain based on two-dimensional gel electrophoresis matrix-assisted laser desorption/ionization MS/MS analysis. *Zebrafish* 2010, 7, 169-177.

Chapter 2

Effects of oxygen on glycolytic enzyme specific activities in liver and skeletal muscle of *Fundulus heteroclitus*

2.1 Abstract

Many aquatic environments are characterized by conditions of low dissolved oxygen (hypoxia), posing significant challenges to organisms that live in these environments. Responses to hypoxia have been well studied in fish, which display physiological, behavioral, and biochemical adjustments to hypoxia. The goal of the present study was to measure the temporal effects of oxygen treatments on the maximal specific activities of nine glycolytic enzymes during chronic exposure (28d) of *Fundulus heteroclitus*. Spectrophotometric enzyme assays were performed on tissues of liver and skeletal muscle of fish exposed to two levels of hypoxia, normoxia, and hyperoxia, and sampled at 0, 8, 14, and 28 d. Analysis of glycolytic enzyme specific activities suggested tissue-specific responses with low oxygen leading to higher enzyme specific activities in liver, but lower specific activities in skeletal muscle. In general, oxygen effects were observed only after two weeks exposure. The duration of the exposure had strong effects on glycolytic enzyme specific activities in both liver and skeletal muscle. The results demonstrated that the effect of different oxygen treatments on enzyme specific activities varied among enzymes and tissues in *Fundulus heteroclitus.*

2.2 Introduction

Estuarine habitats undergo frequent fluctuations in pH, salinity, carbon dioxide, temperature, and dissolved oxygen [1]. Hypoxia occurs when dissolved oxygen is consumed faster than new dissolved oxygen is supplied. In the summer, estuaries have low dissolved oxygen concentrations due to low solubility of oxygen in water at high temperatures. Secondly, the water is not aerated due to lack of wave action, and separates into warmer, less salty, less dense water on the top and colder, more salty, denser water at the bottom. The result is oxygen can't cross the boundary between the two layers and can't be replenished as dissolved oxygen in the bottom layer is used up by the decomposers. Also, algal blooms fueled by warm temperatures and ample supplies of nutrients contribute to hypoxia forming a thick mat on the surface waters and serving as food for decomposers [2, 3].

Low dissolved oxygen (hypoxia) is associated with mass mortality of aquatic animals, declines in fisheries production, and major changes in the types of species found in a given location [4-6]. Several laboratory and field experiments on behavioral responses showed that many fish detect and avoid hypoxia by migrating from low oxygen to oxygenated waters or by engaging in aquatic surface respiration [7, 8]. Some fish were shown to change their feeding habits during the crisis of low oxygen [5]. In response to hypoxia fish also undergo morphological and physiological adjustments including increased number of perfused gill lamellae [9], higher haematocrit [10] and elevated hemoglobin synthesis [11] to improve oxygen extraction and transport. In addition to these adaptations, biochemical adjustments to conserve energy occur, namely by metabolic depression that enables the animals to survive longer periods of hypoxia. This is mediated by general reduction in metabolism, down-regulation of protein synthesis, and control of enzymes involved in aerobic and anaerobic pathways [12, 13].

The up regulation of glycolysis to enhance the production of energy under reduced pO_2 is the hallmark of hypoxic response [13]. Several studies in fish support the hypothesis of up regulation of glycolytic enzymes under hypoxia. However, the changes in enzyme activities are not uniform either throughout the tissues or in different species. Hypoxic exposure of killifish and goldfish resulted in tissue specific effects with increased enzyme activities only in liver but not in skeletal muscle [14, 15]. Also the changes in enzyme activities were species specific where some species showed no changes in enzyme activities [16] with few others showing a decreased enzyme activity during hypoxic exposure [17]. In a recent study by Martinez et al changes in activities of all glycolytic enzymes and those involved in gluconeogeneisis and glycogen metabolism were studied in a multi-tissue perspective using heart, liver, brain and white skeletal muscle from *F. grandis* exposed to hypoxia [18]. The study showed that enzyme activities were low in skeletal muscle and high in liver with smaller changes in brain and heart.

Similar to hypoxia, hyperoxia also occurs naturally in aquatic habitats at daytime when the rate of photosynthesis is highest and oxygen production has exceeded its rate of removal by diffusion, leading to high dissolved oxygen concentrations. Hyperoxia is not as commonly studied, but few studies have shown that short-term exposure to hyperoxia causes gill oxidative cell damage [19]. Studies on salmonids have revealed that fish are prone to reactive oxygen species generated oxidative stress after hyperoxia exposure [20, 21].

The goal of current study was to measure the changes in maximal enzyme specific activities in *Fundulus heteroclitus*, an estuarine teleost fish. *Fundulus heteroclitus*, or mummichog, inhabits salt marshes in the North American Atlantic coast and shows remarkable tolerance to hypoxia, salinity and temperature fluctuations [22]. *F. heteroclitus* was exposed to four different oxygen treatments: hyperoxia, normoxia, moderate hypoxia and severe hypoxia;

the time course of changes in maximal specific enzyme activities of nine glycolytic enzymes was measured at 0, 8, 14 and 28 d. The effects of hyperoxia on maximal enzyme specific activities as a continuum of oxygen effects were also studied.

2.3 Materials and Methods

2.3.1 Experimental design

F. heteroclitus were collected from Canary Creek, a tidal creek of Delaware Bay, during June 2005. Fish were acclimated in the laboratory to experimental temperature and salinity conditions and a 14 h light: 10 h dark cycle for seven days prior to the beginning of the experiment. Fish were fed frozen mysid shrimp (*Mysis relicta*) during the acclimation period. *F. heteroclitus* were injected with Northwest Marine Technology's Visible Implant Elastomer. One of five colors (red, green, blue, orange, or yellow) was implanted on either side of the dorsal fin to distinguish individual fish. After being marked, all fish were placed in experimental tanks for 36 hours prior to onset of oxygen treatments. The experiment consisted of five re-circulating aquarium systems, each with a different dissolved oxygen (DO) level (28 d averages represented): hyperoxia (10.65 mgO_2l^{-1}), normoxia (7.06 mgO_2l^{-1}), moderate hypoxia (2.98 mgO_2l^{-1}), and severe hypoxia (1.18 mgO_2l^{-1}). Each aquarium system consisted of eight 18 L tanks, each of which held seven fish. Dissolved oxygen levels were regulated using the device described by Grecay and Stierhoff [23]. The device regulated each system by measuring DO every 7.5 min and making adjustments, if necessary, by addition of O_2 or N_2 gas. Dissolved oxygen levels were measured each morning prior to feeding or sampling using a handheld YSI Model 55 DO probe; the DO remained stable throughout the experiment (Table 2.1). Tank temperatures were regulated throughout the experiment, ranging from 20.9 and 26.5^{o}C.

Table 2.1 Dissolved oxygen (DO) in experimental tanks measured over 28 d period.

Treatment	Mean (±SD) DO ($mg\ O_2 l^{-1}$)	Min DO ($mg\ O_2 l^{-1}$)	Max DO ($mg\ O_2 l^{-1}$)
Severe Hypoxia	1.18 (0.25)	0.63	1.98
Moderate Hypoxia	2.98 (0.36)	2.06	3.53
Normoxia	7.06 (0.77)	4.69	8.56
Hyperoxia	10.65 (0.95)	7.30	12.77

Ammonia levels were monitored on a daily basis throughout the experiment and partial water changes were done if the levels exceeded above 1.5 mgl^{-1}.

Fish were fed twice per day (0900 h and 1600 h) on frozen *Mysis relicta*. All systems were fed *ad libitum*. Food was removed from all tanks at 1800 h on days prior to a sampling day, giving 15 h for complete gut evacuation prior to the fish being sampled. Tanks were cleaned and fecal matter removed prior to each feeding. Samples taken on days 0, 8, 14, and 28 consisted of the dissection of 40 fish, 8 from each of the five DO treatments. Each fish was measured for length and weight prior to being dissected. Removed fish were replaced with unmarked individuals to maintain seven fish per tank for the duration of the experiment. All animal research conducted in this study conformed to national and institutional guidelines for research on vertebrate animals University of New Orleans IACUC protocol # 073 (Appendix A).

2.3.2 Extract preparation

Fish were sampled at 0, 8, 14, and 28 d. Muscle and liver were dissected, frozen in liquid nitrogen, and stored at – 80°C. Ice-cold homogenization buffer consisting of 100 $mmol^{-1}$ HEPES (*4-(2-hydroxyethyl)-1-piperazineethanesulfonic acid*) pH 7.4, 10 mmol l^{-1} KCl, 0.1 mmol l^{-1} DTT (Dithiothreitol**)** and 0.2% Triton X-100 was used to homogenize the tissues. Twenty to thirty milligrams of tissue were homogenized in nine volumes of buffer using a hand homogenizer for skeletal muscle and power homogenizer for liver (PRO Scientific Inc., Connecticut, USA). Homogenization was done for two 25-second periods placing the tissue on ice after each period. The homogenate was centrifuged for 15 min at 4°C at 2400 x g. Activities were measured on the freshly-prepared supernatants whereas protein content was measured after storage of supernatants at -80°C [18].

2.3.3 Enzyme assays

The nine glycolytic enzymes used in assays were: PGI, phosphoglucoisomerase; PFK, phosphofructokinase; ALD, aldolase; TPI, triosephosphate isomerase; GDH, glyceraldehyde-3-phosphatedehydrogenase; PGK, phospho-glycerokinase; PGM, phosphoglyceromutase; PYK, pyruvate kinase; LDH, lactate dehydrogenase. The linking enzyme and substrate concentrations of glycolytic enzymes for the assay were modified from Martinez et al [18]. The linking enzymes were centrifuged at 12,000 x g for 10 min to remove excess ammonium sulphate and redissolved in assay buffer. All the biochemicals and coupling enzymes were obtained from Sigma Chemical Co. (St.Louis, MO, USA) and Roche Applied Sciences (Indianapolis, IN, USA). Following are the concentrations of co-factors, linking enzymes and substrates in the assay buffer for each glycolytic enzymes assayed:

Concentration of assay buffer: 100 mmol l^{-1} Hepes, 10 mmol l^{-1} KCl pH 7.4 at 25^0C. For PFK, assay buffer of pH 8.2 was used.

Phosphofructokinase (PFK): 7.5 mmol l^{-1} $MgCl_2$, 1.25 mmol l^{-1} ATP (liver) or 2.5 mmol l^{-1} ATP (muscle), 5 mmol l^{-1} AMP, 0.2 mmol l^{-1} NADH, 1 i.u.ml^{-1} aldolase, 10 i.u.ml^{-1} glycerol-3-phosphate dehydrogenase, 29 i.u.ml^{-1} triose phosphate isomerase. Substrate: 5 mmol l^{-1} fructose 6-phosphate (liver), 10 mmol l^{-1} fructose 6- Phosphate (muscle).

Aldolase (ALD): 0.2 mmol l^{-1} NADH, 5 i.u.ml^{-1} glycerol-3-phosphate dehydrogenase, 14.5 i.u.ml^{-1} triose phosphate isomerase. Substrate: 0.75 mmol l^{-1} fructose 1, 6-bisphosphate (muscle, liver)

Triose phosphate isomerase (TPI): 0.2 mmol l^{-1} NADH, 10 i.u.ml^{-1} glycerol-3-phosphate dehydrogenase (muscle, liver). Substrate: 2.9 mmol· l^{-1} glyceraldehyde 3-phosphate (muscle, liver).

Glyceraldehyde-3-phosphate dehydrogenase (GAP): 4 mmol· l^{-1} $MgCl_2$ (muscle) or 1 mmol· l^{-1} $MgCl_2$ (liver), 3.1 mmol l^{-1} ATP (muscle) or 1.55 mmol l^{-1} ATP (liver), 0.2 mmol l^{-1} NADH, 8 i.u.ml^{-1} phosphoglycerokinase. Substrate: 2.8 mmol l^{-1} 3-phosphoglyceric acid (muscle, liver).

Phosphoglycerokinase (PGK): 5 mmol l^{-1} $MgCl_2$, 6.2 mmol· l^{-1} ATP, 0.2 mmol· l^{-1} NADH, 8 i.u.ml^{-1} glyceraldehyde-3-phosphate dehydrogenase. Substrate: 2.8 mmol l^{-1} 3-phosphoglycerate (muscle, liver).

Phosphoglucoisomerase (PGI): 1.25 mmol l^{-1} NADP, 0.5 i.u.ml^{-1} glucose-6-phosphate dehydrogenase. Substrate: 2 mmol l^{-1} fructose 6-phosphate (muscle, liver).

Phosphoglyceromutase (PGM): 5 mmol l^{-1} $MgCl_2$ (liver) or 2.5 mmol l^{-1} $MgCl_2$ (muscle), 65 mmol l^{-1} ADP (liver) or 1.25 mmol l^{-1} ADP (muscle), 0.125 mmol l^{-1}, 2,3-bisphosphoglycerate (liver), 0.062 mmol l^{-1} 2,3-bisphosphoglycerate (muscle),0.22 mmol l^{-1} NADH, 9 mmol l^{-1} glucose (liver) or 4.5 mmol l^{-1} glucose (muscle) , 0.2 i.u.ml^{-1} enolase,0.5 i.u.ml^{-1} pyruvate kinase, 0.75 i.u.ml^{-1} L-lactate dehydrogenase, 3.2 i.u.ml^{-1} hexokinase. Substrate: 1.25 mmol l^{-1} 3-phosphoglycerate (muscle, liver).

Pyruvate kinase (PYK): 10 mmol l^{-1} $MgCl_2$, 7.6 mmol l^{-1} ADP, 0.2 mmol l^{-1} NADH, 0.375 i.u.ml-1 L-lactate dehydrogenase. Substrate: 1 mmol l^{-1} phosphoenolpyruvate (muscle, liver).

Lactate dehydrogenase (LDH): 0.2 mmol l^{-1} NADH. Substrate: 1 mmol l^{-1} pyruvate (muscle and liver).

Substrates, cofactors and linking enzymes were prepared on the same day of tissue homogenization with enzyme activities measured within 3 hours of tissue homogenization. Enzyme activities were measured in quadruplicate on a 96-well microtiter plate (VERSAmax, Molecular Devices, and Sunnyvale, CA, USA) at wavelength of 340 nm at 25°C. The

concentrations of substrates, cofactors and linking enzymes were optimized to give maximal activities. The background rate was measured without the substrate for each enzyme prior to initiating the assay by adding the specific substrate.

2.3.4 Protein assay

The protein content of tissue extracts was determined by the use of the modified bicinchonic acid (BCA) assay [24, 25]. All the reagents for the assay and the protein standard were obtained from Pierce Biochemicals (Rockford, IL, USA) and Sigma Aldrich (St Louis, MO, USA). The concentration of protein standard used was 2 mg/ml BSA. Appropriate dilutions of the tissue extracts (liver and muscle) were prepared so that absorbancies fell within the standard curve. The samples were treated with 0.15% deoxycholate (DOC), vortexed and incubated at room temperature for 10 min. After incubation the tubes were treated with 72% trichloro-acetic acid (TCA), vortexed and placed in swinging bucket rotor and centrifuged at 3800 x g for 30 min at 20°C. Immediately after centrifugation, the supernatants were aspirated and the pellets dissolved in 0.1N NaOH, 5% sodium dodecyl sulfate followed by addition of BCA reagent. The samples were incubated at 60°C for 30 min, and then cooled to room temperature, and the absorbance was read at 562 nm on spectrophotometer (Beckman DU 640 Spectrophotometer, CA, USA).

2.3.5 Calculations and Statistical analysis

Statistical analyses were performed on maximal enzyme specific activities measured in units mg^{-1} of protein. The enzyme specific activities were transformed by taking natural logarithm or square root to achieve normal distribution of data. The effects of oxygen treatment and experimental duration on the transformed enzyme specific activities were measured using two-way analysis of variance (ANOVA). When oxygen or interaction effects were significant

one-way ANOVA was done at individual durations. To determine differences among specific oxygen treatments, pair-wise comparisons were done using Post-hoc Tukey test. All the analyses were done using SYSTAT 10.2 software and $P<0.05$ was considered significant.

2.4 Results

In liver, transformed glycolytic enzyme specific activities were used for analysis but untransformed specific activities were plotted as a function of duration of exposure as shown in figure 2.1. It was observed that different oxygen exposures had selected effect on glycolytic enzyme specific activities. Among the nine glycolytic enzymes phosphoglucoisomerase (PGI), phosphofructokinase (PFK), phoshoglycerokinase (PGK) were significantly affected by oxygen. Post-hoc Tukey tests on enzyme activities measured over the entire experiment (0-28d) 0, 8, 14 and 28 d showed that PGI and PFK were significantly higher in severe hypoxia than normoxia and PGK was significantly higher in severe hypoxia than in moderate hypoxia and normoxia. Similar to liver, transformed glycolytic enzyme specific activities in skeletal muscle were analyzed but untransformed specific activities were plotted as a function of duration of exposure as shown in figure 2.2. Of the nine glycolytic enzymes only aldolase (ALD) had strong oxygen effects. Post-hoc Tukey tests on enzyme activities measured over the entire experiment (0-28d) showed that ALD was significantly lower in severe hypoxia than in moderate hypoxia, normoxia and hyperoxia. Strong interaction effects between treatments and duration of exposure were also seen in enzymes glyceraldehyde-3-phosphate dehydrogenase (GDH) and lactate dehydrogenase (LDH), phosphoglyceromutase (PGM) exhibited an interaction effect that was near to being significant ($P=0.078$). Significant interaction effects suggested an effect of duration on oxygen treatments. Post-hoc Tukey tests on enzyme activities measured at each interval during the experiment (0, 8, 14 and 28 d) showed that PGM and LDH were significantly lower in severe

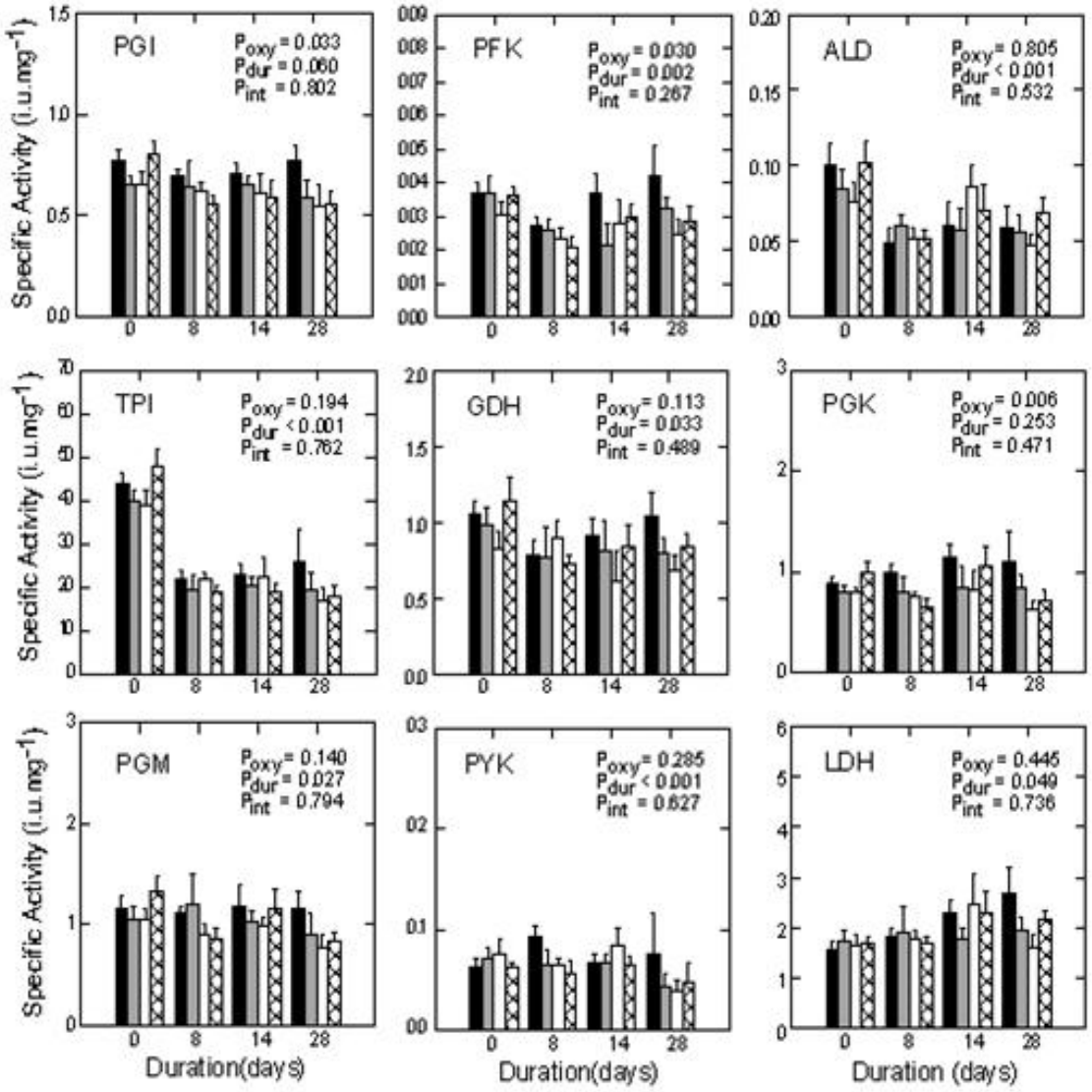

Figure 2.1 Glycolytic enzyme activities (i.u.mg^{-1}) in liver of *Fundulus heteroclitus* held under severe hypoxia (solid bars), moderate hypoxia (grey bars), normoxia (open bars) and hyperoxia (cross hatched bars) for 0, 8, 14 and 28 d. Sample size was eight fish per treatment at each sample interval. P values from two-way ANOVA assessing the effects of experimental duration, oxygen treatment and interaction are shown in inset. Error bars indicate one S.E.M. a, b indicate significant differences between different oxygen treatments at the indicated time points.

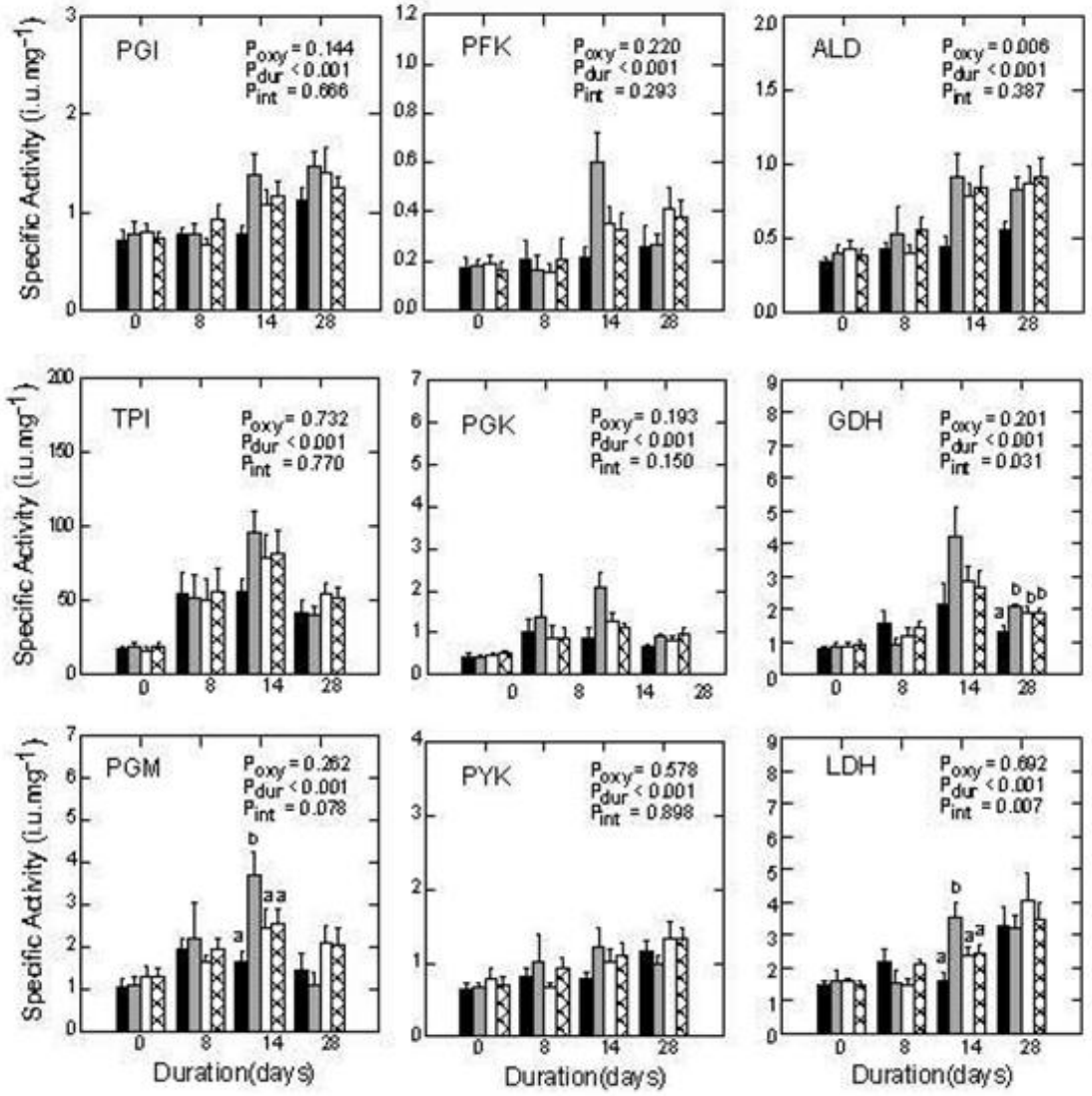

Figure 2.2 Glycolytic enzyme activities (i.u.mg^{-1}) in skeletal muscle of *Fundulus heteroclitus* held under severe hypoxia (solid bars), moderate hypoxia (grey bars), normoxia (open bars) and hyperoxia (cross hatched bars) for 0, 8, 14 and 28 d. Sample size was eight fish per treatment at each sample interval. P values from two-way ANOVA assessing the effects of experimental duration and oxygen treatment and interaction are shown in inset. Error bars indicate one S.E.M. a, b indicate significant differences between different oxygen treatments at the indicated time points.

hypoxia than moderate hypoxia at 14 d. GDH was significantly lower in severe hypoxia than moderate hypoxia, normoxia and hyperoxia at 28 d.

Analyses showed that duration of exposure of fish to different oxygen treatments strongly affected glycolytic enzyme specific activities of liver and skeletal muscle. A general trend towards increased glycolytic enzyme activities in skeletal muscle and decreased enzyme activities in liver were observed regardless of treatment. In liver not all the glycloytic enzymes were affected by duration of exposure. Post-hoc Tukey tests showed that in fish at 0 d, liver PFK, ALD, TPI, PGM and PYK specific activities were greater than in fish sampled at later days. In muscle all the nine glycloytic enzymes were affected by duration of exposure. Post-hoc Tukey tests showed that fish at 0 d had lower specific activities than fish sampled at later days. The time points with greater enzyme specific activities than 0 d were enzyme dependent. In TPI, PGK, GDH and PGM specific enzyme activities were significantly greater by 8 d. In PGI, PFK, ALD, LDH significantly greater changes in specific activities were seen by 14 d and by 28 d in PYK. Strong duration effects on glycloytic enzyme specific activities of liver and skeletal muscle suggest acclimation of fish to lab conditions.

2.5 Discussion

Under hypoxia, animals either reduce metabolic rate or maintain metabolic rate and increase anaerobic metabolism (glycolysis) to match the reduced supply of energy [26]. Studies in fish support increased glycolytic enzyme activities of enzymes involved in carbohydrate metabolism as an adaptation of fish to meet the energy requirements under hypoxia [14, 27, 15, 28, and 29]. The effect of hypoxia on activities of enzymes involved in carbohydrate metabolism is well documented in hypoxia tolerant *F. heteroclitus*. Greaney et al [14] found significantly higher enzyme activities in LDH, MDH and GPI in liver, but not in skeletal muscle of *F.*

heteroclitus during 28 d of chronic hypoxia exposure. In another study, Kramer et al [29] measured enzyme activities of all glycolytic enzymes only in liver tissue where *F. heteroclitus* was exposed to three days of hypoxia. It was seen that only six glycolytic enzymes PGI, ALD, TPI, PGK, PGM and LDH showed significant increase in glycolytic enzyme activities. In *F. grandis*, fewer and smaller changes in the glycolytic enzyme activities were noted in heart and brain while many enzymes were strongly suppressed in skeletal muscle [18]. In liver increased activities of many but not all glycolytic enzymes was observed. However in all these studies the changes in enzyme activities were tissues specific or enzyme specific and even species specific, when studied in different species [16, 30].

The glycloytic enzyme specific activities of nine glycolytic enzymes were measured in *F. heteroclitus* exposed to severe hypoxia, moderate hypoxia, normoxia and hyperoxia over an experimental duration of 28 d. Responses to short-term hypoxia in fish can be very different from those to prolonged hypoxia [15]. Thus, time course of hypoxic exposure is a critical factor in switching to anaerobic metabolism, but very few studies have documented the time course of changes of enzyme activities in fish exposed to long-term hypoxia for all the enzymes and four different oxygen treatments. Exposure to both hyperoxia (high levels of dissolved oxygen, here 145% O_2 saturation) and hypoxia (low levels of dissolved oxygen, here 46% O_2 saturation) may be damaging to aquatic organisms, resulting in suboptimal growth and hence lower biomass production [31]. Therefore the changes in enzyme activities in fish exposed to hyperoxia were also measured.

The measurements suggest significant oxygen effects and interaction effects on few, but not all the glycolytic enzymes. The effects were not uniformly distributed between the two tissues studied, as well as within the glycolytic enzymes. In general a trend towards increased

enzyme activities in liver and decreased enzyme activities in muscle was observed. Lower enzyme activities in skeletal muscle might be due to lower growth rates observed in other teleost species [32] and in *F. heteroclitus* [33]. The negative impact on growth was attributed to loss in skeletal muscle protein to meet energy demands under hypoxia [34-36]. This was also supported in a study by Martinez et al [18] where the soluble protein concentrations were about 20% lower in skeletal muscle extracts of *F. grandis* from hypoxic fish compared to normoxic fish. In addition, behavioral observatory studies on cod [36] and few other selected estuarine organisms [37] revealed decreased locomotion under hypoxia. This could also be a reason for decreased enzyme activities in skeletal muscle where the fish try to conserve energy under chronic hypoxia. In skeletal muscle, GDH was significantly lower in severe hypoxia than moderate hypoxia, normoxia and hyperoxia at 28 d. The higher enzyme activities during hyperoxia (here at 14.5 mgl^{-1}) may due to improved growth as documented in spotted wolffish *Anarhichas minor* [38]. Unlike skeletal muscle, increased glycolytic enzyme specific activities were seen in liver under hypoxia. Higher enzyme activities suggest increased biosynthetic role of this tissue to augment the ATP turnover.Interestingly, the effects of duration of exposure on glycolytic enzyme specific activities in both tissues were also observed. Once again a general trend towards increased glycolytic enzyme specific activities in skeletal muscle and decreased glycloytic enzyme specific activities in liver were observed regardless of treatment. In liver five enzymes were affected by duration and in skeletal muscle all the nine glycolytic enzymes were affected. The glycolytic enzymes and time points affected by duration of exposure were different in both the tissues. This might be due to acclimation of fish to laboratory conditions.

2.6 Conclusions

In aggregate, our results demonstrate that chronic hypoxia alters the capacity for carbohydrate metabolism in *F. heteroclitus*, with the important explanation that the responses are both tissue- and enzyme-specific. The general responses of tissue and skeletal muscle were consistent with results of Martinez et al [18] experiment in *F. grandis*. Also, our experiment supports those studies that documented a tissue and enzyme specific [16, 30, 39] responses of glycolytic enzyme activities to hypoxia.

2.7 References

1] Jensen, F. B., Nikinmaa, M., Weber, R. E., Environmental perturbations of oxygen transport in teleost fishes: causes, consequences, and compensations. In: Rankin, J. C., Jensen, F. B. (Eds.), *Fish Ecophysiology* Chapman & Hall, New York, 1993, 161– 179.

2] Breitburg, D. L., Near-shore hypoxia in the Chesapeake Bay: Patterns and relationships among physical factors. *Estaurine, Coastal and shelf science* 1990, 30, 593-609.

3] Diaz, R. J., Overview of hypoxia around the world. *Jour. of environ. Qual.* 2001, 30, 275-281.

4] Tyson, R. V., Pearson, T. H., Modern and ancient continental shelf anoxia: an overview .pp.1-24. In: R. V.Tyson & T. H. Pearson (ed.) Modern and ancient continental shelf anoxia, Geological society special publication No.58, the Geological Society London. 1991.

5] Diaz, R. J., Rosenberg, R., Marine benthic hypoxia: A review of its ecological effects and the behavioural responses of benthic macrofauna. *Oceanography and Marine Biol.* 1995, 33, 245-303.

6] Alexander, R. B., Smith, R. A., Schwarz, G. E., Effect of stream channel size on the delivery of nitrogen to the Gulf of Mexico. *Nat.* 2000, 403, 758-761.

7] Peterson, M. S. Hypoxia–induced physiological changes in two mangrove swamp fishes: sheephead minnow, Cyprinodon variegates (Myo macrocephalus) during hypoxia exposure. *Comparitive Biochemistry and Physiology* 1990, 77A: 475-482.

8] Love, J. W., Rees, B. B., Seasonal differences in hypoxia tolerance in gulf killifish, *Fundulus grandis* (Fundulidae) Environ. *Biol. of Fishes* 2002, 63, 103–115.

9] Wu, R. S., Woo, N. S., Respiratory responses and tolerance to hypoxia in two marine teleosts, Epinephelus akaara (Temminck & Schlegel) and Mylio macrocephalus (Basilewsky) *Hydrobiologia* 1984, 119, 209-217.

10] Soldatov, A. A., The effect of hypoxia on red blood cells of flounder: a morphologic and autoradiographic study. *Jour. of Fish Biol.* 1996, 48, 321– 328.

11] Kobayashi, M., Nezu, T., Tanaka, Y., Hypoxic induction of hemoglobin synthesis in daphnia magna. *Comp. Biochem. & Physio.* 1990, 97A, 513-517.

12] Storey, K. B., Tissue-specific controls on carbohydrate catabolism during anoxia in goldfish. *Physiol. Zool.* 1987, 60, 601-607.

13] Hochachka, P. W., Somero, G. N., Biochemical adaptation. Princeton University Press, Princeton. 2002.

14] Greaney, G. S., Place, A. R., Cashon, R. E., Smith, G., Powers, D. A., Time course of

changes in enzyme activities and blood respiratory properties of killifish during long-term acclimation to hypoxia. *Physiol.Zool.* 1980, 53, 136-144.

15] Van den Thillart, G., Dalla Via, J., Vitali, G., Cortesi, P., Influence of long-term hypoxia exposure on the energy metabolism of *Solea solea*. I. Critical O_2 levels for aerobic and anaerobic metabolism. *Marine Ecology Progress Series* 1994, 104, 109–117.

16] Shaklee, J. B., Christiansen, J. A., Sidell, B. D., Prosser, C. L., Whitt, G. S., Molecular aspects of temperature acclimation in fish: contributions of changes in enzyme activities and isozyme patterns to metabolic reorganization in the green sunfish. *J. Exp. Zool.* 1977, 201, 1-20.

17] Almeida-Val, V. F., Farias, I. P., Silva, M. P., Duncan, W. P., Val, A. L., Biochemical adjustments to hypoxia by Amazon cichlids. *Braz. J. Med. Biol. Res.* 1995, 28, 1257-1263.

18] Martínez, M. L., Landry, C., Boehm, R., Manning. S., Cheek, A. O., Rees, B. B., Effects of long term hypoxia on enzymes of carbohydrate metabolism in the Gulf killifish, *Fundulus grandis*. *The Jour. of Exp. Biol.* 2006, 209, 3851-3861.

19] Brauner, C. J., Seidelin, M., Madsen, S. S., Jensen, F. B., Effects of freshwater hyperoxia and hypercapnia and their influences on subsequent seawater transfer in Atlantic salmon (*Salmo salar*) smolts. *Can. J. Fish. Aquat. Sci.* 2000, 57, 2054-2064.

20] Lygren, B., Hamre, K., Waagbø, R**.,** Effect of induced hyperoxia on the antioxidant status of Atlantic salmon *Salmo salar* L. fed three different levels of dietary vitamin E. *Aquac. Res.* 2000, 31, 401-407.

21] Ritola, O., Tossavainen, K., Kiuru, T., Lindstrom-Seppa, P., Molsa, H., Effects of continuous and episodic hyperoxia on stress and hepatic glutathione levels in one-summer-old rainbow trout (*Oncorhynchus mykiss*). *J. Appl. Ichthyol.* 2002, 18, 159-164.

22] Burnett, K. G., Bain, L. J., Baldwin, W. S., Callard, G. V., Cohen, S., Di Giulio, R. T., Evans, D. H., Gómez-Chiarri, M., Hahn, M. E., Hoover, C. A., Karchner, *et al.*, *Fundulus* as the premier teleost model in environmental biology:Opportunities for new insights using genomics. *Comp. Biochemis. & Physio. Part D*. 2007, 2, 257–286.

23] Grecay, P. A., Stierhoff, K. L., A device for precisely controlling dissolved oxygen levels in laboratory experiments. *J. Exp. Mar. Biol. Ecol.* 2002, 280, 53-62.

24] Smith, K., Krohn, R. I., Hermanson, G. T., Mallia, A. K., Gartner, F.H., Provenzano, M. D., Fujimoto, E. K., Goeke, N. M., Olson, B. J. and Klenk, D. C., Measurement of protein using bicinchoninic acid. *Anal. Biochem.* 1985, 150, 76-85.

25] Brown, R. E., Jarvis, K. L., Hyland, K. J., Protein measurement using bicinchoninic acid: elimination of interfering substances. *Anal.Biochem.* 1989, 180, 136-139.

26] Boutilier, R. G., St-Pierre, J., Surviving hypoxia without really dying. *Comp. Biochem. Physiol. A* 2000, 126, 481– 490.

27] Johnston, I. A., Bernard, L. M., Ultrastructure and metabolism of skeletal muscle fibres in the tench: effects of long-term acclimation to hypoxia. *Cell Tissue Res.* 1982, 227, 179-199.

28] Zhou, B. S., Wu. R. S. S., Randall, D. J., Lam, P. K. S., Ip, Y. K., Chew, S. F., Metabolic adjustments in the common carp during prolonged hypoxia. *J. Fish Biol.* 2000, 57, 1160-1171

29] Kraemer, L. D., Schulte, P. M., Prior PCB exposure suppresses hypoxia-induced up-regulation of glycolytic enzymes in *Fundulus heteroclitus*. *Comp. Biochem. Physiol.* 2004, 139C, 23-29.

30] Driedzic, W. R., Gesser, H., Johansen, K., Effects of hypoxic adaptation on myocardial performance and metabolism in *Zoarces viviparous*. *Can. J. Zool.* 1985, 63, 821-823.

31] Wedemeyer, G. A., *et al*. Effects of rearing conditions on the health and physiological quality of fish in intensive culture. *Cambridge University Press.* 1997, 62, 35-71.

32] Chabot, D., Dutil, J.-D., Reduce growth of Atlantic cod in nonlethal hypoxic conditions. *J. Fish Biol.* 1999, 55, 472-491.

33] Stierhoff, K. L., Targett, T. E., Grecay, P. A., Hypoxia tolerance of the mummichog: the role of access to the water surface. *J. Fish Biol.* 2003, 63, 580-592.

34] Sullivan, K. M., Somero, G. N., Size- and diet-related variation in enzymic activity and tissue composition in the sablefish, *Anaplopomafimbria*. *Biol. Bull.* 1983, 164, 315-326.

35] Pelletier, D., Guderley, H., Dutil, J.-D., Effects of growth rate, temperature, season, and body size on glycolytic enzymes activities in the white muscle of Atlantic cod (*Gadus morhua*). *J. Exp. Zool.* 1993, 265, 477-487.

36] Martínez, M., Guderley, H., Dutil, J.-D., Winger, P. D., He, P., Walsh, S. J. Condition, prolonged swimming performance and muscle metabolic capacities of cod *Gadus morhua*. *J. Exp. Biol. 2003*, 206, 506-511.

37] Wannamaker, C. M., Rice, J. A., Effects of hypoxia on movements and behavior of selected estuarine organisms from the southeastern United States. *J. Exp. Mar. Biol. Ecol.* 2000, 249, 145-163.

38] Foss, A., Evensen, T. H., Øiestad, V., Effects of hypoxia and hyperoxia on growth and food conversion efficiency in the spotted wolffish *Anarhichas minor* (Olafsen). *Aqua.Resear.* 2002, 33, 437-444.

39] Storey, K. B., Metabolic adaptations supporting anoxia tolerance in reptiles: recent advances. *Comp. Biochem. Physiol. B* 1996, 113, 23-35.

Chapter 3

Tissue sampling and protein recovery from tissues of the gulf killifish, *Fundulus grandis*

3.1 Abstract

Tissue sampling plays an important role in proteomic analysis of biological tissues. Several methods have been used to extract high quality protein; however, there remain concerns as to which method gives the most reproducible and accurate protein profiles for a given tissue. In the current study, the patterns of protein distribution in one-dimensional (1D) gels following flash freezing in liquid nitrogen or immersion in RNA later® were compared for five tissues of the gulf killifish, *Fundulus grandis*: liver, skeletal muscle, brain, gill, and heart. In liver and heart, the protein distribution in 1D gel was better stabilized by flash freezing, while in gill, the 1D protein profile was better preserved by immersion in RNA later®. In skeletal muscle and brain, both approaches yielded similar patterns of protein distribution. Thus, the best approach for tissue sampling is tissue-specific. To identify the proteins that were differentially preserved in liver and gill tissue using these two techniques, LC-MS/MS was used. LC-MS/MS analyses followed by database searching resulted in identification of 17 proteins from seven gel bands in liver and 12 proteins from four gel bands in gill. Identified proteins include enzymes of energy metabolism, heat shock proteins, and structural proteins. These protein identifications for a species without a sequenced genome demonstrate the utility of *F. grandis* as a model organism for environmental proteomic studies in vertebrates.

3.2 Introduction

Tissue sampling and preservation play critical roles in proteomic analyses of biological tissues. Rapidly freezing tissue samples in liquid nitrogen halts protein modification and degradation and it is often accepted as the gold standard for preserving protein integrity [1-5]. However this sampling method is associated with safety concerns of handling liquid nitrogen and it may not be possible where procurement, storage, or transport of cryogens is limited (for example in field studies). In addition, even momentary thawing of frozen tissue during sample storage or processing (e.g., homogenization) can result in protein degradation in previously frozen samples.

Alternatives to flash freezing of tissues have been proposed [6], including use of aqueous ammonium sulfate solutions, commercially available as RNA later® (AMBION). This reagent was originally developed to preserve and isolate high quality, intact RNA by rapidly penetrating fresh tissue and deactivating nucleases [7, 8]. Subsequently, a method was developed for the simultaneous extraction of high quality RNA and protein from tissues preserved in RNA later [9]. Nataliya et al compared the proteome of mice spleen as assessed by 2-dimensional polyacrylamide gel electrophoresis (2D-PAGE) of samples taken in RNA later® compared to those flash frozen [10]. It was seen that use of trireagents (TRIzol reagent® Monophasic solution of phenol and guanidine isothiocyanate from Invitrogen) increased the amount of protein extracted from the sample [10]. In a study performed on human kidney and prostate specimens, 2D PAGE analysis revealed a 50% decrease in the amount of protein that was observed from the ethanol-fixed samples as compared to snap-frozen specimens [11]. Sampling methods have not been systematically optimized, however, for other tissues or for tissues from

other species, and lack of standardized methods hinders the accuracy and reproducibility of proteomic studies.

In the current study, the effects of flash freezing tissues to immersion of tissues in RNA later® on protein profiles of tissues were compared from the gulf killifish, *Fundulus grandis*. This small teleost fish is a common inhabitant of estuaries bordering the Gulf of Mexico, habitats that undergo frequent fluctuations in salinity, temperature, and dissolved oxygen [12]. Due to its high abundance and pronounced tolerance of environmental variation, *F. grandis* and related species have been proposed as model systems to study physiological and molecular adaptations of vertebrates to environmental stress [13]. 1D-SDS-PAGE was used to assess the effects of tissue sampling technique for five tissues, liver, skeletal muscle, brain, gill, and heart. Then LC-MS/MS was used to identify protein bands that were differentially stabilized in gill and liver. The results demonstrate that optimal tissue sampling approach is tissue dependent. Furthermore, the results demonstrate that even in an organism without a sequenced genome, LC-MS/MS, combined with database searching of publically available databases, can be reliably used for protein identification.

3.3 Materials and Methods

3.3.1 Fish maintenance and sample preparation

Fundulus grandis were purchased from a bait store and kept in 40 L aquaria at room temperature (22-26°C) in dechlorinated tap water adjusted to approximately 5 parts per thousand salinity with artificial sea salts (Instant Ocean). Water was aerated and filtered through charcoal and biological filters. Fish were fed *ad libitum* with flake fish food once a day and were fasted 24 h immediately prior to dissection. Fish were sacrificed using an overdose of tricaine methanesulfonate, (MS 222, 1g per L, pH buffered with 4g $NaHCO_3$). Prior to dissection, length,

mass, and sex of the each fish were noted. For these analyses, only male fish were used. All animal research conducted in this study conformed to national and institutional guidelines for research on vertebrate animals protocol # UNO-10-001 (Appendix A).

Liver, gill, skeletal muscle, heart, and brain were harvested by dissection from six or seven fish and either frozen immediately in liquid nitrogen or immersed in 500 μL RNA later® (Ambion, Austin, Texas) at room temperature. For liver, gill, and skeletal muscle, tissues from individual fish were large enough to split into two samples; one for flash freezing, one for RNA later ®. For brain and heart, due to their small size, entire tissues were sampled by one or the other of the two techniques. Accordingly, sample sizes for liver, gill, and skeletal muscle are 6 or 7, while sample sizes for brain and heart are 3 or 4. All samples were stored in -80°C until further analysis.

For all tissues except hearts, samples of 20-50 mg were homogenized in a glass-glass homogenizers (Kontes, Vineland, NJ, USA) in 500 μL lysis buffer containing 7 M urea, 2 M thiourea, 2% CHAPS, 1% ASB-14, 40 mM dithiothreitol (DTT). Hearts (5-10 mg total mass) were homogenized in 200 μL of lysis buffer. Tissue homogenates were made on ice and centrifuged at 2400 x *g* for 15 min at 4°C. The supernatants were stored at -80°C until further analysis. Protein concentrations of the supernatant solutions were determined using Amersham Biosciences 2D Quant kit (GE health care, Piscataway, NJ, USA).

3.3.2 One dimensional gel electrophoresis

After protein quantitation, samples of 20 μg protein were separated by one dimensional gel electrophoresis in 12.5% polyacrylamide (37.5: 1 acrylamide: bisacrylamide) minigels (8 cm x 10 cm x 1mm) according to Laemmli [14]. Prior to electrophoresis, samples were reduced with 100 mM DTT combined with 4x sample buffer (Bio-Rad, Hercules, USA), and heated at 95°C

for 3 min. Electrophoresis was performed in 25 mM Tris, 192 mM glycine, and 0.1% SDS at 150 V for 2 h. Molecular weight markers (Precision Plus Protein Standards; Bio-Rad, Hercules, USA) were included in every gel.

3.3.3 Gel staining and image analysis

For quantitative image analysis, gels were stained using modified Neuhoff's colloidal coomassie protocol [15]. Gels were fixed overnight in 100 ml 50% ethanol: 3% phosphoric acid. Gels were then washed in three 30 min changes of 500 ml distilled water followed by staining in 300 ml of 34% methanol, 17% ammonium sulfate, 3% phosphoric acid, and 0.0066% coomassie brilliant blue G-250 (SERVA, New York, USA). Gels were de-stained in water for three days and imaged using a GS 700 densitometer (BIORAD, Hercules, USA). Images were analyzed using Quantity One software (BIORAD, Hercules, USA). Lanes and bands were manually defined. Lane-based background subtraction was performed using a "rolling disk" method of subtraction with disk size equal to 10. For band quantification, we used trace quantity, which is the area under the curve of pixel intensity versus migration distance. Trace quantity has optical density x mm as units. To test for significant differences in trace quantities of bands from samples prepared by the two techniques, two-sample t-tests assuming equal variances were used. A value of $p \leq 0.05$ was considered statistically significant.

3.3.4 In-gel digestion and peptide extraction

Protein bands were digested and extracted following [16]. In brief, protein bands were excised from gels and cut into 1 mm pieces, placed in micro-centrifuge tubes previously washed with 50% acetonitrile (ACN): 50% Milli–Q water. The gel pieces were equilibrated in 100 mM ammonium bicarbonate for 20 min followed by de-staining with 50 mM ammonium bicarbonate: 50% ACN until coomassie stain was removed. The gel fragments were reduced with 10 mM

DTT for 30 min at 56°C followed by alkylation with 50 mM iodoacetamide in the dark at room temperature for 30 min. Gel pieces were incubated in 30 µl of 50 mM ammonium bicarbonate containing 200 ng of sequencing grade trypsin (Promega, Madison, WI, USA) for 60 min at 4°C, after which the trypsin solution was replaced with equivalent amount of 50 mM ammonium bicarbonate and incubated overnight at 37°C. The resulting peptides were extracted from the gel pieces by vigorous vortex mixing for 5 min in 50 µl of each the following solutions: 1% formic acid; 0.5% formic acid: 50% ACN; and 100% ACN. The extracts were pooled and dried in Speed VAC concentrator (Eppendorf, Hauppauge, NY) and stored at -20°C until further analysis.

3.3.5 LC-MS/MS

LC–MS/MS was performed on Finnigan LTQ^{TM}-ion trap mass spectrometer (Thermo Electron, San Jose, CA) equipped with nano-flow electrospray ionization source. Vacuum-concentrated samples were suspended in 25 µL of 5% acetonitrile and 5% formic acid in a ninety six well microtiter plate and the volume for each sample injection was 6 µL. Electrospray was performed by setting the needle voltage at 2.65 kV. The capillary temperature was held at 200 °C, with a potential of 49 V. Samples were first loaded on a C_{18} trap column and washed with 3% acetonitrile and 0.1% formic acid for 45 min for desalting, then the purified peptides were eluted to a reverse-phase C_{18} analytical column (Pico Frit Column: 75 µm ID, 15 µm tip ID, packed with 5 µm Bio Basic^{TM} C_{18}, 10 cm length, New Objective, Woburn, MA) by a 60 min linear gradient. The mobile phase used for gradient elution consisted of buffer A (0.1% formic acid: 97% water: 3% acetonitrile v/v/v) and buffer B (0.1% formic acid: 3% acetonitrile: 97% water v/v/v) with a flow rate of 200 ~ 500 nL/min. Separated peptides by a gradient of 100% A to 35% A: 65% B were analyzed under the data-dependent acquisition mode set by Xcalibur, 2.2 version (Thermo Electron). After a MS survey scan over the m/z range of 300-2000, the three

most intense precursors were selected and subjected to fragmentation by collision induced dissociation. The normalized collision energy was set at 30% with activation Q value being 0.25 and dynamic exclusion of 120 s. All chemicals were reagent grade or better. Solvents used were HPLC grade

3.3.6 Database searching

The raw data were processed by Bioworks software, version 3.3 (Thermo Electron, San Jose, CA) and tandem mass spectra were searched against a ray-finned fishes protein database (downloaded from NCBI) by using the SEQUEST algorithm. Parameters for SEQUEST database search were set as follows: carbamidomethylation of cysteine (+ 57.02 Da); oxidation of methionine (+ 15.99 Da); and up to three missed cleavage sites. The output for the search results was filtered by cross-correlation score (Xcorr) which must be ≥ 3.0 for the triply charged ions, ≥ 2.5 for the doubly charged ions, and ≥ 2.0 for the singly charged ions. Also, delta correlation score [ΔCn] was set to be ≥ 0.1. A protein was considered identified if 2 or more peptides were identified and the total protein score was less than 10^{-10}. MS/MS spectra of all peptides were manually inspected to ensure the quality of identification.

3.4 Results

3.4.1 Effects of sampling technique on protein stabilization

Patterns of protein distribution were examined by one-dimensional SDS-PAGE for liver, skeletal muscle, brain, gill, and heart from *F. grandis* after sampling by flash freezing in liquid nitrogen or emersion in RNA later® (Figure 3.1). In liver (Fig. 3.1A, B), the staining intensity of several protein bands was greater for flash frozen samples compared to samples taken in RNA later®. These proteins were distributed across the entire range of separated molecular weights.

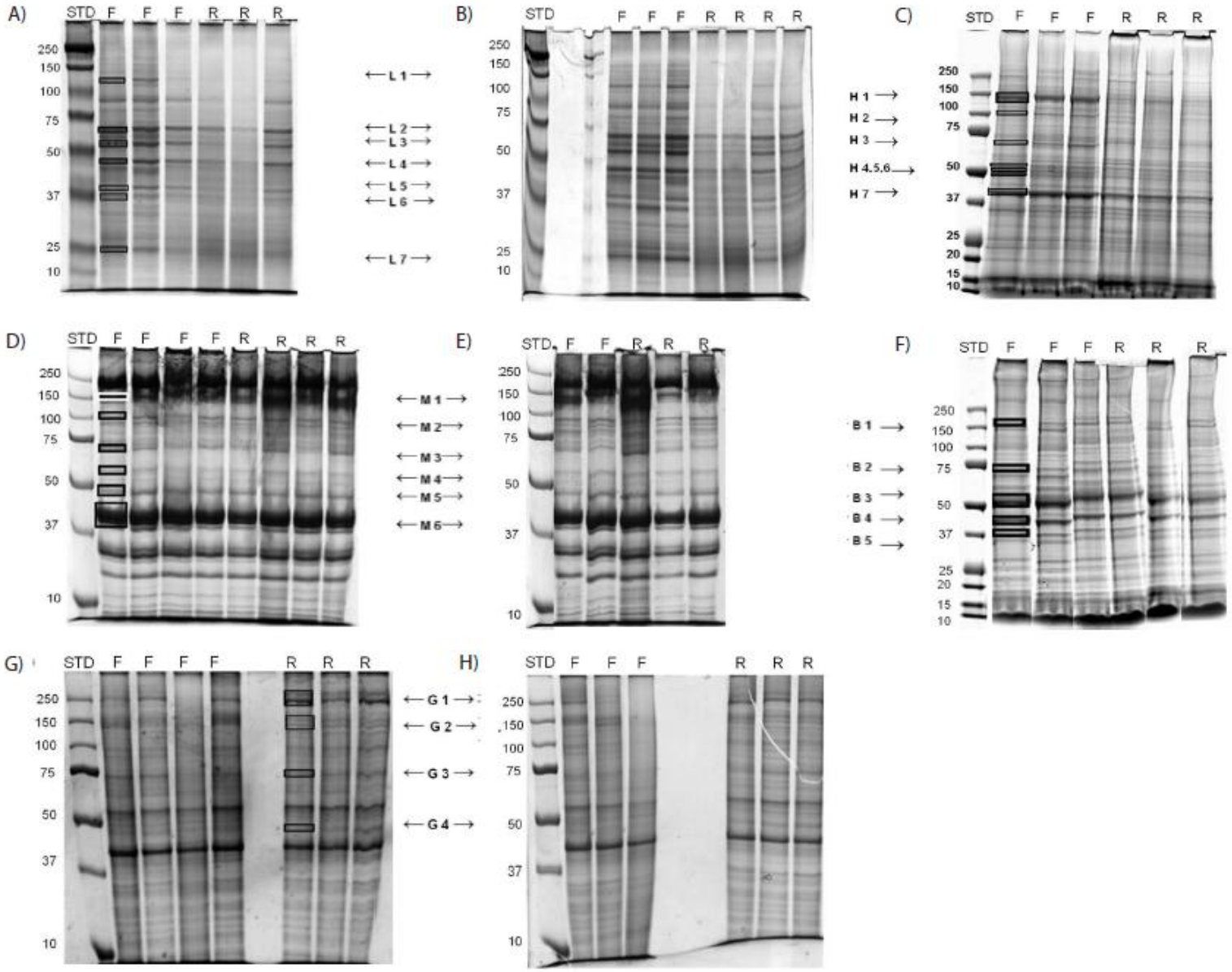
A)
STD F F F R R R
250
150
100
75
50
37
25
10
L 1
L 2
L 3
L 4
L 5
L 6
L 7
B)
STD F F F R R R R
250
150
100
75
50
37
25
10
C)
STD F F F R R R
H 1
H 2
H 3
H 4.5.6
H 7
250
150
100
75
50
37
25
20
15
10
D)
STD F F F F R R R R
250
150
100
75
50
37
10
M 1
M 2
M 3
M 4
M 5
M 6
E)
STD F F R R R
250
150
100
75
50
37
10
F)
STD F F F R R R
B 1
B 2
B 3
B 4
B 5
250
150
100
75
50
37
25
20
15
10
G)
STD F F F F R R R
250
150
100
75
50
37
10
G 1
G 2
G 3
G 4
H)
STD F F F R R R
250
150
100
75
50
37
10

Figure 3.1 Colloidal coomassie stained 1D gel images of *Fundulus grandis* liver (A, B), heart (C), skeletal muscle (D, E), brain (F), and gill (G, H). Protein equivalent to 20 µg was loaded in each lane. Sample sizes were 6 or 7 individual fish for liver, gill, and skeletal muscle, and 3 fish for heart and brain in each treatment. Lanes are labeled by sampling technique, flash frozen samples (F) or immersion in RNA later® (R). Molecular masses were determined by co-migration with protein plus standards from BIORAD (STD). Bands used for quantitative image analysis are indicated with arrows (e.g., L1 - L7, H1 - H7, etc). For liver and gill, the same bands were excised for protein identification by LC-MS/MS (see Tables 3.6 and 3.7).

Table 3.1 Quantitative image analysis of 1D gel band intensities from *F. grandis* liver.

Band [a]	M_r(kDa)	Trace Quantity (Mean ± SEM)		p-value [b]
		Flash frozen	RNA later®	
L1	127	0.342 ± 0.018	0.011 ± 0.003	0.003
L2	64	0.248 ± 0.019	0.129 ± 0.021	0.007
L3	53	0.241 ± 0.028	0.061 ± 0.022	0.001
L4	46	0.268 ± 0.027	0.072 ± 0.020	0.001
L5	38	0.103 ± 0.022	0.038 ± 0.012	0.020
L6	35	0.156 ± 0.040	0.028 ± 0.008	0.003
L7	27	0.209 ± 0.034	0.070 ± 0.025	0.002

[a] Band number corresponds to Figure 3.1 A, B. [b] p-values calculated using t-test: two sample assuming equal variances. $p \leq 0.05$ is considered significant.

Table 3.2 Quantitative image analysis of 1D gel band intensities from *F. grandis* heart.

Band [a]	M_r(kDa)	Trace Quantity (Mean ± SEM)		p-value [b]
		Flash frozen	RNA later®	
H1	141	0.193 ± 0.011	0.033± 0.010	<0.001
H2	103	0.032 ± 0.001	0.012 ± 0.000	<0.001
H3	68	0.046 ± 0.009	0.019 ± 0.003	0.041
H4	55	0.032 ± 0.004	0.023 ± 0.004	0.218
H5	52	0.037 ± 0.015	0.009 ± 0.001	0.126
H6	50	0.031 ± 0.004	0.019 ± 0.002	0.060
H7	41	0.286 ± 0.008	0.122 ± 0.027	0.004

[a] Band number corresponds to Figure 3.1 C. [b] p-values calculated using t-test: two sample assuming equal variances. $p \leq 0.05$ is considered significant.

Table 3.3 Quantitative image analysis of 1D gel band intensities from *F. grandis* skeletal muscle.

Band	M_r(kDa)	Trace Quantity (Mean ± SEM)		p-value [a]
		Flash frozen	RNA later®	
M1	153	0.378 ± 0.099	0.187 ± 0.029	0.072
M2	103	0.114 ± 0.012	0.094 ± 0.005	0.146
M3	71	0.094 ± 0.020	0.079 ± 0.021	0.605
M4	58	0.046 ± 0.012	0.045 ± 0.006	0.985
M5	49	0.203 ± 0.035	0.166 ± 0.017	0.338
M6	42	2.031 ± 0.142	1.738 ± 0.134	0.163

[a] Band number corresponds to Figure 3.1 D, E. [b] p-values calculated using t-test: two sample assuming equal variances. $p \leq 0.05$ is considered significant.

Table 3.4 Quantitative image analysis of 1D gel band intensities from *F. grandis* brain.

Band [a]	M_r(kDa)	Trace Quantity (Mean ± SEM)		p-value [b]
		Flash frozen	RNA later®	
B1	159	0.066 ± 0.026	0.070 ± 0.028	0.921
B2	72	0.100 ± 0.029	0.070 ± 0.024	0.471
B3	51	0.502 ± 0.089	0.507 ± 0.099	0.972
B4	42	0.335 ± 0.062	0.284 ± 0.061	0.594
B5	35	0.097 ± 0.029	0.074 ± 0.027	0.595

[a] Band number corresponds to Figure 3.1 F. [b] p-values calculated using t-test: two sample assuming equal variances. $p \leq 0.05$ is considered significant.

Table 3.5 Quantitative image analysis of 1D gel band intensities from *F. grandis* gill.

Band [a]	M_r (kDa)	Trace Quantity (Mean ± SEM)		p-value [b]
		Flash frozen	RNA later®	
G1	250	0.085 ± 0.022	0.240 ± 0.039	0.004
G2	140	0.187 ± 0.050	0.082 ± 0.008	0.083
G3	70	0.073 ± 0.017	0.122 ± 0.015	0.061
G4	46	0.032 ± 0.005	0.063 ± 0.008	0.006

[a] Band number corresponds to Figure 3.1 G, H. [b] p-values calculated using t-test: two sample assuming equal variances. $p \leq 0.05$ is considered significant.

The intensities of seven bands (L1 – L7) ranging from M_r 127 kD to 27 kD were determined by quantitative image analysis; all were found to be higher for flash-frozen samples (Table 3.1). heart showed a pattern similar to liver, having more intense protein staining in flash frozen samples than in samples taken in RNA later® (Figure 3.1C). Seven bands were selected for image analysis (Table 3.2); four were significantly more intense in flash frozen samples ($p < 0.05$, t-tests), while one was marginally higher in flash frozen samples ($0.10 > p > 0.05$, t-test). Skeletal muscle showed a pattern in which the protein staining intensities were similar in the two tissue sampling approaches (Figure 3.1D, E). Seven gel regions corresponding to discrete protein bands were selected for image analysis (M1 –M7): none were found to be statistically different between samples obtained by flash freezing or by immersion in RNA later® (Table 3.3). Brain, like skeletal muscle, seemed to be equally well preserved using either technique (Figure 3.1F, Table 3.4). In gill (Figure 3.1G, H) greater staining intensities were observed in samples taken in RNA later® than in flash frozen samples. In addition, the staining intensities among replicate samples was more reproducible for samples taken in RNA later®, especially for higher molecular weight proteins (>75 kD). In particular, two flash frozen samples had poor staining of high molecular weight proteins, presumably due to protein degradation. Four regions (G1 – G4) were selected for quantitative image analysis (Table 3.5). Two areas of staining (G1 and G4) were significantly more intense in samples taken in RNA later® ($p < 0.05$, *t*-tests), and one (G3) was marginally elevated in RNA later® ($0.10 > p > 0.05$, *t*-test). One gel region (G2) was marginally higher in flash frozen samples ($0.10 > p > 0.05$, *t*-test). The staining intensity of this region (ca. 140 kD) appeared to be inversely related to the staining intensity in the region of 250 kD (G1), suggesting possible degradation of the 250 kD protein band(s) giving rise to 140 kD

products in flash frozen samples. This suggestion was supported by LC-MS/MS identification of proteins in these gel bands (see Discussion).

3.4.2 Protein identification by LC-MS/MS

The tryptic digests of the gel bands excised from liver and gill samples were subjected to LC-MS/MS, and the mass spectra were searched against actinopterygii fish reference sequences using the SEQUEST algorithm. Using this approach, 17 proteins were identified in seven gel bands from liver (Table 3.6). Many of the identified proteins are involved in carbohydrate metabolism, a well-known function of vertebrate liver. Identified carbohydrate metabolism enzymes include glycogen phosphorylase, fructose bisphosphate aldolase-B, triosephosphate isomerase, glyceraldehyde-3-phosphate dehydrogenase, phosphoglycerate kinase, enolase, and aconitase. In addition to proteins of carbohydrate metabolism, other identifications included proteins involved in protein synthesis (elongation factor alpha, nascent polypeptide associated complex alpha, ribosomal protein SA), cell structure (actin and keratin), and one-carbon metabolism (adenosyl homocysteinase). In gill, a total of 12 proteins were identified from four gel bands (Table 3.7). The proteins identified are involved in biological functions such as ion transport (Na^+/K^+ ATPase), cell structure (myosin heavy chain), stress (heat shock protein 9, heat shock cognate 70 kDa), and protein turnover (poly A binding protein, proteasome 26S subunit ATPase 3). Zebrafish hypothetical protein Zgc:73056 was identified in both liver and gill. BLAST performed on this unnamed protein showed that protein is likely to be form of alpha enolase [17, 18]. In support of this, enolase 3-2 was also identified in the same protein bands in liver and gill.

Table 3.6 LC-MS/MS protein identifications from 1D gel bands from *F. grandis* liver.

Band[a]	Protein Name	Peptides[b]	Species Matched	P (pro)	Score	M_r (kDa)	Accession No.
L1	aconitase 1	3	*Danio rerio*	4.81E-12	30.27	98.9	NP_001030155
L1	glycogen phosphorylase, liver	5	*Danio rerio*	1.65E-10	60.30	111.5	NP_001008538
L2	keratin 8	5	*Danio rerio*	1.57E-13	84.29	57.7	NP_956374
L3	adenosylhomocysteinase	6	*Danio rerio*	4.15E-13	78.34	47.9	NP_954688
L3	enolase 3-2	5	*Salmo salar*	7.06E-13	54.31	47.3	NP_001133193
L3	zgc:73056	5	*Danio rerio*	4.19E-12	84.30	47.3	NP_956989
L3	elongation factor 1-alpha	3	*Oryzias latipes*	4.32E-11	54.24	50.4	NP_001098132
L4	actin, cytoplasmic 1	14	*Salmo salar*	1.00E-30	302.36	41.8	NP_001116997
L4	enolase 3-2	3	*Salmo salar*	3.22E-14	22.34	47.3	NP_001133193
L4	zgc:73056	4	*Danio rerio*	8.16E-13	56.33	47.3	NP_956989
L4	ribosomal protein SA	3	*Danio rerio*	4.74E-11	30.28	34.0	NP_957346
L4	phosphoglycerate kinase 1	3	*Danio rerio*	1.46E-10	30.23	44.7	NP_998552
L5	actin, cytoplasmic 1	6	*Salmo salar*	6.44E-12	60.29	41.7	NP_001116997
L5	GAPDH	7	*Salmo salar*	4.55E-10	70.22	35.9	NP_001117033
L6	aldolase B, fructose-bisphosphate	4	*Salmo salar*	6.28E-12	50.25	39.2	NP_001117099
L6	nascent polypeptide-associated,alpha	3	*Danio rerio*	4.14E-11	40.24	23.4	NP_775371
L7	triosephosphate isomerase 1	6	*Danio rerio*	2.64E-10	70.26	26.8	NP_705954

[a] Band number corresponds to Figure 3.1 A, B.

[b] Peptide sequences and individual Xcorr score are in Appendix B.

Table 3.7 LC-MS/MS protein Identifications of 1D gel bands from *F. grandis* gill.

Band[a]	Protein Name	Peptides[b]	Species Matched	P(pro)	Score	M_r(kDa)	Accession
G1	myosin heavy chain larval type 2	5	*Oryzias latipes*	1.81E-13	76.31	221.5	NP_001155230
G1	myosin, heavy polypeptide 1.1, skeletal muscle	13	*Danio rerio*	3.56E-13	180.36	222.0	NP_001124138
G1	myosin, heavy polypeptide 10, non-muscle	2	*Danio rerio*	6.41E-11	30.29	228.9	XP_683046
G2	ATPase, Na+/K+ transporting, alpha 3b polypeptide	2	*Danio rerio*	1.33E-11	20.20	112.6	NP_571760
G2	myosin, heavy polypeptide 1.1, skeletal muscle	2	*Danio rerio*	2.32E-10	20.33	222.0	NP_001124138
G3	heat shock protein 9	2	*Danio rerio*	4.80E-11	32.22	73.9	NP_958483
G3	poly A binding protein, cytoplasmic 1 a	2	*Danio rerio*	5.41E-11	30.22	70.7	NP_001026846
G3	heat shock cognate 70 kDa protein	10	*Oncorhynchus mykiss*	9.89E-10	78.27	71.2	NP_001117704
G4	enolase 3-2	2	*Salmo salar*	8.75E-13	20.30	47.3	NP_001133193
G4	zgc:73056	5	*Danio rerio*	8.79E-11	46.29	47.3	NP_956989
G4	proteasome 26S subunit ATPase 3	3	*Oryzias latipes*	2.33E-10	50.22	47.8	NP_001153918
G4	elongation factor 1-alpha	2	*Oryzias latipes*	8.99E-10	20.24	50.4	NP_001098132

[a] Band number corresponds to Figure 3.1 G, H.

[b] Peptide sequences and individual Xcorr score are in Appendix B.

Out of a total of 29 proteins identified in the two tissues, 17 best matched proteins from *Danio rerio* (Zebrafish), 7 matched proteins from *Salmo salar* (black salmon), 4 matched proteins from *Oryzia latipes* (Japanese medaka), and one matched a protein from *Oncorhynchus mykiss* (rainbow trout). Nearly all of the identified proteins in both tissues had observed molecular weights in the gels (Tables 3.1, 3.2) within 20% of the predicted molecular weights for the intact proteins (Tables 3.6, 3.7). One notable exception was that myosin heavy chain (predicted M_r = 222 kDa) was identified as one of the gill proteins migrating at 140 kDa (G2), potentially as a result of partial proteolysis.

3.5 Discussion

One-dimensional gel electrophoresis and quantitative image analysis of five tissues of *F. grandis* demonstrate differences in the protein profile following two tissue sampling techniques: flash freezing in liquid nitrogen vs. immersion in RNA later®. Moreover, the approach that better preserved intact, high-molecular weight proteins differed among tissues. It is speculated that, whether the flash-freezing or RNA later® was more effective reflects a balance between the time to halt proteases during the initial sampling and the time required to completely homogenize the tissue. For liver and heart, the infiltration of the tissue by RNA later® may have taken more time than rapid freezing to inhibit endongenous proteases. Then, because of the soft consistency (liver) or small size (heart), homogenization in lysis buffer was rapid and thawing was minimal, thereby minimizing proteolyis during tissue lysis. Gill tissue, on the other hand, is comprised of thin sheets of tissue, the gill lamellae, supported by the bony gill arch. In this tissue, penetration by RNA later®, and protease inhibition, is expected to be quite fast. Tissue homogenization, however, of the gills took longer due to the presence of the gill arch. This delay would allow frozen tissues to thaw, albeit briefly, leading to partial proteolysis in flash frozen samples. The

longer homogenization time for gills would be less deleterious for samples taken in RNA later®, since the protein denaturant remains present during the homogenization process. The similarity in protein profiles of skeletal muscle and brain after both approaches for tissue sampling suggest equivalent protein stabilization by flash freezing and immersion in RNA later®. Other tissue specific factors, specifically the type and concentration of proteases, are also likely involved in determining which tissue sampling approach is better.

One observation from the analysis of gill tissue supports proteolysis as a major factor determining the difference in protein profiles between the two sampling approaches. The area of protein staining indicated as G2 was present in higher intensity in flash frozen samples, which based upon the intensities of other gel bands appeared to be more degraded than the corresponding samples in RNA later® (Figure 3.1, Table 3.2). Identification by LC-MS/MS of proteins in this band showed the presence of myosin heavy chain (Table 3.7), although the molecular weight estimate in 1D gel electrophoresis was only about 50% of the intact molecular weight. It has long been known that myosin heavy chain (220 - 230 kD) is cleaved into heavy meromyosin (ca. 130 kD) and light meromyosin (ca. 100 kD) by limited proteolytic digestion [19] In our gill samples, band G1 was identified as myosin heavy chain and had an estimated molecular weight of the intact polypeptide. In flash-frozen samples, the intensity of this band decreased and the intensity of band G2 increased, which had an estimated molecular weight nearer to the values expected for heavy meromyosin. Thus, its increased intensity in flash frozen samples is consistent with myosin proteolyis in the flash frozen gill samples.

Comparisons performed in adrenal tumor samples [20] and a pilot study involving rat kidney samples suggested that both storage methods are equal with regard to protein stabilization. However, in other experiments performed on rat brain snap-frozen heat dried

samples tissue samples stored at ambient conditions were shown to preserve protein integrity [21]. In mice spleen cells, 2D proteome analysis showed RNA later® as a better storage method to preserve proteins [10]. Our results with *F. grandis* tissues is in agreement with previous studies which suggest that type of storage method to preserve protein integrity depends on type of tissue under analysis. The use of RNA later® for protein preservation in tissues where it was equally or more effective than flash-freezing provides an alternative to the use of liquid nitrogen or other cryogens. This consideration might be particularly important in settings where availability, transport, or use of cryogens is difficult for logistical or safety concerns, for example in field or laboratory teaching settings.

Another aspect of this study that deserves mention is that LC-MS/MS was successfully used to identify proteins from an organism without a sequenced genome. The fish species used in this study (*F. grandis*) and its close relatives have been proposed as model systems for studies of environmental biology [13]. Herein, proteins were identified from 1D gels based upon matches to sequence data from other fish species. Identified proteins had between 2 and 14 peptides matching database sequences, there was good agreement between observed and predicted molecular weights, and all matches were highly significant ($p < 10^{-10}$). These observations suggest that these fish are amenable to proteomic analyses and support the use of these species as tractable models for environmental studies.

3.6 Conclusions

The degradation of proteins during sample preparation is a major concern in proteomic analyses. To address this problem we compared the protein profiles in 1D gels after two sampling approaches: freezing in liquid nitrogen and immersion of fresh tissues in RNA later®. The study shows that, in *F. grandis*, the method of tissue preservation was tissue specific: liver

and heart proteins were better preserved by flash freezing; gill proteins were better preserved in RNA later®; and brain and muscle proteins were equally well preserved by the two approaches. Furthermore, protein identifications using LC-MS/MS identified 17 proteins in liver and 12 proteins in gill involved in various physiological functions. These results demonstrate the utility of LC-MS/MS combined with database searching for reliable protein identification in a fish without a sequenced genome and support the use of *F. grandis* and its close relatives as model organisms for environmental proteomic studies in vertebrates.

3.7 References

1] Chu, W. S., Liang, Q., Liu, J., Wei, M.Q., Winters, M., Liotta, L., Sandberg, G., Gong, M., A nondestructive molecule extraction method allowing morphological and molecular analyses using a single tissue section. *Lab Investigations* 2005, 85, 1416-1428.

2] Perlmutter, M.A., Best, C.J.M., Gillespie, J.W., Gathright, Y., Gonzalez, S., Velasco, A., Linehan, W.M., Emmert-Buck, M.R., Chuaqui, R.F., Comparison of snap freezing versus ethanol fixation for gene expression profiling of tissue specimens. *Journal of Molecular Diagnostics* 2004, 6, 371-377.

3] Harris, R.J., Preservation of biological materials by freeze-drying. *Nature* 1951, 168, 851–853.

4] Boe, J., Greaves, R.I., Observations on the biological properties of B.C.G. treated by freeze drying. *Acta Tuberc. Scand.* 1950, 24, 38–46.

5] Hershko, A., Ciechanover, A., Mechanisms of intracellular protein breakdown. *Annual Review of Biochemistry* 1982, 51, 335-364.

6] Guo, T., Wang, W., Rudnick, P.A., Song, T., Li, J., Zhuang, Z., Weil, R.J., DeVoe, D.L., Lee, C.S., Balgley, B.M. Proteome analysis of microdissected formalin fixed and paraffin embedded tissue specimens. *J. Histochem. Cytochem*. 2007, 55, 763-772.

7] Allewell, N.M., Sama, A., The effect of ammonium sulfate on the activity of ribonuclease A. *Biochemica et Biophysica Acta* 1974,341, 484-488.

8] Lader, E.S., Methods and reagents for preserving RNA in cell and tissue samples. *US Patent* 2001, 6, 204, 375.

9] Rodrigo, M.C., Martin, D.S., Redetzke, R.A. and Eyster, K.M. A method for the extraction of high-quality RNA and protein from single small samples of arteries and veins preserved in RNA later. *Journal of Pharmacological and Toxicological Methods* 2002, 47, 87-92.

10] Nataliya, I.L., Dominic, M. D., Ivan, C. G., Two-dimensional gel electrophoresis characterization of the mouse leukocyte proteome, using a tri-reagent for protein extraction. *Proteomics* 2005, 5, 2202-2209.

11] Gillespie, J.W., Best, C.J.M., Bichsel, V.E., Cole, K.A., Greenhut, S.F., Hewitt, S.M., Ahram, M., Gathright, Y.B., et al., Evaluation of non-formalin tissue fixation for molecular profiling studies. *American Journal of Pathology* 2002,160, 449-457.

12] Jensen, F.B., Nikinmaa, M., Weber, R.E., Environmental perturbations of oxygen transport in teleost fishes: causes, consequences, and compensations. In: Rankin, J.C., Jensen, F.B. (Eds.), *Fish Ecophysiology. Chapman & Hall, New York* 1993, 161– 179.

13] Burnett, K.G., Bain, L.J., Baldwin, W.S., Callard, G.V., Cohen, S., Di Giulio, R.T., Evans, D.H., Gómez-Chiarri, M., Hahn, M.E., Hoover, C.A., *et al*., *Fundulus* as the premier teleost model in environmental biology:Opportunities for new insights using genomics. *Comparative Biochemistry and Physiology. Part D* 2007, 2, 257–286.

14] Laemmli, U.K. Cleavage of structural proteins during the assembly of the head of bacteriophage T4. *Nature* 1970, 227, 680-5.

15] Peisker. K., Application of neuhoff's optimized coomassie brilliant blue G250 [C. I. Acid Blue 90] ammonium sulphate-phosphoric acid protein staining to ultra-thin polyacrylamide gels on polyester films. *Electrophoresis* 1988, 5, 236-238.

16] Havlis, J., Thomas, H., Sebela, M., Shevchenko, A., Fast-response proteomics by accelerated in-gel digestion of proteins. *Analytical Chemistry* 2003, 75, 1300-1306.

17] Stephen, F. A., Thomas, L. M., Alejandro, A. S., Jinghui, Z., Zheng, Z., Webb, M., David, J. L., Gapped BLAST and PSI-BLAST: a new generation of protein database search programs. *Nucleic Acids Research* 1997, 25, 3389-3402.

18] Stephen, F., Altschul, J. C., Wootton, E. M., Richa, A., Aleksandr, M., Alejandro A. S., Yi-Kuo, Yu., Protein database searches using compositionally adjusted substitution matrices. *FEBS Journal* 2005, 272, 5101-5109.

19] Eckert, R.; Randall, R.; Augustine, G. *Animal physiology: Mechanisms and Adaptations*, Fifth Edition. ISBN 0-716-71937-1.

20] Johnsen, I.K., Hahner, S., Brière, J.J., Ozimek, A.., Gimenez-Roqueplo, A.P., Hantel, C., Adam, P., Bertherat, J., Beuschlein, F., Evaluation of a standardized protocol for processing adrenal tumor samples: Preparation for a european adrenal tumor bank. *Hormone Metabolism Research* 2010 42, 93-101.

21] Theodore R. S., Ani C. K., David R. H., Daniel, P.,Holschneider., Snap-frozen brain tissue sections stored with desiccant at ambient laboratory conditions without chemical fixation are resistant to degradation for a minimum of 6 Months. *Applied Immunohistochemistry Molecular Morphology* 2009, 17, 165–171.

Chapter 4

2DE-MALDI-TOF/TOF tandem MS for evaluation of protein expression patterns in tissues of the model fish species, *Fundulus grandis*

4.1 Abstract

Current proteome investigations use two dimensional gel electrophoresis (2DE) coupled with mass spectrometry (MS) to separate and identify proteins from complex mixtures. The technique of 2DE-MS was employed to investigate patterns of protein abundance in multiple tissues of *Fundulus grandis*, a small teleost fish that inhabits marshes of the Gulf of Mexico. Due to its high tolerance of physiochemical variation (e.g., temperature, oxygen, salinity) *F. grandis* presents itself as a model organism to study physiological and molecular adaptations to environmental stress. A total of 864 protein spots were excised from all the five tissues and 394 were identified for an identification rate of 46%. Out of 394 total spots, 253 were identified as non-redundant proteins. PANTHER functional annotation tool was used to categorize proteins into various molecular functions. PANTHER retrieved GO terms for 45% of the non-redundant proteins submitted for analysis.The proteins were categorized into various molecular functions including catalytic activity, structure molecule activity, binding and transport, etc. The 2DE maps and protein identifications provided by this work could be used as resources in future studies of protein expression in *F. grandis* and other fish exposed to environmental stressors and help to elucidate proteomic responses of vertebrates to environmental stress.

4.2 Introduction

During recent years, proteomics has emerged as a powerful tool for the study of biological systems. Proteome technologies are extensively being used for separation and characterization of highly complex protein mixtures [1]. Two dimensional polyacrylamide gel electrophoresis (2D-PAGE), followed by mass spectrometry (MS) or tandem mass spectrometry (MS/MS) is an effective method for quantitative analysis of complex protein mixtures. Proteomic approaches have been employed in fish biology to address several questions pertaining to fish that includes but not limited to physiology, development and effect of pollutants. However proteome studies in fish are still limited due to lack of genetic information available for the most fish under investigation [2].

The zebrafish or *Danio rerio*, a tropical freshwater fish belonging to the minnow family cyprinidae, is an important vertebrate model in scientific research for proteomic studies. The protein expression profiles of zebrafish whole embryos [3-6] and embryonic mesodermal cells and ectodermal cells [7] have been studied using 2DE MALDI-TOF/TOF. In addition, proteomic analyses have been done in single oocytes to demonstrate molecular variability between phenotypically similar oocytes of the same or different fish specimens [8]. In addition to understanding developmental processes, zebrafish have also been used as a model to test the effect of aquatic pollutants on the proteome of embryos [10] and adult liver and brain [11, 12]. Proteomics was used in zebrafish to establish the cytosolic proteome of the liver [13] and the gill [14] of adult fish and in more general physiological studies related to the changes in the skeletal muscle proteome under hypoxia [15].

Proteomics in non-model fish species have been reported in fish that were commercially important in aquaculture and in fish that serve as environmental reporters. The salmonids,

especially Atlantic salmon (*Salmo salar*) and rainbow trout (*Oncorhynchus mykiss*), are commercially important cultured fish. The effects of X-ray exposure on rainbow trout [16], viral infection and stress in Atlantic salmon [17, 18], and the effect of anoxia in crucian carp (*Carassius carassius*) have been investigated [19]. In another study, adult brain of the Atlantic salmon was used as an experimental model for neuronal tissue regeneration after injury [20]. Aquatic toxicology in non-model fish species used proteomics to monitor the exposure of heavy metals including cadmium in Japanese flounder (*Paralichthys olivaceus)* brain [21], zinc in rainbow trout (*Oncorhynchus mykiss)* gills [22], biological toxins in medaka (*Oryzias latipes)* liver [23], and undefined pollutant mixtures in goldfish *(Carassius auratus)* liver [24].

In all the above mentioned studies, the choice of technique was 2DE-MS or MS/MS though there were differences in type of instrumentation employed for experiments. Because of poorly characterized genomes for species other than zebrafish, MS/MS was preferred and the database search was improved by using peptide mass fingerprinting and MS/MS fragmentation data. The fish proteome reports published to date used a great variety of methods with similar protein identification rates. In all these studies the average identification rate was 57% [10, 18, 25- 27]. In general, more positive identifications are expected in methods that use zebrafish-specific databases. However, there are studies reported in literature where using similar proteomic tools, the protein identification rates are very similar for zebrafish [15], Atlantic salmon [20] or rainbow trout [28]. Currently, development of methods for the improvement of protein identification in non-model species is very active area of research in proteomics.

Fundulus is a diverse and widespread genus of small teleost fishes, with many related species inhabiting species inhabiting a wide range of aquatic habitats of North America. They are abundant, small in size, adaptive to various environments, and easy to maintain in lab. These fish

are exposed to various environmental fluctuations like salinity, temperature, pH and oxygen that occur on a regular basis in these habitats. *Fundulus* species thus present themselves as models to examine basic physiological processes and adaptations to environmental change [29]. Proteomic studies in *Fundulus* have been limited due to lack of sequenced genome. The availability of expressed sequence tags and cDNA made some microarray analyses possible to study individual variation in gene expression, affect of polymorphism on tissue-specific expression on cardiac physiology [30, 31]. Although a recent study examined variation in cardiac protein expression using two-dimensional difference gel electrophoresis (2D-DIGE) [32]. In this study, however, only a limited number of protein identifications were reported (< 50 out of > 600 spots).

The goal of current study is to investigate patterns of protein abundance in various tissues of *Fundulus grandis*, a small teleost fish that inhabits marshes of the Gulf of Mexico using two-dimensional gel electrophoresis (2DE) coupled with mass spectrometry (MS). Also, the study is aimed at employing gene ontology web-based tools to annotate molecular functions for the proteins identified from most abundant protein spots in the tissues of liver, skeletal muscle, brain, gill and heart. The 2DE maps and protein identifications provided by this work could be used as resources in future studies of protein expression in this and other fish exposed to environmental stressors and they can help to elucidate proteomic responses of vertebrates to environmental stressors.

4.3 Materials and methods

4.3.1 Fish maintenance and sample preparation

Fundulus grandis were purchased from a bait store and kept in 40 L aquaria at room temperature (22-26°C) in dechlorinated tap water adjusted to approximately 5 parts per thousand salinity with artificial sea salts (Instant Ocean). Water was aerated and filtered through charcoal

and biological filters. Fish were fed *ad libitum* with flake fish food once a day and were fasted 24 h immediately prior to dissection. Fish were sacrificed using an overdose of tricaine methanesulfonate (MS 222, 1g per L, pH buffered with 4g $NaHCO_3$). Prior to dissection, length, mass, and sex of the each fish were noted. For these analyses, only male fish were used. All animal research conducted in this study conformed to national and institutional guidelines for research on vertebrate animals protocol # UNO-10-001 (Appendix A).

Liver, skeletal muscle, heart, and brain were harvested by dissection from six or seven fish frozen immediately in liquid nitrogen. Gill tissues were preserved in RNA later®. For all tissues except hearts, samples of 20-50 mg were homogenized in glass-glass homogenizers (Kontes, Vineland, NJ, USA) in 500 µL lysis buffer containing 7 M urea, 2 M thiourea, 2% CHAPS, 1% ASB-14, 40 mM dithiothreitol (DTT). Hearts (5-10 mg total mass) were homogenized in 200 µL of lysis buffer. Tissue homogenates were made on ice and centrifuged at 2400 x *g* for 15 min at 4°C. The supernatants were stored at -80°C until further analysis. Protein concentrations of the supernatant solutions were determined using Amersham Biosciences 2D Quant kit (GE health care, Piscataway, NJ, USA).

4.3.2 One dimensional gel electrophoresis

After protein quantitation, samples of 20 µg protein were separated by one dimensional gel electrophoresis in 12.5% polyacrylamide (37.5: 1 acrylamide: bisacrylamide) minigels (8 cm x 10 cm x 1mm) according to Laemmli [33]. Prior to electrophoresis, samples were reduced with 100 mM DTT combined with 4x sample buffer (Bio-Rad, Hercules, USA), and heated at 95°C for 3 min. Electrophoresis was performed in 25 mM Tris, 192 mM glycine, and 0.1% SDS at 150 V for 2 h. Molecular weight markers (Precision Plus Protein Standards; Bio-Rad, Hercules, USA) were included in every gel.

4.3.3 Two dimensional gel electrophoresis

Protein equivalent to 600 µg was prepared for 2D electrophoresis by tricholoroacetic acid-deoxycholate/acetone precipitation [34] to remove excess salts and buffers and then resuspended in rehydration buffer containing 7 M urea, 2 M thiourea, 2 % CHAPS, 40 mM DTT, 0.5% IPG buffer and 1% bromophenol blue. First dimension (IEF) was performed using commercially available immobilized pH gradient (IPG) strips (GE health care, Piscataway, NJ, USA) with Ettan IPGphor II Isoelectric Focusing Unit (GE health care, Piscataway, NJ, USA). For tissues other than skeletal muscle samples were loaded on 13 cm 3-10 NL IPG strips by active rehydration overnight in a total volume of 250 µL. IEF was performed using a five step protocol: 30 V for 10 h (active rehydration); 500 V for 1h (linear); 1000 V for 1 h (gradient); 8000 V for 2 h 30 min (gradient); 8000 V for 55 min (linear). Total electrophoresis was performed at 20 kVh while the current was limited to 50 µA per strip. For skeletal muscle, protein was cup-loaded for first dimension electrophoresis. The IPG strips were rehydrated overnight in 250 µL of rehydration buffer containing destreak solution (12 µL in mL rehydration solution) without dithiothreitol. The sample was applied and IPG strips were focused in IEF following a three step protocol: 500 V for 1 min (gradient); 4000 V for 1 h 30 min (gradient); 8000 V for 1 h 50 min (linear). Total electrophoresis was performed at 8.8 kVh. Current was limited to 50 µA per strip. The IPG strips were frozen in -80°C until further analysis. Prior to second dimension electrophoresis the IPG strips were equilibrated for 10 min twice, first in equilibration buffer (6 M urea, 75 mM Tris HCl pH 8.8, 29.3% (v/v) glycerol, 2% SDS(w/v) containing 1% DTT followed by another 10 mins in equilibration buffer containing 2.5% iodoacetamide. Second dimension was SDS PAGE employing 1x Laemmli SDS electrophoresis buffer (25 mM Tris base, 192 mM glycine, 0.1% SDS buffer). Gels were 12.5% polyacrylamide

(37.5: 1 acrylamide: bisacrylamide) (16 cm x 18 cm x 1mm). The equilibrated IPG strips were fixed on the top of the gel using agarose sealing solution (25 mM Tris base, 192 mM glycine, 0.1% SDS, 0.5% agarose, 0.002% bromophenol blue). Second dimension gels were electrophoresed at 15 mA per gel for 15 mins followed by 60 mA per gel for 3 h at 25°C.

4.3.4 Staining and image analysis

After 2DE gels, were stained using modified Neuhoff's colloidal comassie protocol [35]. Gels were fixed overnight in 100 mL 50% ethanol: 3% phosphoric acid. Gels were then washed in three 30 min changes of 500 mL distilled water followed by staining in 300 mL of 34% methanol, 17% ammonium sulfate, 3% phosphoric acid, and 0.0066% comassie brilliant blue G-250 (SERVA, New York, USA). Gels were de-stained in water for three days and imaged using a GS 700 densitometer (BIORAD, Hercules, USA). The gels were then analyzed using PDQUEST ^{TM} 2D analysis software (BIORAD, Hercules, USA) for spot cutting. The most abundant 192 spots for liver, brain, gill and heart and 96 for skeletal muscle were excised from gels and subjected to trypsin digestion for identification by mass spectrometry.

4.3.5 Spot cutting, trypsin digestion and MALDI

The most abundant spots from PDQUEST^{TM} 2D analysis software were excised from the gels using EXQuest^{TM} spotcutter (BIORAD, Hercules, USA). The spots were collected in 96 well plates and trypsin digested using sequencing-grade trypsin (Promega, Madison, WI, USA) following the protocol from Investigator Progest^{TM} automatic trypsin digester (Genomic Solutions, MI, USA). The concentration of trypsin in each well was 130 ng. A saturated solution of α-cyano-4-hydroxycinnamic acid (CHCA) was prepared in 50:50 acetonitrile: water containing 0.1% TFA (matrix solution). The tryptic digests from 96 well plates was mixed with

equal volume of matrix solution (1:1) and a sample volume of 0.6 µL was spotted on MALDI plates. CHCA was obtained from Sigma (Aldrich, St.Louis, USA).

4.3.6 Mass spectrometry

The masses of the tryptic digested peptides were determined using MALDI-TOF/TOF. The MS and MS/MS spectra were acquired using 4800 MALDI-TOF/TOF mass spectrometer (Applied Biosystems, Foster City, CA) in the positive reflectron mode. The total accelerating voltage was (+) 20,000 V with a delay time of 510 ns. Peptide mass fingerprints were acquired using 400 laser shots in a mass range between m/z 800 and 4000. Two trypsin autolysis peaks at m/z 842 and 2211 were used as internal standards for MS calibration. The ten most intense peptide precursors were selected for MS/MS product ion acquisitions and the MS/MS spectra were acquired using 1000 laser shots.

4.3.7 Protein identifications

The MS spectra were transferred to GPS explorer software™ version 3.6 that used an underlying search algorithm of a locally installed copy of the Mascot software programs, version 2.1 (Matrix Science; http://www.matrixscience.com). The data were searched against the Actinopterygii fishes subset of the non-redundant sequences deposited with NCBI database (updated as of 14 July 2010). Parameters for MASCOT database search were set as follows: fixed modification = carbamidomethylation of cysteine residues; variable modification = oxidation of methione residues; maximum missed cleavages = 1; mass tolerance = 100 ppm; and MS/MS fragment tolerance = 0.5 Da. Significant matches from the search were determined from MASCOT score that is given by relation, Score = -10 x log [P] where P is probability of a match occurring by random chance. The spots identified as unknown proteins, were BLASTed [36] to determine potential homologous proteins.

4.3.8 GO annotation

Out of the total identified spots, non-redundant proteins were submitted to web-based GO annotation tool PANTHER, Protein ANalysis THrough Evolutionary Relationships [37]. The analysis was performed on non-redundant proteins using the gene ontology terms: Molecular function, Biological process and Cellular component. The GI accession numbers of identified proteins were uploaded on PANTHER software and the proteins were categorized based on molecular function in all five tissues. The distribution of proteins between different molecular function categories was demonstrated as pie-chart diagram using web- based tools available on PANTHER.

4.4 Results and Discussion

Proteins were separated on 2D gels and visualized with colloidal comassie blue stain. Representative 2D gel images of liver, skeletal muscle, brain, gill and heart of *F. grandis* (Figure 4.1) depict a well distributed protein profile in five tissues between pH ranges 3-10. Very slight streaking was observed in all the tissues that are most likely from impurities in the sample, which can interfere with focusing in the first dimension [38]. However streaking did not interfere with protein spot resolution and almost all the gels had well resolved spots. The colloidal comassie stained 2DE preparative gels in five tissues of *F. grandis* resolved more than ~ 600 spots in liver, more than ~ 400 spots in brain, gill and heart, and more than ~200 spots in skeletal muscle. The most abundant 192 spots from liver, brain gill and heart including 96 spots from skeletal muscle were excised from the preparative gels, trypsin digested and analyzed by MALDI-TOF/TO.

In *F. grandis* tissues, 96 spots (56%) from liver, 46 spots (47.9%) from skeletal muscle, 101 spots (52.6%) from brain, 67 spots (34.9%) from gill and 84 spots (43.8%) from heart were identified. A total of 864 spots were excised from all the five tissues and 394 spots were

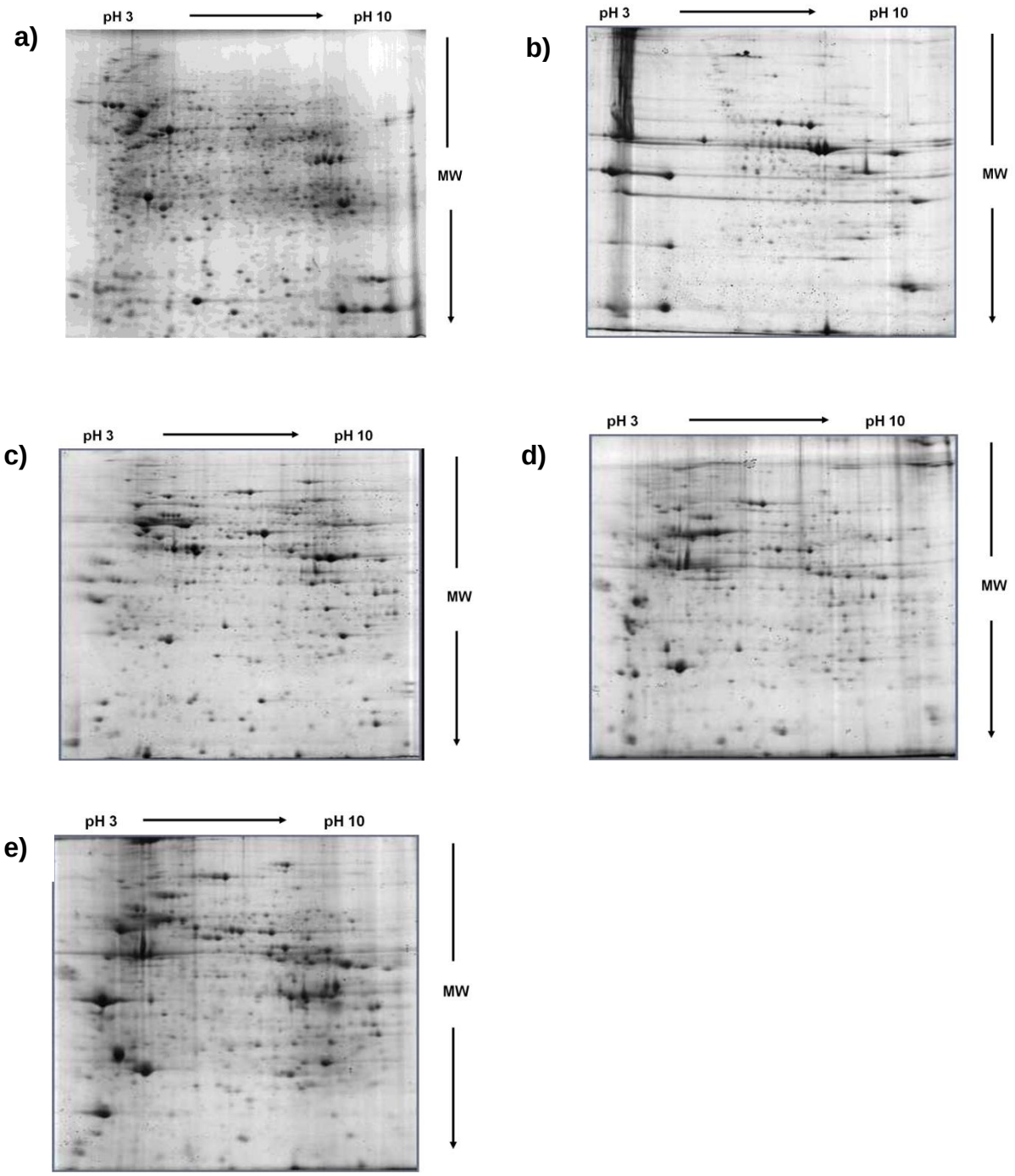

Figure 4.1 Representative preparative gel images of five tissues from *F. grandis* a) liver, b) skeletal muscle, c) brain, d) gill and e) heart. The gels were stained with colloidal comassie blue. Protein equivalent to ~600 µgms was loaded on each of the gels.

identified giving an identification rate of 46% (Appendix C). The proteins identified as hypothetical, predicted, novel, or by an alphanumeric code (e.g., Zebrafish Genome Collection [ZGC] proteins) were BLASTed to obtain potential homologs [36]. Most of the protein identifications were homologous to proteins of zebrafish (Danio rerio) than any other species and these accounted for 45% (178/394) of the identifications. However this expected result given the genome of zebrafish has been sequenced. The possible reasons for inability in identifying other proteins could be due to poor MS or MS/MS spectra that could not be characterized or lack of homologous proteins in actinopterygii database. In our experiments, the first 96 spots had average identification rates of 63% compared to an average of 27% identification rate for the next 96 most abundant spots. Therefore, major fractions of unidentified proteins are from second set of 96 spots that were lower in intensity and did not yield useful MS/MS spectra for further identifications.

Previously, Kling et al achieved 41% identification rate using 2DE MALDI-TOF/TOF in a zebrafish cell line [11]. In another study 2-DIGE MS/MS identified 8 out of 12 proteins in zebrafish liver [25] and 8 out of 31 proteins in zebrafish brain [12]. Bosworth et al reported 29 out of 40 protein identifications in zebrafish skeletal muscle [15]. In non-model fish species protein identification rates ranged from as low as 27% to as high as 90%. Similar identification rates were seen in *Salmosalar* (24/53) [20] and *Onchorhynkus mykiss* (19/33) [28]. In Chinese rare minnow (*Gobiocypris rarus*) liver using 2DE MALDI-TOF/TOF the investigators were able to identify 23 out of 84 proteins [39] and in *Sparus aurata* muscle 2DE MALDI-TOF/TOF identified 9 out of 10 proteins [40]. For non model species not many studies reported identifications in gill and heart using 2DE MALDI-TOF/TOF. The identification rates in our study are similar to those observed in other fish species including zebrafish. Thus, our data

Table 4.1 Protein identifications in tissues of *Fundulus grandis.*

Tissue	#Spots	# Identified	% ID	%Sequence coverage	Peptides matched
				Mean (Range)	**Mean (Range)**
Liver	192	96	50.0	24.83 (7-70)	9 (2-70)
Muscle	96	46	47.9	30.72 (6-60)	12 (4-23)
Brain	192	101	52.6	24.59 (4-49)	9 (1-24)
Gill	192	67	34.9	33.42 (4-70)	11 (1-26)
Heart	192	84	43.8	30.49 (4-70)	12 (2-50)

suggest potential use of 2DE MALDI-TOF/TOF to identify proteins in *F. grandis* even though its genome has not been sequenced.

Protein identifications were based on matches that had mascot scores greater than 61 proteins were identified with peptide matches ranging from a minimum of 1 peptide to a maximum of 70 peptides. Figure 4.2 is a frequency distribution of the number of matched peptides for the identified proteins from all the tissues of *F. grandis*. More than 90% of proteins were identified by 5-20 peptides. Figure 4.3 is frequency distribution of % sequence coverage for total identified proteins. The majority of proteins were identified by 15-45% sequence coverage. In our experiment, confidence on the goodness of protein identification method was derived from Mascot score, the number of peptides identified for the protein, and the coincidence of expected and measured pI and molecular weights. However, there is always a certain probability that the sequence had been wrongly identified, and thus typically a decoy database search is performed using identical search parameters, against a database in which the sequences have been reversed or randomized. The validation of protein identifications through decoy database search yielded a false discovery rate of 1.46% that corresponds to 13 spots out of 864 analyzed spots. The false discovery rate was within the range deemed to be acceptable (0.1% to 5%) [41, 42].

With 394 protein spots identified in five tissues, there was considerable redundancy among identifications. For example, more than five spots were annotated as muscle-type creatine kinase in skeletal muscle. These could represent post-translational modifications or degradation products of the same protein. To reduce redundancy in the dataset all those spots identified as muscle-type creatine kinase were considered to represent one non redundant protein. Accordingly, the numbers of non-redundant protein identifications were 52 in liver, 22 in skeletal muscle, 71 in brain, 54 in gill, and 51 in heart. Thus, the number of non-redundant

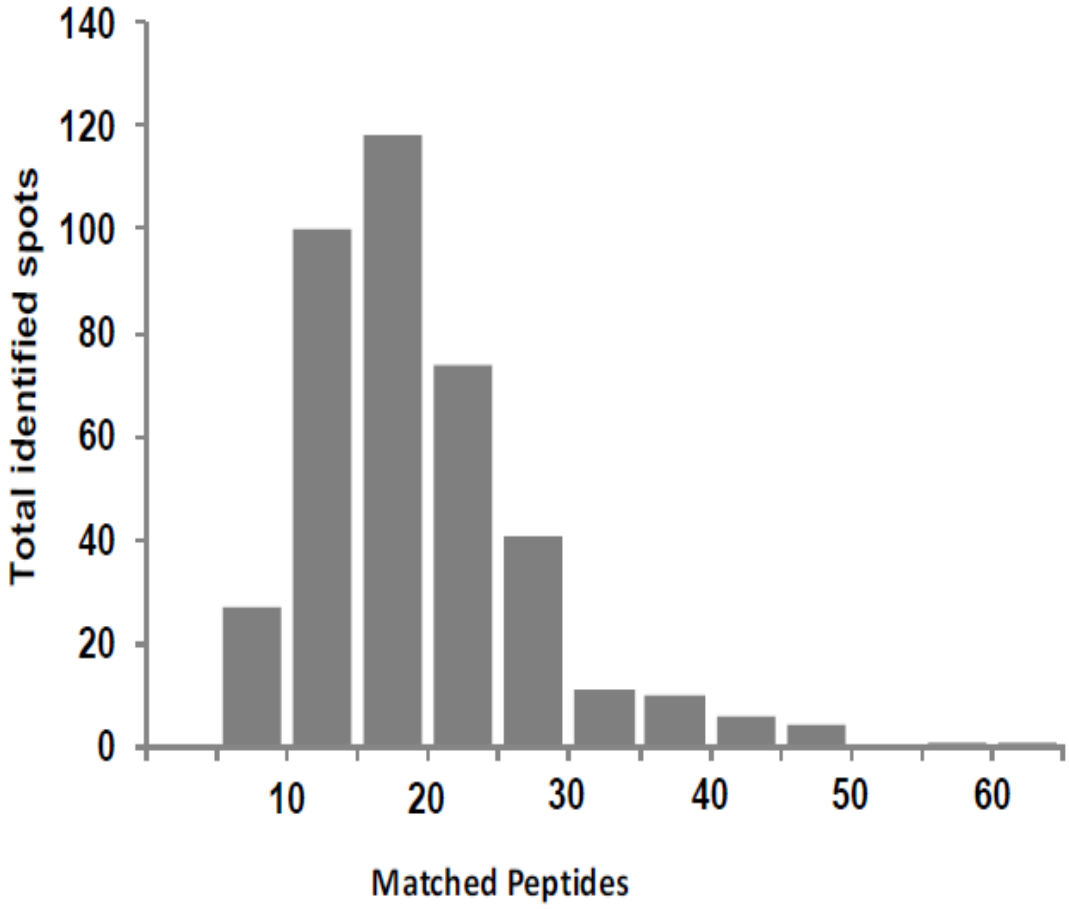

Figure 4.2 Frequency distribution histogram of peptides matched from protein identifications in tissues of *Fundulus grandis*. X-axis number of matched peptides, Y-axis total identified spots

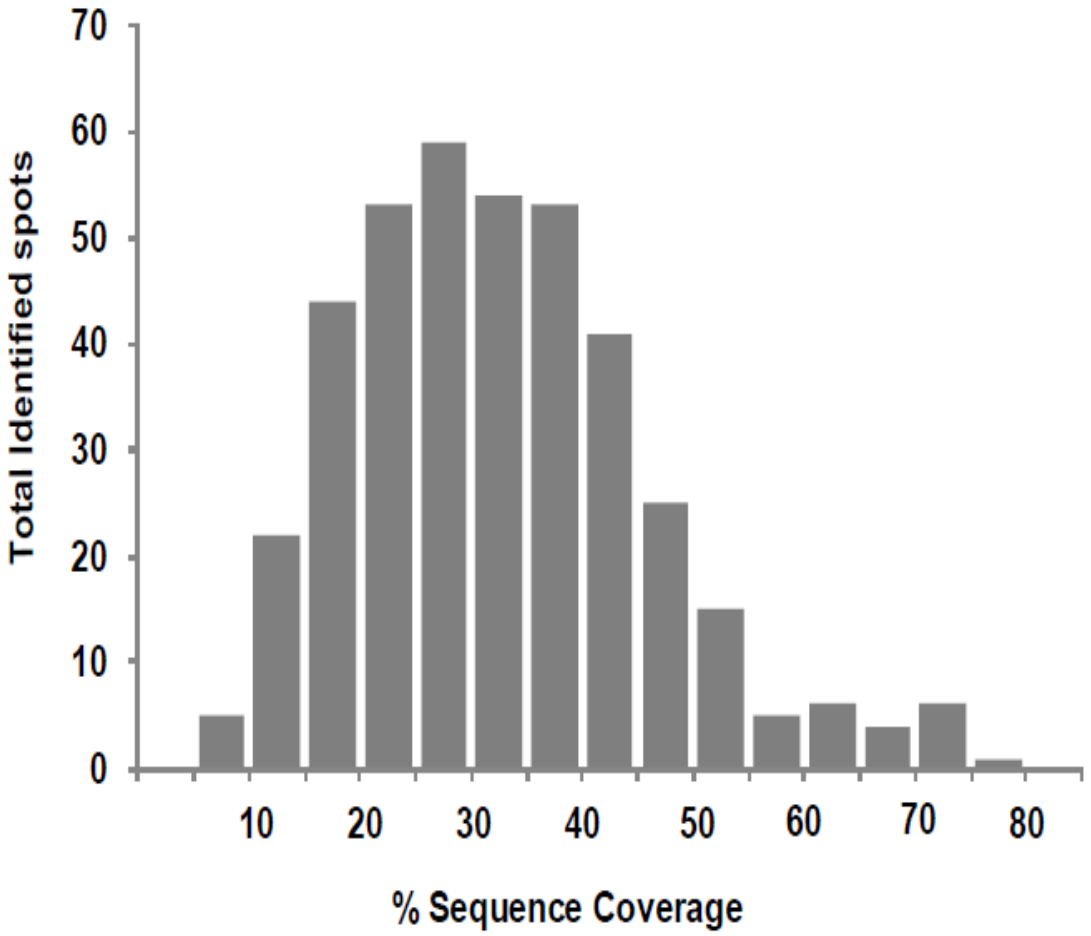

Figure 4.3 Frequency distribution histogram showing the % sequence coverage in five tissues of *Fundulus grandis*. X-axis number % sequence coverage, Y-axis total identified spots.

protein identifications was 253, which represents a conservative estimate of the number of proteins identified in these five tissues.

Still, with 253 proteins from five tissues, it was necessary to employ bioinformatic analyses to understand the potential functional relationships among this large and complex data set. Gene ontology annotations were done on the non-redundant proteins from five tissues using web-based functional annotation tool PANTHER that classifies genes by their molecular functions [37]. For the GO annotations, zebrafish homologs to 253 non-redundant proteins were obtained using Blink from pubmed. Zebrafish homologs were available for only 233 proteins. Of the 233 proteins submitted for analysis on PANTHER, GO annotations were retrieved for 106 proteins (45% of the non-redundant proteins). PANTHER was not able to annotate molecular function to all the proteins due to limitation in available GO annotations for zebrafish on web-based annotation tools. The output from GO analysis gives; GO term associated with the molecular function and percent of gene hits against total # function hits which is total number of genes mapped divided by total functional hits. The results of the ontology analyses for non-redundant proteins from five tissues are depicted as pie diagrams (Figure 4.4). In several cases, multiple proteins were identified matching a single GO term annotated to a particular molecular function and thus number of function hits are greater than total mapped genes. The results of these analyses show catalytic activity enzymes (light purple) as highest fraction of proteins in all tissues; however liver showed slightly greater fraction than other tissues which identifies the important molecular functions specific to liver. Motor activity proteins were identified as higher fraction in skeletal muscle that supports the important functions of muscle.

Table 4.2 List of non-redundant proteins identified from liver tissue in *F. grandis.*

Actin, Beta
Adenosylmethionine (S) synthase isoform type-1
Alanine-glyoxylate aminotransferase
Aldolase-B
Aminoacyl tRNA synthase complex-interacting multifunctional protein 1
Amylase-3 protein
ATP synthase beta subunit-like, mitochondrial
Betaine homocysteine methyltransferase
Calreticulin
Catalase
Cytochrome b-c1 complex subunit 1, mitochondrial
E1 protein 14-3-3
Endoplasmin
Enolase 1, (alpha)
Enolase, beta
Ferritin H3
Fructose-1,6-bisphosphatase 1
Fumarylacetoacetase
Glucose-regulated protein 78 kDa
Glutamate dehydrogenase 1
Glutathione peroxidase 1b
Glutathione-S-transferase, theta
Glyceraldehyde 3-phosphate dehydrogenase
Glycogen phosphorylase, liver form
Heart-type fatty acid-binding protein
Heat shock 60 kD protein 2
Hydroxyphenylpyruvate dioxygenase -4-
Interleukin-1 receptor-associated kinase, 4, similar to
Interleukin-1 receptor-like protein
Keratin 18
Lactate dehydrogenase B
Lengsin
Manganese-containing superoxide dismutase precursor
Methionine adenosyltransferase I, alpha
Myosin heavy chain
Peroxiredoxin 4-like
Phenylalanine hydroxylase
Phosphoenolpyruvate carboxykinase
Phosphoglycerate kinase 1
Polypeptide, beta
Profilin 2
Protein disulfide-isomerase

Table 4.2 Continued

Putative oncoprotein nm23
Rab6 interacting protein homolog family member (elks-1)-like
Reverse transcriptase
Squamous cell carcinoma antigen recognized by T-cells 3
Succinate-CoA ligase, GDP-forming beta subunit
Triosephosphate isomerase B
Trypsin
Tryptophan hydroxylase 1, non-neuronal
Tubulin, alpha
Zinc finger SWIM domain-containing protein KIAA0913

Table 4.3 List of non-redundant proteins identified from muscle tissue in *F. grandis*

Actin (F) capping protein, alpha-1 subunit
Actin, Alpha, skeletal
Adenylate kinase
Creatine kinase CKM2 , muscle-type
Creatine kinase, brain
Creatine kinase-like,sarcomeric mitochondrial
Enolase 1, (alpha)
Enolase, Beta
Fructose-bisphosphate aldolase A
Glyceraldehyde 3-phosphate dehydrogenase
Isocitrate dehydrogenase 2 (NADP+), mitochondrial
Myosin binding protein H-like
Myosin, light polypeptide 2, skeletal muscle
PDZ and LIM domain protein 7 isoform a
Phosphoglycerate mutase 2 (muscle)
Triosephosphate isomerase B
Tropomyosin1-1 , skeletal muscle
Troponin putative fast skeletal muscle
Troponin T3b, skeletal, fast isoform 2
Warm temperature-acclimated 65kDa protein

Table 4.4 List of non-redundant proteins identified from brain tissue in *F. grandis*

Aconitate hydratase, mitochondrial
Actin , beta
Adenylate kinase
ATP synthase beta subunit-like,Mitochondrial
ATP synthase subunit alpha, mitochondrial
ATPase B subunit, V-type
ATPase subunit A (V-)
Brain-type fatty acid binding protein
Carbonic anhydrase, Cytoplasmic
Cofilin 2, like
Creatine kinase
Creatine kinase, brain
Dihydrolipoamide succinyltransferase
Dihydrolipoyllysine-residue succinyltransferase component
of 2-oxoglutarate dehydrogenase complex, mitochondrial
Dihydropyrimidinase-like 5
Dj-1 protein
Enolase , Gamma
Enolase 1, alpha
Enolase 2
Enoyl-CoA hydratase, mitochondrial
Fascin
Fructose-bisphosphate aldolase C
Fumarate hydratase precursor
Gefiltin
Gfap protein
Glial fibrillary acidic protein
Glutamate dehydrogenase 3
Glutamate oxaloacetate transaminase 2
Glutamine synthetase
Glyceraldehyde-3-phosphate dehydrogenase
Heat shock 60 kD protein 1
heat shock cognate 71
Heterogeneous nuclear ribonucleoprotein A0
HSP70
Intermediate filament protein , class III
Internexin neuronal intermediate filament protein, alpha
Isocitrate dehydrogenase NADP , mitochondrial
Isocitrate dehydrogenase 3 (NAD+) alpha, Similar to
Lactate dehydrogenase B
Malate dehydrogenase A,Cytosolic
Malate dehydrogenase, mitochondrial
Manganese-containing superoxide dismutase precursor

Table 4.4 Continued

Monooxygenase-3-/tryptophan 5-monooxygenase activation protein, gamma polypeptide
NSFL1 cofactor p47
Oncoprotein nm23, putative
Peroxiredoxin-2
Phosphatidylethanolamine binding protein
Phosphoglycerate kinase
phosphoglycerate kinase 1
Pkm2 protein
Prohibitin
Proteasome alpha 1 subunit, similar to
Proton ATPase subunit E 1 V-type
Psma2 protein
Pyruvate dehydrogenase E1 alpha 1
Stress-70 protein, mitochondrial
Succinyl-CoA ligase GDP-forming subunit alpha, mitochondrial
Synaptosome-associated protein 25a
Synuclein , gamma1-
Thioredoxin-dependent peroxide reductase, mitochondrial
Triosephosphate isomerase A
Tubulin ,alpha
Tubulin beta-2A chain
Tubulin,beta
Tubulin-4, alpha 8 like
Valosin containing protein
Voltage-dependent anion-selective channel protein 1
Warm temperature-acclimated 65kDa protein

Table 4.5 List of non-redundant proteins identified from gill tissue in *F. grandis*

Actin, alpha, cardiac muscle 1a
Actin, beta
Actin, skeletal alpha
Actin-F-capping protein subunit beta
Adenylate kinase
Adenylyl cyclase-associated protein 1
Aldolase A
ATP synthase,F1, beta subunit
Calmodulin-A= Full; Short=CaM A
Condensin-2 complex subunit D3
Coronin-1A
Creatine kinase CKM2, muscle-type
Creatine kinase,Muscle-type
Cytokeratin type I , enveloping layer, like
Cytoplasmic carbonic anhydrase
Domain-containing protein 1, COMM
Enolase 1 isoform b
Enolase 3-2
Fructose-bisphosphate aldolase C
Glucose-regulated protein, 78 kDa
Glyceraldehyde-3-phosphate dehydrogenase
Heat shock cognate 70
Heat shock protein 60
Heat shock protein Hsp27 , low molecular weight
Heterogeneous nuclear ribonucleoprotein A/B ,
Hypothetical protein LOC100124602
Keratin 18
Keratin E3-like protein, type II
Keratin, type II cytoskeletal 8
Krt4 protein
Lactate dehydrogenase B
Malate dehydrogenase, mitochondrial
Myosin, heavy polypeptide 10,non-muscle
Myosin, light polypeptide 2, skeletal muscle
Nuclease diphosphate kinase B
Nucleoside diphosphate kinase
Peroxiredoxin-1
Phosphoglycerate kinase 1
Proteasome 20S, beta subunit
Proteasome subunit alpha type 2
Proteasome subunit alpha type-4
Proteasome subunit alpha type-6
Protein kinase C, receptor for activated
Pyruvate kinase muscle isozyme

Table 4.5 Continued

Serine/cysteine proteinase inhibitor
Triosephosphate isomerase B
Tropomyosin 3 isoform
Tropomyosin, slow myotomal muscle
Tropomyosin2
Tropomyosin4-1
Tubulin beta-1 chain
Tubulin, alpha 8 like 3-1
Uracil phosphoribosyltransferase homolog; RecName: Full
Warm temperature acclimation-related 65kDa protein

Table 4.6 List of non-redundant proteins identified from heart tissue in *F. grandis*

Aconitate hydratase, mitochondrial
Actin, fast myotomal muscle
Actin, skeletal alpha-
Acyl-CoA dehydrogenase, mitochondrial isoform 1, medium-chain specific
Adenylate kinase
Aldolase A fructose-bisphosphate
ATP synthase beta subunit-like, mitochondrial
ATP synthase subunit alpha, mitochondrial
Creatine kinase brain isoform
Creatine kinase-like, sarcomeric mitochondrial
Cytochrome b-c1 complex subunit 1, mitochondrial
Desmin;TPA:
Dihydrolipoyl dehydrogenase, mitochondrial
Dystrophin, putative
Enolase 1, (alpha)
Enolase, beta
Enoyl-CoA hydratase, mitochondrial
Fructose-bisphosphate aldolase C
Fumarate hydratase precursor
Glial fibrillary acidic protein; GFAP
Glutamate dehydrogenase 3
Glutamate oxaloacetate transaminase 2
Glyceraldehyde-3-phosphate dehydrogenase
Heat shock 60 kD protein 1
Heat shock cognate 71
HSP70
Hydroxyacyl-coenzyme A dehydrogenase, mitochondrial
Isocitrate dehydrogenase 3 ,(NAD+) alpha, Similar toE6
Isocitrate dehydrogenase NADP , mitochondrial
Keratin
Ketoacyl (3-)-CoA thiolase, mitochondrial
Lactate dehydrogenase B
Lectin , C-type
Malate dehydrogenase, mitochondrial
Manganese superoxide dismutase
Methylmalonate-semialdehyde dehydrogenase acylating , mitochondrial
Myosin, light chain 6, alkali, smooth muscle and non-muscle like
NADH dehydrogenase ubiquinone iron-sulfur protein 3, mitochondrial
Nuclear ribonucleoprotein A/B isoform 1, heterogeneous
Phosphoglycerate kinase 1
Phosphoglycerate mutase 2 (muscle)
Pkm2 protein
Prohibitin
Transferrin variant A
Transferrin, putative

Table 4.6 Continued
Triosephosphate isomerase B
Tropomyosin , cardiac
Tubulin, beta
Ubiquinol-cytochrome c reductase core I protein
Uncoupling protein 3, mitochondrial
Warm-temperature-acclimation-related-65kDa- protein-like-protein

The tissues were different from each other in terms of diversity in molecular functions. Out of five tissues, brain was the most complex as demonstrated by the greatest number pie wedges compared to other tissues (Figure 4.4). Complexity of brain was greater than gill, and gill was greater than heart. The tissues of heart and liver showed similar pattern of diversification for molecular functions. Muscle was least complex of all the tissues which again support the 2D gel image of muscle that demonstrated comparatively simple protein profile than other tissues. It should be noted that the GO annotations retrieved are for identifications of the most abundant protein spots from the gel.The inability in retrieving GO annotations for remaining 55% proteins is due to limitations associated with web-based GO annotation tools. First, the existing annotation databases are incomplete and for all sequenced organisms only a subset of known genes are functionally annotated [43]. Electronically only 25% of gene annotations are available for *Danio rerio* [44]. Also some of the information may not be precise because it is not experimentally verified. Second, the GO analysis is limited to those categories present in database because GO cannot annotate function if the functional category is not available in database. Third, a single process might appear more significant in the results if the genes associated with that biological process are annotated more than the others [45].

A)

Liver 31 Genes; 26 Function hits

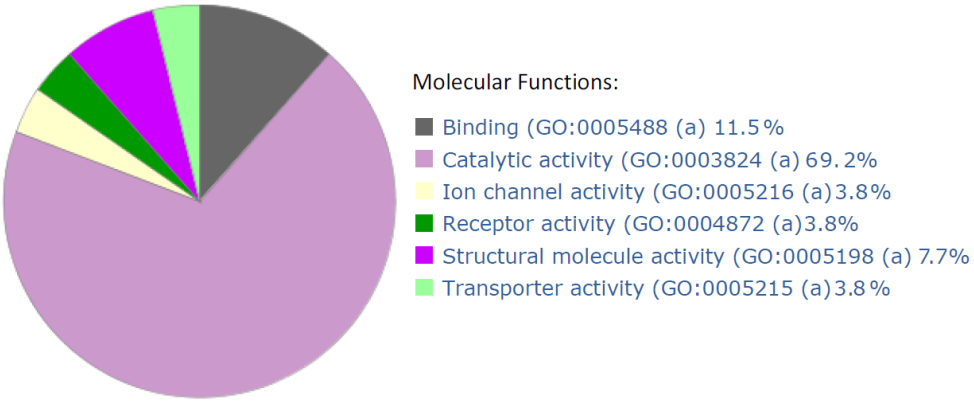

B)

Muscle 12 Genes; 18 Function hits

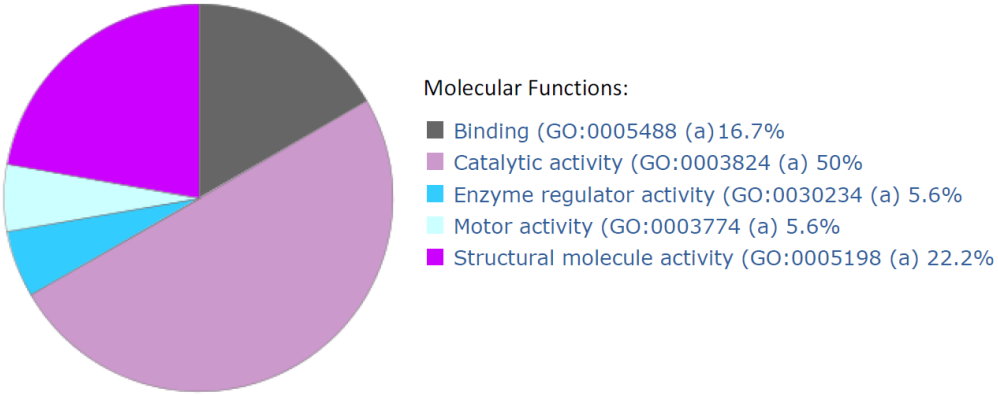

C)

Brain 48 Genes; 69 Function hits

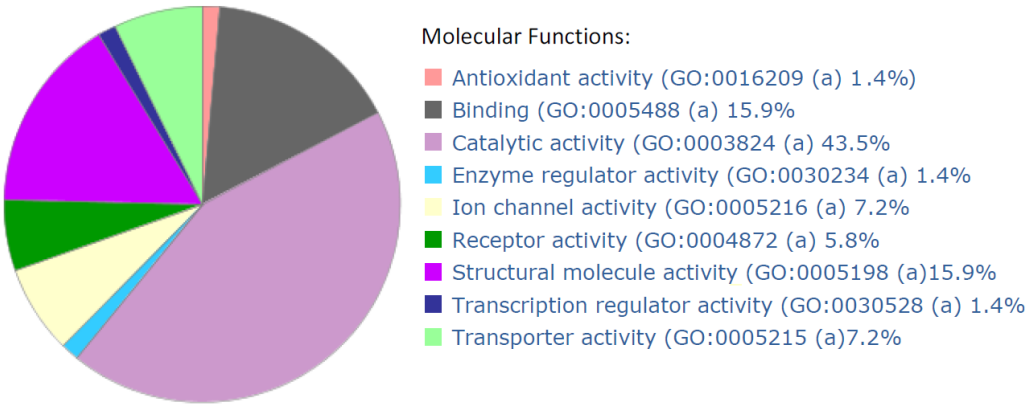

D)

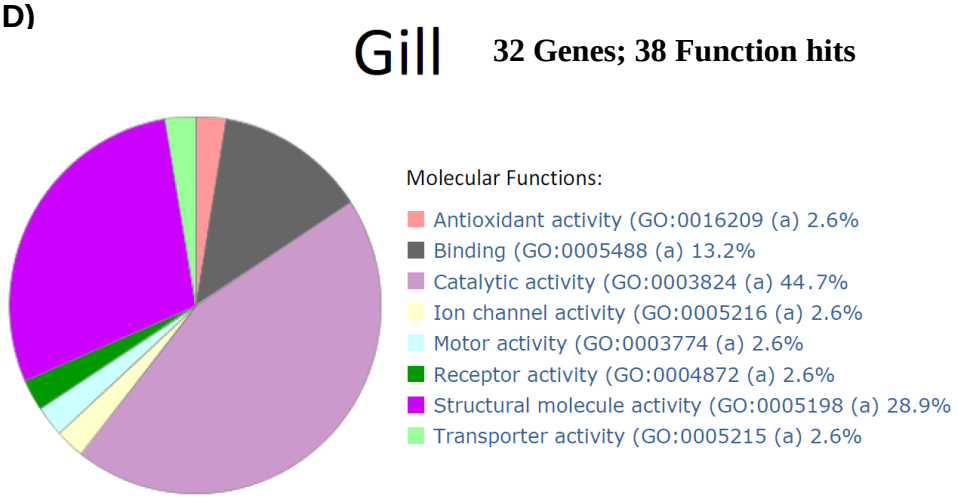

E)

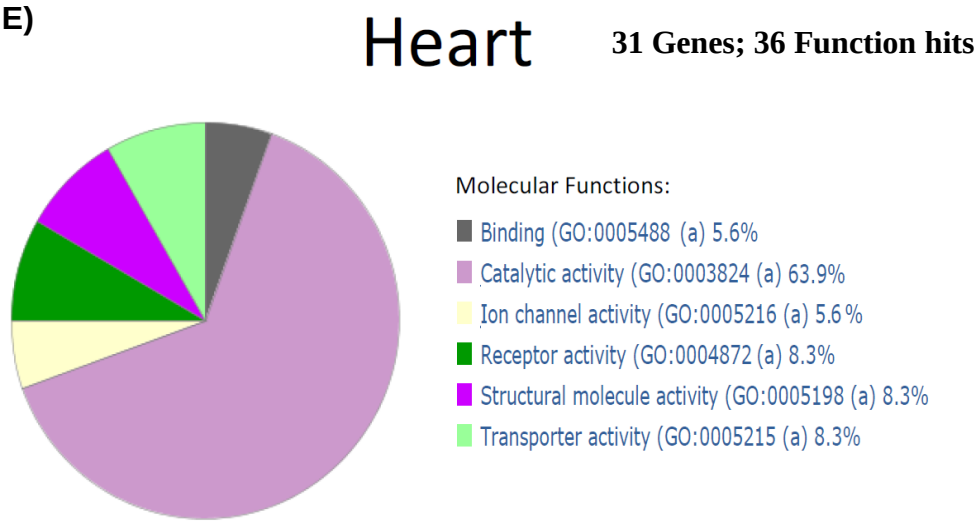

Figure 4.4 Gene ontology analyses of five tissues of *F. grandis* A) liver, B) muscle, C) brain, D) gill, E) heart. The pie charts depict the molecular function annotation of identified proteins. a) Percent of gene hit against total # genes; b) percent of gene hit against total # function hits.

4.5 Conclusions

In this study, large-scale proteome profile was presented in tissues of liver, skeletal muscle, brain, gill and heart of a teleost fish *F. grandis* tissue using 2DE MALDI-TOF/TOF. Previously, using 2DE MALDI-TOF/TOF in other fish species investigators achieved 45% identification rate in *Salmosalar* [19] , 58% in *Onchorhynkus mykiss*, [28] 30% in *Gobiocyprus rarus* liver [39] , and 46% in *Carassus auratus* liver [24]. The results thus demonstrate comparable protein identification rates of *F. grandis* to other fish species using similar proteomic tools. The proteins were identified with an estimated false-positive matching rate of 1.46% in fish without a sequenced genome. However there is gap in knowledge associated with GO annotations that highlight the need for improved bioinformatics. Despite the limitations, the coverage of protein identifications in a fish with unsequenced genome suggests that *Fundulus* species may serve as models for environmental proteomic studies. Though there is a need to focus on refining the technique for improved protein identification rate and GO annotations, the study presents the utility of 2DE MALDI-TOF/TOF to investigate patterns of protein abundance in various tissues of *F. grandis*. The 2DE maps and protein identifications along with GO annotations provided by this work could be used as resources in future studies of protein expression in this and other fish exposed to environmental stressors and help to elucidate proteomic responses of vertebrates to environmental stress.

4.6 References

1] Aebersold, R., Mann, M., Mass spectrometry-based proteomics. *Nature* 2003, 422,198-207.

2] Martyniuk, C. J., Denslow, N. D., Towards functional genomics in fish using quantitative proteomics. *General and Comparative Endocrinology* 2009, 164, 135-141.

3] Tay, T. L., Lin, Q., Seow, T. K., Tan, K. H. *et al.*, Proteomic analysis of protein profiles during early development of the zebrafish, *Danio rerio*. *Proteomics* 2006, 6, 3176–3188.

4] Lucitt, M. B., Price, T. S., Pizarro, A., Wu, W. *et al*., Analysis of the zebrafish proteome during embryonic development. *Mol. Cell. Proteomics* 2008, 7, 981–994.

5] Lemeer, S., Jopling, C., Gouw, J., Mohammed, S. *et al.*, Comparative phosphoproteomics of zebrafish fyn/yes morpholino knockdown embryos. *Mol. Cell. Proteomics* 2008, 7, 2176–2187.

6] Lemeer, S., Ruijtenbeek, R., Pinkse, M. W. H., Jopling, C.*et al.*, Endogenous phosphotyrosine signaling in zebrafish embryos. *Mol. Cell. Proteomics* 2007, 6, 2088–2099.

7] Link, V., Carvalho, L., Castanon, I., Stockinger, P. *et al*., Identification of regulators of germ layer morphogenesis using proteomics in zebrafish. *J. Cell Sci.* 2006, 119, 2073–2083.

8] Ziv, T., Gattegno, T., Chapovetsky, V., Wolf, H. *et al.*, Comparative proteomics of the developing fish (zebrafish and gilthead seabream) oocytes. *Comp. Biochem. Physiol.D Genomics Proteomics* 2008, 3, 12–35.

9] Knoll-Gellida, A., Andre, M., Gattegno, T., Forgue, J. *et al.*, Molecular phenotype of zebrafish ovarian follicle by serial analysis of gene expression and proteomic profiling, and comparison with the transcriptomes of other animals. *BMC Genomics* 2006, 7, 46, 1-28.

10] Undel, G., Benndorf, D., von Bergen, M., Altenburger, R.et al., Vitellogenin cleavage products as indicators for toxic stress in zebra fish embryos: a proteomic approach. *Proteomics* 2007, 7, 4541–4554.

11] Kling, P., Forlin, L., Proteomic studies in zebrafish liver cells exposed to the brominated flame retardants HBCD and TBBPA. *Ecotoxicol. Environ. Saf.* 2009, 7, 1985–1993.

12] Damodaran, S., Dlugos, C. A., Wood, T. D., Rabin, R. A., Effects of chronic ethanol administration on brain protein levels: a proteomic investigation using 2-D DIGE system. *Eur. J. Pharmacol.* 2006, 547, 75–82.

13] Wang, N., MacKenzie, L., De Souza, A. G., Zhong, H. et al., Proteome profile of cytosolic component of zebrafish liver generated by LC-ESI MS/MS combined with trypsin digestion and microwave-assisted acid hydrolysis. *J. Proteome Res.* 2006, 6, 263–272.

14] De Souza, A. G., Maccormack, T. J., Wang, N., Li, L., Goss,G. G., Large-scale proteome profile of the zebrafish (*Danio rerio*) gill for physiological and biomarker discovery studies. *Zebrafish* 2009, 6, 229–238.

15] BosworthIV, C. A., Chou, C. W., Cole, R. B., Rees, B., Protein expression patterns in zebrafish skeletal muscle: initial characterization and the effects of hypoxic exposure. *Proteomics* 2005, 5, 1362–1371.

16] Smith, R. W., Wood, C. M., Cash, P., Diao, L. *et al.*, Apolipoprotein AI could be a significant determinant of epithelial integrity in rainbow trout gill cell cultures: a study in functional proteomics. *Biochim. Biophys. Acta* 2005, 1749, 81–93.

17] Booy, A. T., Haddow, J. D., Ohlund, L. B., Hardie, D. B. *et al*., Application of isotope coded affinity tag (ICAT)analysis for the identification of differentially expressed proteins following infection of atlantic salmon (*Salmo salar*) with infectious hematopoietic necrosis virus (IHNV) or *Renibacterium salmoninarum* (BKD). *J. Proteome Res.* 2005, 4, 325–334.

18] Martin, S. A. M., Mohanty, B. P., Cash, P., Houlihan, D. F. *et al*., Proteome analysis of the Atlantic salmon (*Salmo salar*) cell line SHK-1 following recombinant IFN-gamma stimulation. *Proteomics* 2007, 7, 2275–2286.

19] Smith, R. W., Cash, P., Ellefsen, S., Nilsson, G. E., Proteomic changes in the crucian carp brain during exposure to anoxia. *Proteomics* 2009, 9, 2217–2229.

20] Zupanc, M. M., Wellbrock, U. M., Zupanc, G. K. H., Proteome analysis identifies novel protein candidates involved in regeneration of the cerebellum of teleost fish. *Proteomics* 2006, 6, 677–696.

21] Zhu, J.-Y., Huang, H.-Q., Bao, X.-D., Lin, Q.-M. *et al*., Acute toxicity profile of cadmium revealed by proteomics in brain tissue of *Paralichthys olivaceus*: potential role of transferrin in cadmium toxicity. *Aquat. Toxicol.* 2006, 78,127–135.

22] Hogstrand, C., Balesaria, S., Glover, C. N., Application of genomics and proteomics for study of the integrated response to zinc exposure in a non-model fish species, the rainbow trout. *Comp. Biochem. Physiol. B Biochem. Mol.Biol.* 2002, 133, 523–535.

23] Mezhoud, K., Praseuth, D., Puiseux-Dao, S., Franc-ois, J. C.*et al.*, Global quantitative analysis of protein expression and phosphorylation status in the liver of the medaka fish (*Oryzias latipes*) exposed to microcystin-LR. *Aquat.Toxicol.* 2008, 86, 166–175.

24] Wang, J., Wei, Y., Wang, D., Chan, L. *et al*., Proteomic study of the effects of complex environmental stresses in the livers of goldfish (*Carassius auratus*) that inhabit Gaobeidian Lake in Beijing, China. *Ecotoxicology* 2008, 17, 213–220.

25] De Wit, M., Keil, D., Remmerie, N., Ven, K. v. d., *et al.*, Molecular targets of TBBPA in zebrafish analyzed through integration of genomic and proteomic approaches. *Chemosphere* 2008, 74, 96-105.

26] Wulff, T., Hoffmann, E. S., Roepstorff, P., Jessen, F.,Comparison of two anoxia models in rainbow trout cells by a 2-DE and MS/MS-based proteome approach. Proteomics 2008, 8, 2035–2044.

27] Rime, H., Guitton, N., Pineau, C., Bonnet, E. et al., Postovulatory ageing and egg quality: A proteomic analysis of rainbow trout coelomic fluid. *Repr. Biol. Endocr*. 2004, 2, 26.

28] Wulff, T., Jessen, F., Roepstorff, P., Hoffmann, E.S., Long term anoxia in rainbow trout investigated by 2-DE and MS/MS. P*roteomics* 2008, 8, 1009–1018.

29] Burnett, K. G., Bain, L. J., Baldwin, W. S., Callard, G. V., *et al.*, *Fundulus* as the premier teleost model in environmental biology: Opportunities for new insights using genomics. *Comparative Biochemistry and Physiology Part D: Genomics and Proteomics* 2007, 2, 257-286.

30] Oleksiak, M.F., Roach, J.L., Crawford, D.L., Natural variation in cardiac metabolism and gene expression in *Fundulus heteroclitus*. *Nat. Genet.* 37, 2005, 67–72.

31] Whitehead, A., Crawford, D.L., Variation within and among species in gene expression: raw material for evolution. *Mol. Ecol.* 2006, 15, 1197–1211.

32] Rees, B. B., Andacht, T., Skripnikova, E., Crawford, D. L., Population proteomics: Quantitative variation within and among populations in cardiac protein expression. *Molecular Biology and Evolution* 2011, 28, 1271-1279

33] Laemmli, U.K. Cleavage of structural proteins during the assembly of the head of bacteriophage T4. *Nature* 1970, 227, 680-685.

34] Damerval, C., De Vienne, D., Zivy, M., Thiellement, H., Technical improvements in two-dimensional electrophoresis increase the level of genetic variation detected in wheat-seedling proteins. *Electrophoresis* 1986, *7*, 52-54.

35] Peisker. K., *Electrophoresis* 1988, 5, 236-238.

36] Altschul, S.F., Gish, W., Miller, W., Myers, E.W. & Lipman, D.J. Basic local alignment search tool. *J. Mol. Biol.* 1990, 215, 403-410.

37] Mi, H., Lazareva-Ulitsky, B., Loo, R., Kejariwal, A., *et al.*, The PANTHER database of protein families, subfamilies, functions and pathways. *Nucleic Acids Research* 2005, *33*, D284-D288.

38] Görg, A., Obermaier, C., Boguth, G., Harder, A., *et al.*, The current state of two-dimensional electrophoresis with immobilized pH gradients. *Electrophoresis* 2000, 21, 1037-1053.

39] Zhong, X., Xu, Y., Liang, Y., Liao, T., Wang, J., The Chinese rare minnow (Gobiocypris rarus) as an in vivo model for endocrine disruption in freshwater teleosts: a full life-cycle test with diethylstilbestrol. *Aquatic Toxicology* 2005, 71, 85-95.

40] Schiavone, R., Zilli, L., Storelli, C., Vilella, S., Identification by proteome analysis of muscle proteins in sea bream *Sparus aurata European Food Research and Technology* 2008, 227, 1403-1410.

41] Reiter, L., Claasen, M., Schrimpf, S. P., Jovanovic, M. *et al.*, Protein identification false discovery rates for very large proteomics datasets generated by tandem mass spectrometry. *Mol. Cell. Proteomics* 2009, 8, 2405–2417.

42] Huber, L. A., Is proteomics heading in the wrong direction? *Nat. Rev. Mol. Cell Biol.* 2003, 4, 74–80.

43] King, O. D., Foulger, R. E., Dwight, S. S., White, J. V., Roth, F. P., Predicting gene function from patterns of annotation. *Genome Research* 2003, 13, 896-904.

44] Lomax, J., Get ready to GO! A biologist's guide to the Gene Ontology. *Briefings in Bioinformatics* 2005, 6, 298-304.

45] Khatri, P., Drăghici, S., Ontological analysis of gene expression data: current tools, limitations, and open problems. *Bioinformatics* 21, 3587-3595.

Chapter 5

Conclusions

The dissertation focuses on the use of traditional enzymatic methods and the development and application of current proteomic approaches in *F. heteroclitus and F. grandis*. Initially the temporal effects of oxygen treatments on the maximal specific activities of nine glycolytic enzymes were measured under chronic exposure (28 d) in *Fundulus heteroclitus* (chapter 2). The study demonstrated that chronic hypoxia alters the capacity for carbohydrate metabolism in *F. heteroclitus*, with the important explanation that the responses are both tissue- and enzyme-specific. The measurements suggested significant oxygen effects and interaction between oxygen and duration effects on few, but not all the glycolytic enzymes. The effects were not uniformly distributed between the two tissues studied, as well as within the glycolytic enzymes. In general trends towards increased enzyme activities in liver and decreased enzyme activities in muscle were observed. Interestingly, the effects of duration of exposure on glycolytic enzyme specific activities showed a general trend towards increased glycolytic enzyme specific activities in skeletal muscle and decreased glycloytic enzyme specific activities in liver regardless of treatment. The experiment supports those studies that documented a tissue and enzyme specific responses of glycolytic enzyme activities to hypoxia [1-3].

Maximal enzyme activity measurements in glycolytic enzymes reflects changes in only subset of proteins, and thus to understand changes on a more global scale recent proteomic approaches were used that led to chapter 3 and chapter 4. As a first step, in chapter 3 the experiments were aimed to address the problem of protein degradation during sample preparation that is a major concern in proteomic analyses. For this the protein profiles of *F. grandis* were

compared in 1D gels after two sampling approaches: freezing in liquid nitrogen and immersion of fresh tissues in RNA later®. The study showed that the method of tissue preservation was tissue specific, liver and heart proteins were better preserved by flash freezing; gill proteins were better preserved in RNA later®; and brain and muscle proteins were equally well preserved by the two approaches. Furthermore, protein identifications using LC-MS/MS identified several proteins in liver and gill involved in various physiological functions. These results demonstrate the utility of LC-MS/MS combined with database searching for reliable protein identification in a fish without a sequenced genome and support the use of *F. grandis* and its close relatives as model organisms for environmental proteomic studies in vertebrates.

Chapter 4 investigates the patterns of protein abundance in multiple tissues of *Fundulus grandis* using advanced two-dimensional gel electrophoresis coupled with mass spectrometry (2DE-MS/MS). Database searching resulted in the identification of multiple proteins from liver, skeletal muscle, brain, gill, and heart. Identified proteins include enzymes of energy metabolism, heat shock proteins, and structural proteins. The protein identification rate was approximately 40-50% for all the tissues for a species without a sequenced genome, demonstrating the utility of *F. grandis* as a model organism for environmental proteomic studies in vertebrates. A total of 253 non-redundant proteins were identified in all the tissues. GO annotations from total 253 non-redundant proteins were performed and majorities were classified as proteins with catalytic activity (57.5%) and structure molecule activity (23.6%).

5.1 Future directions

Over the years studies of responses of fish to environmental stressors has been of great interest to biologists. Further experiments on responses of fish to low oxygen might be of interest in hypoxia related investigations. Results from duration of exposure of fish to different oxygen

treatments at 14 d and 28 d that affected glycolytic enzyme specific activities in the tissues of *Fundulus* could be used for hypoxia studies. At these time points 2DE-MS/MS can be used to compare hypoxic fish to normoxic fish for the proteins up/down regulated under hypoxia. 2DE-MS/MS along with cDNA microarray technology to understand patterns of mRNA expression will provide an integrated view of gene expression as a possible adaptation of fish to hypoxic environments.

The generated 2DE maps and protein identifications from five tissues of *F. heteroclitus* can be submitted to 2DE databases. The 2DE databases contain 2DE data, like gel images, protein identifications, and experimental information before and after separation. Through these databases the 2DE information is accessible through World Wide Web (www.) These databases are available on EXpasy proteomics website. The world 2D PAGE repository contains data from 21 published articles, holding 28 reference maps for 18 species, about 5700 identified spots as of March 2011 [4]. The 2DE databases can be created and published for public access using software like "The Make2D-DB II Package" [5]. Using this package one can publish information like picture of gel image, protein identifications, molecular weight, pI, protein identifiers i.e accession numbers, spot numbers, x and y co-ordinates of the spots on the gel image [6]. Furthermore protein identifications can be used to design specific hypotheses to investigate the function of single proteins, protein–protein interactions, or whole biochemical pathways.

The results from chapter 3 and 4 demonstrate the utility of LC-MS/MS and 2DE-MS/MS techniques in a species without a sequenced genome. However, these techniques have to be refined further to increase the identification rate and functional annotation. Nevertheless limitations associated with gene ontology, incomplete annotations even for organisms with sequenced genomes, and level of confidence in web programs that perform annotations

highlights the need for improved bioinformatics analyses [7]. The combination of improved proteomic techniques, progression of genomic sequencing of nonmodel organisms, and improved bioinformatics should increase the applicability of these advanced techniques in understanding fish physiology.

5.2 References

1] Shaklee, J. B., Christiansen, J. A., Sidell, B. D., Prosser, C. L., Whitt, G. S., Molecular aspects of temperature acclimation in fish: Contributions of changes in enzyme activities and isozyme patterns to metabolic reorganization in the green sunfish. *Journal of Experimental Zoology* 1977, 201, 1-20.

2] Driedzic, W. R., Gesser, H., Johansen, K., Effects of hypoxic adaptation on myocardial performance and metabolism in *Zoarces viviparous Can. J. Zool.* 1985, 63, 821-823.

3] Storey, K. B., Tissue-specific controls on carbohydrate catabolism during anoxia in goldfish. *Physiol. Zool.* 1987, 60, 601-607.

4] http://world-2dpage.expasy.org/repository/

5] Mostaguir, K., Hoogland, C., Binz, P.-A., Appel, R. D., The Make 2D-DB II package: Conversion of federated two-dimensional gel electrophoresis databases into a relational format and interconnection of distributed databases. *Proteomics* 2003, 3, 1441-1444.

6] Hoogland, C., Mostaguir, K., Appel, R. D., in: Walker, J. M. (Ed.), *The Proteomics Protocols Handbook*, Humana Press 2005, 259-266.

7] Lomax, J., Get ready to GO! A biologist's guide to the gene ontology. *Briefings in Bioinformatics* 2005, 6, 298-304.

Appendix A

University of New Orleans

Institutional Animal Care and Use Committee (IACUC)

DATE: May 4, 2005

TO: Bernard B. Rees, Ph.D.

FROM: Gerald J. LaHoste, Ph.D.
Chairman

RE: *IACUC Protocol No.* **073**
Entitled: **Hypoxia-inducible gene expression in fish**

Your application for the use of animals in research (referenced above) has been approved for a three-year period beginning May 4, 2005 and expiring May 4, 2008.

❖ A Member of the Louisiana State University System Committed to Equal Opportunity ❖

Appendix A

Institutional Animal Care and Use Committee

UNIVERSITY OF NEW ORLEANS

DATE: February 2, 2010

TO: Dr. Bernard Rees

FROM: Steven G. Johnson, Ph.D.
Chairman

RE: *IACUC Protocol* # **UNO-10-001**
Entitled: **Identifying biomarkers of low oxygen exposure in estuarine fish.**

Your application for the use of animals in research (referenced above) has been approved for a 9 months beginning February 2, 2010 and expiring November 1, 2010. Please note that an annual/final report must be provided to the UNO IACUC.

The University of New Orleans has an Animal Welfare Assurance on file with the Office of Laboratory Animal Welfare (OLAW), National Institute of Health. The assurance is A3299-01.

❖UNIVERSITY OF NEW ORLEANS Institutional Animal Care and Use Committee❖

Appendix B

Table B.1 LC-MS/MS protein Identifications of 1D gel bands from *F. grandis* liver.

Band	Protein Name	Accession #	Peptides	Peptide sequences	Xcorr	ΔCn
L1	aconitase 1	NP_001030155	3	Q.GDLVAAGVLSGNR.N	3.41	0.42
				K.FVEFFGPGVAQLSIADR.A	4.75	0.55
				R.VILQDFTGVPAVVDFAAM*R.D	5.47	0.63
L1	liver glycogen phosphorylase	NP_001008538	5	K.VIPATDLSEQISTAGTEASGTGNM*K.F	4.28	0.50
				K.LITSVADVVNND.P	3.99	0.43
				R.GIVGVENVAELK.K	3.80	0.43
				K.DGWQVEEADDWLR.Y	4.39	0.37
				R.DFNVGDYIQAVLDR.N	2.99	0.13
L2	keratin 8	NP_956374	5	K.DVDEAYM*NKVELEAK.L	2.88	0.32
				R.IKDLEDALQR.A	2.75	0.21
				K.M*KLEADLHNM*QGLVEDFK.N	4.24	0.39
				K.LEADLHNM*QGLVEDFK.N	3.84	0.39
				K.LESLTDEINFLR.Q	3.61	0.38
L3	adenosylhomocysteinase	NP_954688	6	K.KLDEEVAAAHLDK.L	5.36	0.44
				K.VAVVAGYGDVGK.G	3.66	0.54
				K.VADISLAEWGR.K	3.81	0.45
				K.DGQPLNM*ILDDGGDLTNLVHQK.Y	2.87	0.37
				K.YPLGVYFLPK.K	3.63	0.43
				R.VIVTEIDPINALQAAM*EGYEVTTM*DEAC#K.E	5.99	0.57
L3	enolase 3-2	NP_001133193	5	K.DATNVGDEGGFAPN.I	3.49	0.39
				R.AAVPSGASTGVHEALELR.D	5.08	0.51
				N.ILENNEALELLK.T	4.37	0.27
				K.DATNVGDEGGFAPNILENNEALELLK.T	6.18	0.36
				K.VNQIGSVTESIKAC#K.L	4.42	0.37

Table B.1 Continued

Band	Protein Name	Accession #	Peptides	Peptide sequences	Xcorr	ΔCn
L3	zgc:73056	NP_956989	5	F.M*ILPVGASSFK.E	2.79	0.33
				Q.DATNVGDEGGFAPNILENK.E	5.76	0.48
				R.AAVPSGASTGIYEALELR.D	3.89	0.38
				K.LAM*QEFM*ILPVGASSFK.E	5.51	0.54
				R.AAVPSGASTGIYEALELR.D	4.19	0.55
L3	elongation factor 1-alpha	NP_001098132	3	K.LIPQKPM*VVEPFSNYPPLGR.F	3.33	0.35
				R.VETGVLKPGM*VVTFAPPNLTTEVK.S	4.40	0.35
				K.IGYNPAAVAFVPISGWH.G	4.77	0.55
L4	actin, cytoplasmic 1	NP_001116997	14	R.TTGIVM*DSGDGVTHTVPIYEGYALPH.A	4.51	0.43
				D.FEQEM*GTAASSSSLEK.S	5.43	0.30
				K.QEYDESGPSIVHR.K	3.07	0.45
				L.SGGTTM*YPGIADR.M	3.26	0.44
				G.YSFTTTAER.E	2.19	0.39
				R.GYSFTTTAER.E	3.32	0.40
				N.TVLSGGTTM*YPGIADR.M	4.15	0.51
				K.IWHHTFYNELR.V	2.75	0.16
				R.KDLYANTVLSGGTTM*YPGIADR.M	5.80	0.51
				R.VAPEEHPVLLTEAPLNPK.A	4.34	0.30
				R.AVFPSIVGR.P	2.24	0.19
				K.SYELPDGQVITIGNER.F	4.06	0.28
				K.LC#YVALDFEQEM*GTAASSSSLEK.S	5.60	0.11
L4	enolase 3-2	NP_001133193	3	K.VNQIGSVTESIKAC#K.L	4.30	0.44
				K.DATNVGDEGGFAPNILENNEALELLK.T	6.86	0.43
				R.HIADLAGHKDVILPCPAFNVINGGSHAGNK.L	3.29	0.05
L4	zgc:73056	NP_956989	4	Q.DATNVGDEGGFAPNILENK.E	5.81	0.49
				R.HIADLAGNPEVILPVPAFNVINGGSHAGNK.L	6.65	0.41
				K.LAMQEFM*ILPVGASSFK.E	4.78	0.20
				R.AAVPSGASTGIYEALELR.D	2.96	0.26

Table B.1 Continued

Band	Protein Name	Accession #	Peptides	Peptide sequences	Xcorr	ΔCn
L4	ribosomal protein SA	NP_957346	3	R.AIVAIENPADVC#VISSR.N	5.55	0.52
				R.ADHQPLTEASYVNIPTIALC#NTDSPLR.Y	5.14	0.46
L4	phosphoglycerate kinase 1	NP_998552	3	K.LGDVYVNDAFGTAHR.A	4.58	0.48
				K.YSLEPVAAELK.N	3.61	0.39
				K.DC#VGPDVEKACADPPAGSVILLENLR.F	2.76	0.18
L5	actin, cytoplasmic 1	NP_001116997	6	K.QEYDESGPSIVHR.K	2.44	0.19
				R.GYSFTTTAER.E	3.18	0.46
				K.IWHHTFYNELR.V	3.15	0.38
				R.VAPEEHPVLLTEAPLNPK.A	4.13	0.29
				K.SYELPDGQVITIGNER.F	4.96	0.27
				R.TTGIVM*DSGDGVTHTVPIYEGYALPHA ILR.L	5.72	0.44
L5	glyceraldehyde-3-phosphate dehydrogenase	NP_001117033	7	K.ITVFHERDPAN.I	3.30	0.40
				K.ITVFHERDPANIK.W	2.58	0.03
				K.ITVFHERDPANIK.W	3.34	0.35
				K.VVSNASC#TTNC#LAPLAK.V	4.32	0.49
				N.VSVVDLTVR.L	2.88	0.25
				R.VPTPNVSVVDLTVR.L	3.65	0.28
				R.VPTPNVSVVDLTVR.L	3.84	0.44
L6	aldolase B, fructose-bisphosphate	NP_001117099	4	K.VDKGTAGLNGTDGETTTQ.G	3.80	0.34
				K.VDKGTAGLNGTDGETTTQGLDGLSER. C	5.05	0.49
				K.GTAGLNGTDGETTTQGLDGLSER.C	4.70	0.40
				K.ALNDHHVYLEGTLLKPN.M	4.16	0.28
L6	nascent polypeptide-associated	NP_775371	3	K.IEDLSQQAQLAAAEK.F	4.90	0.53
				K.SPASDTYIVFGEAK.I	4.42	0.41
				K.NILFVITKPDVYK.S	4.24	0.40
L7	triosephosphate isomerase 1	NP_705954	6	R.IIYGGSVTGGTC#K.E	4.53	0.52
				K.TNVSEAVANSVR.I	4.86	0.38

Table B.1 Continued

Band	Protein Name	Accession #	Peptides	Peptide sequences	Xcorr	ΔCn
				R.RHVFGESDELIGQK.V	5.26	0.50
				R.HVFGESDELIGQK.V	4.86	0.55
				K.GAFTGEISPAMIK.D	4.19	0.39
				K.VVLAYEPVWAIGTGK.T	4.69	0.46

Table B.2 LC-MS/MS protein Identifications of 1D gel bands from *F. grandis* gill.

Band	Protein Name	Accession #	Peptide	Peptide sequences	Xcorr	ΔCn
G1	myosin heavy chain larval type 2	NP_001155230	5	K.QKYEESQAELEGAQK.E	3.09	0.34
				K.LAQESIM*DLENDKQQSDEK.L	3.95	0.22
				R.VALLHSQNTSLLNTK.K	4.85	0.46
				R.DLEEATLQHEATAAALR.K	5.07	0.43
				K.NLQQEISDLTEQIGETGK.S	6.13	0.00
G1	myosin, heavy polypeptide 1.1, muscle	NP_001124138	13	R.KVAEQELVDASER.V	4.59	0.51
				K.KM*EGDLNEM*EIQLSHANR.Q	4.13	0.38
				K.IEDEQSLGAQLQK.K	4.29	0.30
				R.IEELEEEIEAER.A	4.40	0.30
				K.AGLLGTLEEM*RDEK.L	3.98	0.38
				K.NKDPLNESVVQLYQK.S	4.77	0.34
				K.ALQEAHQQTLDDLQAEEDKVNTLTK.S	6.76	0.48
				K.VLNASVIPEGQFIDNKK.A	4.12	0.36
				R.LQGEVEDLM*IDVER.A	4.54	0.45
				K.TKLEQQVDDLEGSLEQEK.K	5.19	0.41
				K.TPGLM*ENFLVIHQLR.C	5.51	0.39
				K.M*QGSLEDQIIAANPLLEAYGNAK.T	5.47	0.35
				K.NLQQEISDLTEQLGETGK.S	6.13	0.04
G1	PREDICTED: myosin, heavy polypeptide 10,	XP_683046	2	K.VEDM*AELTC#LNEASVLHNLK.D	3.18	0.04
				R.TQLEELEDELQATEDAK.L	4.41	0.40
G2	ATPase, Na+/K+ transporting,	NP_571760	2	K.VDNSSLTGESEPQTR.S	3.92	0.45
				K.GVGIISEGNETVEDIAAR.L	4.01	0.52
G2	myosin, heavy polypeptide 1.1, muscle	NP_001124138	2	K.ALQEAHQQTLDDLQAEEDKVNTLTK.S	6.67	0.44
				K.VLNASVIPEGQFIDNKK.A	3.03	0.15
G3	heat shock protein 9	NP_958483	2	K.DAGQIAGLNVLR.V	3.13	0.32
				R.VINEPTAAALAYGLDK.T	4.42	0.54
G3	poly A binding protein, cytoplasmic 1 a	NP_001026846	2	R.SKVDEAVAVLQAHQAK.E	4.36	0.43
				R.ALDTM*NFDVIK.G	3.01	0.26
G3	heat shock cognate 70 kDa protein	NP_001117704	10	K.STAGDTHLGGEDFDNR.M	3.32	0.42

Table B.1 Continued

Band	Protein Name	Accession #	Peptides	Peptide sequences	Xcorr	ΔCn
				K.M*KEIAEAYLGK.T	3.37	0.32
				K.M*DKAQVHDIVLVGGSTR.I	3.98	0.00
				K.FELTGIPPAPR.G	3.20	0.36
				R.IINEPTAAAIAYGLDKK.V	4.24	0.46
				K.DAGTISGLNVLR.I	3.49	0.26
				R.IINEPTAAAIAYGLDKK.V	3.89	0.38
				K.LLQDFFNGK.E	2.84	0.22
				R.FEELNADLFR.G	3.12	0.28
G4	enolase 3-2	NP_001133193	2	V.PSGASTGVHEALELR.D	4.89	0.45
				K.DATNVGDEGGFAPNILENNEALELLK.T	6.09	0.42
G4	zgc:73056	NP_956989	5	K.IDQFM*LELDGTENK.S	4.43	0.43
				Q.DATNVGDEGGFAPNILENK.E	5.85	0.46
				K.LAM*QEFM*ILPVGASSFK.E	5.62	0.54
				L.PVPAFNVINGGSHAGNK.L	3.71	0.40
				R.GNPTVEVDLYTE.R	2.18	0.29
G4	proteasome 26S subunit ATPase 3	NP_001153918	3	R.TM*LELLNQLDGFQPNM*QVK.V	4.05	0.33
				K.LAGPQLVQM*FIGDGAK.L	4.24	0.52
				K.DSYLILETLPTEYDSR.V	4.48	0.36
G4	elongation factor 1-alpha	NP_001098132	2	K.LIPQKPM*VVEPFSNYPPLGR.F	3.34	0.38
				R.VETGVLKPGM*VVTFAPPNLTTEVK.S	4.86	0.32

Appendix C

Table C.1 List of total identified proteins from Mascot database search of *Fundulus grandis* liver

SSP	Protein Name	Species	Mascot score	Sequence coverage	Matched peptides	Mr (kDa)	pI	Accession#
6613	phosphoenolpyruvate carboxykinase	*Oncorhynchus mykiss*	179	17%	12	69.66	8.14	gi|185134359
4410	lengsin	*Danio rerio*	65	22%	11	75.87	6.65	gi|72384345
5506	phosphoenolpyruvate carboxykinase	*Oncorhynchus mykiss*	86	15%	13	69.66	8.14	gi|185134359
5702	cytochrome b-c1 complex subunit 1 mitochondrial	*Danio rerio*	61	11%	10	52.14	6.28	gi|41387118
5502	beta-enolase	*Danio rerio*	70	18%	10	47.08	5.99	gi|47551317
4715	Enolase 1	*Danio rerio*	65	21%	11	47.04	6.16	gi|37590349
7212	glutathione peroxidase 1b	*Danio rerio*	81	11%	6	15.96	7.74	gi|237825135
3507	methionine adenosyltransferase I alpha	*Danio rerio*	70	27%	10	43.26	6.32	gi|41054082
1701	79 kDa glucose-regulated protein	*Danio rerio*	215	24%	22	73.98	5.05	gi|47085775
6609	like 4-hydroxyphenylpyruvate dioxygenase	*Danio rerio*	70	18%	9	44.01	6.21	gi|41054723
7602	4-hydroxyphenylpyruvate-dioxygenase	*Gillichthys mirabilis*	68	10%	2	13.26	9.43	gi|10121623
1405	14-3-3 E1 protein	*Fundulus heteroclitus*	72	50%	12	14.27	5.15	gi|52001207
7404	aldolase-B	*Fundulus heteroclitus*	61	10%	2	20.76	5.96	gi|24473730
6708	Beta-enolase	*Osmerus mordax*	204	10%	2	20.76	5.96	gi|47210809
2812	heat shock 60 kD protein 2	*Danio rerio*	116	22%	15	61.16	5.56	gi|31044489
7302	betaine homocysteine methyltransferase	*Danio rerio*	111	10%	4	44.64	6.61	gi|56121765
7302	tropomyosin1-2	*Takifugu rubripes*	69	25%	8	29.27	4.93	gi|28557124
8308	heat shock cognate 71	*Rivulus marmoratus*	175	25%	22	70.48	5.23	gi|37925913
4205	non-neuronal tryptophan hydroxylase 1	*Takifugu rubripes*	70	8%	6	57.31	8.11	gi|47208716
1301	tyrosine 3-monooxygenase	*Danio rerio*	96	30%	16	27.38	4.68	gi|47085905
6313	peroxiredoxin 4-like	*Danio rerio*	139	27%	12	28.91	6.41	gi|292613542
4805	phenylalanine hydroxylase	*Danio rerio*	73	16%	12	51.32	5.60	gi|41054599
3510	tubulin alpha-4A chain	*Danio rerio*	106	23%	14	50.43	5.05	gi|41152353
4801	phenylalanine hydroxylase	*Danio rerio*	84	16%	13	51.32	5.60	gi|41054599
8508	fructose-1 6-bisphosphatase 1	*Danio rerio*	109	32%	13	36.78	6.90	gi|47085885

Table C.1 Continued

SSP	Protein Name	Species	Mascot score	Sequence coverage	Matched peptides	Mr (kDa)	pI	Accession#
5707	Zgc:55316 protein	*Danio rerio*	73	13%	9	47.40	6.48	gi|45219818
1501	succinate-CoA ligase GDP-forming beta subunit	*Danio rerio*	136	15%	12	46.62	5.53	gi|189525094
7610	phosphoenolpyruvate carboxykinase	*Tetraodon nigroviridis*	90	20%	17	69.66	8.14	gi|185134359
7102	aldolase-B	*Fundulus heteroclitus*	218	70%	15	20.76	5.96	gi|24473730
3604	glycogen phosphorylase liver form	*Oreochromis mossambicus*	182	19%	22	93.65	6.56	gi|45383372
1512	squamous cell carcinoma antigen recognized by T-cells 3	*Danio rerio*	65	12%	17	109.51	5.12	gi|71834402
3205	ferritin H3	*Oryzias latipes*	62	37%	8	13.61	5.84	gi|4585816
4105	lactate dehydrogenase B	*Danio rerio*	92	9%	8	36.48	7.00	gi|388124
4505	methionine adenosyltransferase I alpha	*Danio rerio*	98	19%	11	43.26	6.32	gi|41054081
4204	glutathione-S-transferase theta	*Fundulus heteroclitus*	262	51%	10	16.34	5.70	gi|52001203
5103	putative oncoprotein nm23	*Ictalurus punctatus*	125	31%	8	17.32	8.52	gi|10180968
807	calreticulin	*Danio rerio*	87	10%	9	47.33	4.48	gi|41054373
5409	Glutamate dehydrogenase 1	*Danio rerio*	61	22%	13	59.92	8.46	gi|28277658
5710	Enolase 1 (alpha)	*Danio rerio*	87	33%	15	47.04	6.16	gi|37590349
4203	peroxiredoxin-2	*Danio rerio*	124	21%	6	21.84	5.93	gi|50539996
8402	unnamed protein product	*Tetraodon nigroviridis*	69	8%	40	521.48	4.86	gi|47216756
5705	Enolase 1 (alpha) Danio rerio	*Danio rerio*	185	15%	11	47.39	6.16	gi|37590349
7605	like 4-hydroxyphenylpyruvate dioxygenase	*Danio rerio*	65	13%	8	44.18	6.21	gi|41054723
7306	triosephosphate isomerase B	*Danio rerio*	162	27%	11	26.66	6.90	gi|47271422
2503	zinc finger SWIM domain-containing protein KIAA0913	*Danio rerio*	61	34%	8	19.07	9.37	gi|301612620
2611	Rab6 interacting protein homolog family member (elks-1)-like	*Danio rerio*	81	19%	29	104.80	6.64	gi|189520472
3208	ferritin H3	*Oryzias latipes*	102	37%	10	13.61	5.84	gi|4585816
7608	similar to 4-hydroxyphenylpyruvate dioxygenase	*Danio rerio*	69	15%	8	44.01	6.21	gi|41054723
203	carnitine deficiency-associated gene 1	*Danio rerio*	67	27%	22	78.84	6.43	gi|50539694

Table C.1 Continued

SSP	Protein Name	Species	Mascot score	Sequence coverage	Matched peptides	Mr (kDa)	pI	Accession#
1708	mitochondrial ATP synthase beta subunit-like	*Danio rerio*	175	23%	14	55.22	5.09	gi|47218629
6104	aldolase-B	*Fundulus heteroclitus*	216	70%	15	20.76	5.96	gi|24473730
2811	tubulin alpha-4A chain	*Danio rerio*	137	34%	16	50.43	5.05	gi|41152353
7509	glyceraldehyde 3-phosphate dehydrogenase	*Oncorhynchus mykiss*	98	27%	10	35.94	8.63	gi|15010816
8210	glyceraldehyde 3-phosphate dehydrogenase	*Oncorhynchus mykiss*	100	27%	10	36.06	8.63	gi|15010816
8306	triosephosphate isomerase B	*Xiphophorus maculatus*	199	45%	15	26.48	7.60	gi|15149252
2607	keratin 18	*Danio rerio*	100	37%	20	41.25	5.07	gi|29335504
4102	heart-type fatty acid-binding protein	*Fundulus heteroclitus*	119	36%	7	14.75	5.74	gi|15072477
1805	endoplasmin	*Danio rerio*	339	15%	20	89.29	4.88	gi|38016165
8510	aldolase-B	*Fundulus heteroclitus*	230	70%	15	20.76	5.96	gi|24473730
3201	myosin heavy chain	*Cyprinus carpio*	64	13%	30	220.85	5.68	gi|56790034
1607	hsc71	*Paralichthys olivaceus*	79	23%	17	71.11	5.23	gi|39979269
8502	glyceraldehyde 3-phosphate dehydrogenase	*Oncorhynchus mykiss*	100	27%	10	36.06	8.63	gi|15010816
809	protein disulfide-isomerase	*Danio rerio*	127	20%	15	54.78	4.74	gi|193788703
8505	aldolase-B	*Fundulus heteroclitus*	230	70%	15	20.76	5.96	gi|24473730
3703	beta actin	*Dicentrarchus labrax*	338	49%	20	41.71	5.29	gi|27805142
2303	similar to interleukin-1 receptor-associated kinase 4	*Danio rerio*	70	30%	11	41.74	5.66	gi|41055831
2704	simple type II keratin K8a (S1)	*Oncorhynchus mykiss*	124	34%	14	35.68	4.72	gi|185132941
6806	catalase	*Oplegnathus fasciatus*	61	10%	8	59.83	8.34	gi|52354832
6209	triosephosphate isomerase B	*Danio rerio*	96	19%	6	26.66	6.90	gi|47271422
8503	Alanine-glyoxylate aminotransferase	*Platichthys flesus*	111	15%	5	30.14	8.93	gi|60417200
6312	heat shock cognate 71	*Rivulus marmoratus*	212	15%	14	70.48	5.23	gi|37925912
3509	beta tubulin	*Notothenia coriiceps*	110	11%	10	49.76	4.78	gi|10242162
5205	ferritin heavy polypeptide 1	*Danio rerio*	86	16%	7	20.71	5.67	gi|18858719
7210	manganese-containing superoxide dismutase precursor	*Danio rerio*	95	14%	6	24.99	8.29	gi|41152470

Table C.1 Continued

SSP	Protein Name	Species	Mascot score	Sequence coverage	Matched peptides	Mr (kDa)	pI	Accession#
4413	interleukin-1 receptor-like protein	*Salmo salar*	65	23%	11	36.45	9.40	gi|185136291
6606	similar to 4-hydroxyphenylpyruvate dioxygenase	*Danio rerio*	75	17%	11	44.01	6.21	gi|41054723
3311	actin	*Oreochromis mossambicus*	126	37%	9	20.48	5.28	gi|4376058
3506	phosphoglycerate kinase 1	*Danio rerio*	147	26%	13	44.11	7.01	gi|47087077
3502	S-adenosylmethionine synthase isoform type-1	*Danio rerio*	114	11%	8	42.60	6.60	gi|41054081
6310	triosephosphate isomerase B	*Danio rerio*	153	37%	11	26.66	6.90	gi|47271422
8413	fructose-1 6-bisphosphatase 1	*Danio rerio*	66	10%	6	36.78	6.90	gi|47085885
3709	keratin 18	*Danio rerio*	64	30%	17	41.25	5.07	gi|29335504
4108	profilin 2	*Danio rerio*	78	7%	4	15.22	7.66	gi|41152213
6008	glutathione-S-transferase theta	*Fundulus heteroclitus*	78	18%	4	16.16	5.70	gi|52001203
1413	beta actin	*Hippoglossus hippoglossus*	80	24%	10	37.36	5.46	gi|45237481
1403	skeletal muscle tropomyosin1-2	*Takifugu rubripes*	92	38%	15	32.78	4.69	gi|22415765
2103	aminoacyl tRNA synthase complex-interacting	*Danio rerio*	63	33%	13	33.37	8.73	gi|113951751
5003	glutathione-S-transferase theta	*Fundulus heteroclitus*	121	18%	4	16.16	5.70	gi|52001203
1104	mitochondrial ATP synthase alpha-subunit	*Cyprinus carpio*	95	16%	11	59.53	9.33	gi|14009437
1102	Anopheles gambiae str. PEST AGAP012555-PA	*Anopheles gambiae str.*	61	32%	6	11.19	10.19	gi|158284403
2703	keratin 8	*Danio rerio*	141	38%	17	35.68	4.72	gi|29335502
5101	liver fatty acid binding protein	*Fundulus heteroclitus*	83	42%	10	14.13	9.06	gi|52001213
9105	aldolase-B	*Fundulus heteroclitus*	180	31%	11	20.42	5.96	gi|24473730
9101	liver fatty acid binding protein	*Fundulus heteroclitus*	175	34%	9	14.13	9.06	gi|52001213
9109	hemoglobin beta chain	*Decapterus maruadsi*	113	20%	6	16.18	8.07	gi|13241084
8106	beta globin	*Paramisgurnus dabryanus*	131	17%	6	16.20	7.14	gi|22135542

Table C.2 List of total identified proteins from Mascot database search of *Fundulus grandis* skeletal muscle

SSP	Protein Name	Species	Mascot score	Sequence coverage	Matched peptides	Mr (kDa)	pI	Accession#
6304	muscle-type creatine kinase CKM2	*Oreochromis mossambicus*	343	36%	23	42.69	6.44	gi|21694043
4503	muscle-type creatine kinase CKM2	*Oreochromis mossambicus*	161	30%	16	42.69	6.44	gi|21694043
7602	isocitrate dehydrogenase 2 (NADP+), mitochondrial	*Danio rerio*	345	33%	24	46.82	6.57	gi|47224185
3814	warm temperature-acclimated 65kDa protein	*Fundulus heteroclitus*	73	54%	5	7.76	7.08	gi|52430344
6302	muscle-type creatine kinase CKM2	*Oreochromis mossambicus*	131	16%	8	42.69	6.44	gi|21694043
6301	creatine kinase muscle isoform 2	*Chaenocephalus aceratus*	68	17%	8	42.66	6.44	gi|31322099
7104	PDZ and LIM domain protein 7 isoform	*Mus musculus*	99	7%	8	54.67	8.40	gi|166197681
6702	Beta-enolase	*Danio rerio*	142	24%	16	47.08	5.99	gi|47210809
605	skeletal alpha-actin	*Sparus aurata*	416	46%	24	41.84	5.28	gi|6653228
8108	PDZ and LIM domain protein 7 isoform	*Mus musculus*	98	7%	7	54.67	8.46	gi|166197681
5702	Enolase 1, (alpha	*Danio rerio*	115	17%	7	47.04	6.16	gi|37590349
8601	sarcomeric mitochondrial creatine kinase-like	*Danio rerio*	174	34%	10	20.48	9.01	gi|292617951
8107	phosphoglycerate mutase 2 (muscle)	*Danio rerio*	193	27%	9	28.81	8.83	gi|41056123
4401	F-actin capping protein alpha-1 subunit	*Danio rerio*	152	19%	7	32.69	5.65	gi|289547471
9203	fast troponin T isoform a	*Danio rerio*	63	8%	3	27.77	9.45	gi|31580579
7403	muscle-type creatine kinase CKM2	*Oreochromis mossambicus*	515	39%	25	42.69	6.44	gi|21694043
4504	muscle-type creatine kinase CKM2	*Oreochromis mossambicus*	153	24%	13	42.69	6.44	gi|21694043
604	skeletal alpha-actin	*Sparus aurata*	277	35%	21	41.84	5.28	gi|6653228
6704	beta-enolase	*Danio rerio*	302	31%	18	47.08	5.99	gi|47551317
8402	glyceraldehyde 3-phosphate dehydrogenase	*Oncorhynchus mykiss*	113	16%	8	35.94	8.63	gi|15010816
6502	muscle-type creatine kinase CKM2	*Oreochromis mossambicus*	124	17%	8	42.69	6.44	gi|21694043
8101	triosephosphate isomerase B	*Danio rerio*	271	30%	13	26.66	6.9	gi|47271422
5706	alpha enolase-1	*Amia calva*	215	26%	11	39.06	5.54	gi|11999247
9102	tropomyosin 3	*Danio rerio*	99	44%	16	28.83	4.76	gi|41393141

Table C.2 Continued

SSP	Protein Name	Species	Mascot score	Sequence coverage	Matched peptides	Mr (kDa)	pI	Accession#
5508	muscle-type creatine kinase CKM3	*Oreochromis mossambicus*	351	37%	25	42.69	6.44	gi|21694043
6501	muscle-type creatine kinase CKM5	*Oreochromis mossambicus*	135	25%	16	42.69	6.44	gi|21694043
7105	Adenylate kinase	*Salmo salar*	227	36%	16	21.41	7.66	gi|213512310
2608	skeletal alpha-actin	*Sparus aurata*	460	41%	22	41.84	5.28	gi|6653228
5504	muscle-type creatine kinase CKM2	*Oreochromis mossambicus*	263	31%	20	42.69	6.44	gi|21694043
2106	Myosin light chain 1, skeletal muscle Isoform	*Liza ramado*	309	35%	16	20.05	4.54	gi|7994632
4803	myosin binding protein H-like	*Salmo salar*	72	14%	11	53.60	6.04	gi|213511568
6504	muscle-type creatine kinase CKM2	*Oreochromis mossambicus*	587	41%	27	42.69	6.44	gi|21694043
6503	muscle-type creatine kinase CKM2	*Oreochromis mossambicus*	397	36%	25	42.69	6.44	gi|21694043
9202	troponin T3b, skeletal, fast isoform 2	*Danio rerio*	89	6%	3	26.40	9.61	gi|31795559
8401	glyceraldehyde-3-phosphate dehydrogenase	*Paralichthys olivaceus*	162	24%	10	36.02	8.54	gi|6635240
101	myosin, light polypeptide 2 , skeletal muscle	*Danio rerio*	116	40%	9	16.53	4.39	gi|18859049
6707	myosin, light polypeptide 2, skeletal muscle	*Danio rerio*	136	44%	10	16.53	4.39	gi|18859049
8507	fructose-bisphosphate aldolase A	*Danio rerio*	266	17%	12	39.23	8.45	gi|41282154
9101	putative fast skeletal muscle troponin	*Paralichthys olivaceus*	126	60%	9	10.09	9.7	gi|32454282
2303	skeletal muscle tropomyosin1-1	*Takifugu rubripes*	468	40%	24	32.70	4.69	gi|22415763
1604	skeletal alpha-actin	*Sparus aurata*	460	41%	22	41.84	5.28	gi|6653228
1602	skeletal alpha-actin	*Sparus aurata*	460	41%	22	41.84	5.28	gi|6653228
2102	unnamed protein product	*Tetraodon nigroviridis*	266	50%	15	16.53	4.39	gi|47217809
1603	skeletal alpha-actin	*Sparus aurata*	460	41%	22	41.84	5.28	gi|6653228
405	skeletal muscle tropomyosin1-1	*Takifugu rubripes*	468	40%	24	32.70	4.69	gi|22415763
7501	muscle-type creatine kinase CKM2	*Oreochromis mossambicus*	343	36%	23	42.69	6.44	gi|21694043

Table C.3 List of total identified proteins from Mascot database search of *Fundulus grandis* brain

SSP	Protein Name	Species	Mascot score	Sequence Coverage	Matched peptides	Mr (kDa)	pI	Accession#
4802	stress-70 protein, mitochondrial	*Danio rerio*	90	21%	13	51.77	5.39	gi|54262125
6303	glyceraldehyde-3-phosphate dehydrogenase	*Astatotilapia burtoni*	100	14%	7	35.83	6.40	gi|51895785
6601	fascin	*Danio rerio*	163	26%	14	47.04	8.35	gi|115494998
5102	enoyl-CoA hydratase, mitochondrial	*Salmo salar*	86	9%	4	36.33	5.85	gi|213511865
4501	Pkm2 protein	*Danio rerio*	72	21%	15	58.08	6.36	gi|45501385
3603	V-type ATPase B subunit	*Oncorhynchus mykiss*	180	30%	18	55.70	5.46	gi|4929105
6103	thioredoxin-dependent peroxide reductase, mitochondrial	*Danio rerio*	68	4%	4	26.85	8.89	gi|65301457
7507	fumarate hydratase precursor	*Danio rerio*	63	7%	5	54.83	8.98	gi|41055718
5606	fascin	*Danio rerio*	89	22%	12	47.04	8.35	gi|115494998
5406	Phosphoglycerate kinase	*Salmo salar*	85	15%	6	44.11	7.01	gi|213511822
7001	manganese-containing superoxide dismutase	*Danio rerio*	69	13%	6	24.99	8.29	gi|41152470
4302	beta tubulin	*Notothenia coriiceps*	164	27%	19	49.76	4.78	gi|10242162
3801	V-ATPase subunit A	*Fundulus heteroclitus*	284	35%	32	68.41	5.43	gi|14915706
6305	glyceraldehyde-3-phosphate dehydrogenase	*Astatotilapia burtoni*	151	22%	7	35.83	6.40	gi|51895785
105	triosephosphate isomerase A	*Xiphophorus maculatus*	143	25%	12	26.75	4.61	gi|15149254
7105	Adenylate kinase	*Salmo salar*	168	32%	13	21.41	7.66	gi|213512310
5001	phosphatidylethanolamine binding protein	*Danio rerio*	63	18%	7	20.84	6.89	gi|54312133
4401	glutamine synthetase	*Oncorhynchus mykiss*	70	5%	4	33.08	6.86	gi|21666325
7103	triosephosphate isomerase B	*Xiphophorus maculatus*	294	39%	15	26.48	7.60	gi|15149252
5202	malate dehydrogenase, mitochondrial	*Danio rerio*	104	23%	12	35.51	8.56	gi|47085883
6204	voltage-dependent anion-selective channel protein	*Danio rerio*	223	32%	12	30.54	6.53	gi|47221743
3501	creatine kinase, brain	*Danio rerio*	180	14%	9	42.86	5.49	gi|27545193
3602	alpha tubulin	*Gillichthys mirabilis*	125	32%	9	31.83	5.35	gi|16517095
3601	class III intermediate filament protein Danio	*Chaenocephalus*	87	23%	15	51.26	5.03	gi|38374177
3103	peroxiredoxin-2	*Danio rerio*	120	14%	5	21.84	5.93	gi|50539996
8605	glutamate dehydrogenase 3	*Oncorhynchus mykiss*	146	27%	20	59.56	8.26	gi|21666614
3704	warm temperature-acclimated 65kDa protein	*Fundulus heteroclitus*	63	26%	4	7.76	7.08	gi|52430344

Table C.3 Continued

SSP	Protein Name	Species	Mascot Score	Sequence Coverage	Matched peptides	Mr (kDa)	pI	Accession#
8107	V-type proton ATPase subunit E 1	*Danio rerio*	156	37%	22	25.97	8.47	gi|27545261
8004	muscle cofilin 2	*Danio rerio*	136	29%	5	18.76	6.84	gi|37681759
3003	cofilin 2, like	*Danio rerio*	173	33%	10	18.74	6.82	gi|47271384
8604	ATP synthase subunit alpha, mitochondrial	*Danio rerio*	296	28%	19	59.65	9.23	gi|11632597
2203	beta tubulin	*Chionodraco*	285	31%	22	49.72	4.74	gi|10242186
6806	aconitate hydratase, mitochondrial	*Danio rerio*	207	17%	18	86.87	6.61	gi|38707983
4005	putative oncoprotein nm23	*Ictalurus punctatus*	125	31%	7	17.20	8.52	gi|10180968
7305	lactate dehydrogenase B	*mummichog*	209	38%	17	36.16	7.64	gi|388130
2603	gefiltin	*Danio rerio*	94	21%	15	54.39	5.23	gi|18858755
3404	creatine kinase, brain	*Danio rerio*	150	20%	10	42.86	5.49	gi|27545193
2601	gefiltin	*Danio rerio*	130	23%	18	54.39	5.23	gi|18858755
4101	cytoplasmic carbonic anhydrase	*Oncorhynchus mykiss*	66	5%	2	28.16	5.46	gi|41059441
6706	Pkm2 protein	*Danio rerio*	194	25%	24	58.08	6.36	gi|45501385
9302	glutamate oxaloacetate transaminase 2 Danio	*Tetraodon nigroviridis*	109	21%	16	47.43	8.93	gi|41053395
2801	heat shock cognate 71 Rivulus marmoratus	*Danio rerio*	435	40%	31	70.48	5.23	gi|37925912
8204	voltage-dependent anion channel	*Gillichthys mirabilis*	96	11%	2	19.00	8.54	gi|16517086
2401	beta-actin	*Morulius calbasu*	219	39%	19	41.73	5.16	gi|18034011
7205	voltage-dependent anion-selective channel protein	*Danio rerio*	272	35%	13	30.54	6.53	gi|47777306
8301	cytosolic malate dehydrogenase A	*Oryzias latipes*	101	14%	7	36.25	7.59	gi|29242789
1606	heat shock 60 kD protein 1	*Danio rerio*	103	23%	14	61.16	5.56	gi|31044489
4513	Enolase 1, (alpha)	*Danio rerio*	182	31%	15	47.04	6.16	gi|37590349
1501	enolase 2	*Danio rerio*	138	22%	15	46.81	4.77	gi|51467931
5	gamma1-synuclein	*Takifugu rubripes*	64	18%	2	6.73	3.59	gi|76253695
6409	fructose-bisphosphate aldolase C	*Oryzias latipes*	98	16%	8	35.70	6.36	gi|46849375
5002	cofilin 2, like	*Danio rerio*	220	38%	12	18.74	6.82	gi|47271384
7202	malate dehydrogenase, mitochondrial	*Danio rerio*	225	30%	16	35.51	8.56	gi|47085883
2609	Gfap protein	*Danio rerio*	164	28%	21	51.09	5.34	gi|46329793
8404	creatine kinase	*Takifugu rubripes*	193	23%	17	46.45	8.73	gi|8575804

Table C.3 Continued

SSP	Protein name	Species	Mascot score	Sequence Coverage	Matched peptides	Mr (kDa)	pI	Accession#
1701	internexin neuronal intermediate filament	*Danio rerio*	75	15%	12	64.71	4.79	gi|41054736
1506	Gamma-enolase	*Salmo salar*	224	19%	16	56.41	5.42	gi|213513750
6402	phosphoglycerate kinase 1	*Danio rerio*	148	23%	12	44.69	6.47	gi|47087077
1603	Tubulin beta-2A chain	*Salmo salar*	124	32%	19	38.44	4.83	gi|291190198
1503	mitochondrial ATP synthase beta subunit-like	*Danio rerio*	228	40%	21	55.11	5.09	gi|66773080
8104	triosephosphate isomerase B	*Xiphophorus maculatus*	384	44%	16	26.48	7.60	gi|15149252
2608	glial fibrillary acidic protein	*Danio rerio*	80	31%	17	42.13	5.03	gi|40538766
2409	creatine kinase, brain	*Danio rerio*	217	26%	14	42.86	5.49	gi|27545193
7302	glyceraldehyde-3-phosphate dehydrogenase	*Astatotilapia burtoni*	95	21%	6	35.83	6.40	gi|51895785
2403	beta actin	*Dicentrarchus labrax*	411	48%	24	41.71	5.29	gi|27805142
2102	Enolase 1, (alpha)	*Danio rerio*	207	40%	20	47.04	6.16	gi|37590349
5503	predicted protein	*Nematostella vectensis*	76	7%	4	95.79	7.17	gi|156382697
1602	beta tubulin	*Notothenia coriiceps*	508	49%	34	49.76	4.78	gi|10242162
5101	Psma2 protein	*Danio rerio*	101	26%	9	25.74	6.01	gi|37747972
5201	similar to proteasome alpha 1 subunit	*Monodelphis domestica*	82	21%	8	35.99	10.70	gi|126332430
401	HSP70	*Dicentrarchus labrax*	103	16%	14	71.32	5.31	gi|38882982
2104	prohibitin	*Danio rerio*	185	43%	14	29.67	5.28	gi|41152028
5301	Similar to isocitrate dehydrogenase 3 (NAD+) alpha	*Danio rerio*	121	29%	14	39.96	7.04	gi|29124437
8105	heat shock cognate 71	*Rivulus marmoratus*	106	18%	15	70.48	5.23	gi|37925912
2803	valosin containing protein	*Danio rerio*	83	21%	20	89.37	5.14	gi|41393119
3310	beta tubulin	*Notothenia coriiceps*	119	20%	15	49.76	4.78	gi|10242162
2305	alpha tubulin	*Gillichthys mirabilis*	112	38%	14	31.83	5.35	gi|16517095
4507	alpha-1 enolase-1	*Salmo trutta*	62	18%	7	39.90	5.33	gi|11999265
6405	isocitrate dehydrogenase [NADP], mitochondrial	*Danio rerio*	187	29%	20	46.82	6.57	gi|41054651
4602	dihydrolipoyllysine-residue succinyltransferase component of 2-oxoglutarate dehydrogenase	*Danio rerio*	62	14%	8	44.67	8.35	gi|41393131
4004	dj-1 protein	*Oryzias latipes*	77	16%	8	19.94	5.83	gi|157278183

Table C.3 Continued

SSP	Protein Name	Species	Macot score	Sequence coverage	Matched peptides	Mr (kDa)	pI	Accession#
1504	NSFL1 cofactor p47	*Gallus gallus*	97	12%	9	40.49	5.04	gi|71894957
6711	dihydropyrimidinase-like 5	*Danio rerio*	139	18%	14	57.71	7.94	gi|66392186
7309	heterogeneous nuclear ribonucleoprotein A0	*Danio rerio*	68	7%	5	51.58	8.65	gi|47086749
5718	dihydropyrimidinase-like 5	*Danio rerio*	62	14%	10	57.71	7.94	gi|66392186
6602	fascin	*Danio rerio*	122	12%	11	47.04	8.35	gi|115494998
5403	pyruvate dehydrogenase E1 alpha 1	*Danio rerio*	127	17%	18	43.27	7.56	gi|50539866
107	3-monooxygenase/tryptophan 5-monooxygenase activation protein, gamma polypeptide	*Danio rerio*	81	29%	11	28.22	4.86	gi|49227280
1815	heat shock cognate 71	*Rivulus*	304	34%	29	70.48	5.23	gi|37925912
6404	isocitrate dehydrogenase [NADP], mitochondrial	*Danio rerio*	205	30%	21	46.82	6.57	gi|41054651
9203	succinyl-CoA ligase [GDP-forming] subunit alpha, mitochondrial	*Danio rerio*	64	21%	10	32.62	9.07	gi|52138570
7308	glyceraldehyde-3-phosphate dehydrogenase	*Astatotilapia*	186	14%	8	35.83	6.40	gi|51895785
5717	Pkm2 protein	*Danio rerio*	102	22%	16	58.08	6.36	gi|45501385
7608	mitochondrial ATP synthase alpha-subunit	*Cyprinus carpio*	80	21%	14	59.53	9.33	gi|14009437
9206	voltage-dependent anion-selective channel protein 2	*Danio rerio*	64	10%	7	29.99	8.91	gi|41054601
4514	Enolase 1	*Danio rerio*	115	28%	12	47.04	6.16	gi|37590349
102	synaptosome-associated protein 25a	*Danio rerio*	138	34%	13	22.84	4.57	gi|56207906
7612	ATP synthase subunit alpha, mitochondrial	*Danio rerio*	349	35%	25	58.10	9.30	gi|116325975
1405	B-actin	*Pagrus major*	123	33%	13	41.81	5.30	gi|6693629
1604	tubulin, alpha 8 like 4	*Danio rerio*	313	40%	20	47.87	5.14	gi|41055710
1002	brain-type fatty acid binding protein	*Oryzias latipes*	91	46%	6	14.94	5.08	gi|171544945

Table C.4 List of total identified proteins from Mascot database search of *Fundulus grandis* gill

SSP	Protein Name	Species	Mascot score	Sequence Coverage	Matched peptides	Mr (kDa)	pI	Accession #
9406	fructose-bisphosphate aldolase A	*Danio rerio*	203	25%	20	39.74	8.45	gi|41282154
7104	Proteasome subunit alpha type-4	*Salmo salar*	81	44%	15	29.60	7.57	gi|47550827
3203	myosin, heavy polypeptide 10, non-muscle	*Fundulus heteroclitus*	68	12%	23	268.74	5.68	gi|292614613
5301	heterogeneous nuclear ribonucleoprotein A/B	*Haplochromis burtoni*	106	19%	11	35.33	5.67	gi|108744009
2604	tubulin alpha 8-like 3a protein	*Danio rerio*	254	44%	23	50.72	4.93	gi|267567402
1608	F1 ATP synthase beta subunit	*Gillichthys seta*	282	51%	28	53.95	5.15	gi|226441961
2606	keratin, type II cytoskeletal 8	*Danio rerio*	145	33%	16	35.74	4.72	gi|41056085
8101	triosephosphate isomerase B	*Xiphophorus maculatus*	354	62%	20	26.76	7.60	gi|15149252
6702	coronin-1A	*Danio rerio*	111	15%	10	51.37	6.24	gi|41055464
4003	Peroxiredoxin-1	*Anoplopoma fimbria*	192	27%	9	22.02	6.51	gi|229366432
8203	lactate dehydrogenase B	*Fundulus heteroclitus*	171	44%	17	36.49	7.00	gi|388144
2802	78 kDa glucose-regulated protein	*Salmo salar*	302	39%	34	74.15	5.05	gi|213511032
7205	malate dehydrogenase, mitochondrial	*Danio rerio*	263	38%	18	35.97	8.56	gi|47085883
7102	low molecular weight heat shock protein Hsp27	*Poeciliopsis lucida*	107	12%	5	22.63	6.24	gi|1835583
8202	glyceraldehyde-3-phosphate dehydrogenase	*Salmo salar*	100	25%	10	36.03	7.81	gi|185133678
6402	phosphoglycerate kinase 1	*Danio rerio*	99	20%	11	44.51	7.01	gi|47087077
9101	heat shock cognate 70	*Fundulus heteroclitus macrolepidotus*	113	30%	15	71.05	5.27	gi|77999572
8103	COMM domain-containing protein 1	*Danio rerio*	68	61%	9	21.33	5.48	gi|113674991
3801	heat shock cognate 70	*Fundulus heteroclitus macrolepidotus*	418	48%	33	71.05	5.27	gi|77999572
5101	cytoplasmic carbonic anhydrase	*Oncorhynchus mykiss*	98	5%	2	28.39	5.46	gi|41059441
3605	keratin, type II cytoskeletal 8	*Danio rerio*	340	43%	20	35.68	4.72	gi|41056085
1303	tropomyosin 3 isoform 0	*Danio rerio*	244	36%	20	32.93	4.71	gi|45387763
7402	muscle-type creatine kinase CKM2	*Oreochromis mossambicus*	142	30%	16	42.98	6.44	gi|21694043
206	slow myotomal muscle tropomyosin	*Salmo trutta*	232	25%	16	32.66	4.71	gi|3063940

Table C.4 Continued

SSP	Protein Name	Species	Mascot Score	Sequence Coverage	Matched peptides	Mr (kDa)	pI	Accession#
7403	muscle-type creatine kinase	*Siniperca chuatsi*	513	44%	25	43.12	6.32	gi|255502901
2603	warm temperature acclimation-related 65kDa protein	*Xiphophorus hellerii*	174	17%	11	48.30	5.35	gi|86610887
2504	keratin 18	*Epinephelus coioides*	159	25%	12	33.55	4.75	gi|189498197
1	Full=Calmodulin-A; Short=CaM A	*Oryzias latipes*	85	33%	6	15.35	4.08	gi|49037466
9304	GAPDH	*Salmo salar*	205	29%	11	36.03	7.81	gi|185133678
8402	fructose-bisphosphate aldolase C	*Oryzias latipes*	243	30%	12	36.04	6.36	gi|46849375
207	tropomyosin4-1	*Takifugu rubripes*	194	38%	17	28.68	4.65	gi|28557136
3402	skeletal alpha-actin	*Sparus aurata*	559	48%	23	41.84	5.28	gi|6653228
7002	nuclease diphosphate kinase B	*Gillichthys mirabilis*	135	33%	8	17.21	6.82	gi|10121713
2405	beta-actin	*Oncorhynchus mykiss*	124	24%	9	42.01	5.38	gi|8886013
8107	triosephosphate isomerase B	*Danio rerio*	757	52%	21	26.95	6.90	gi|47271422
1607	Tubulin beta-1 chain	*Salmo salar*	522	58%	38	50.21	4.79	gi|47228186
9407	Fructose-bisphosphate aldolase A	*Osmerus mordax*	285	32%	15	40.20	8.26	gi|225706996
3602	keratin, type II cytoskeletal 8	*Danio rerio*	205	36%	14	35.74	4.72	gi|41056085
9602	adenylyl cyclase-associated protein 1	*Danio rerio*	76	26%	14	49.71	8.52	gi|41054003
3702	serine/cysteine proteinase inhibitor	*Fundulus heteroclitus*	71	14%	6	22.86	5.01	gi|52430384
2406	skeletal muscle actin	*Sparus aurata*	306	35%	17	42.19	5.28	gi|6653228
1404	type I cytokeratin, enveloping layer,	*Danio rerio*	127	15%	6	41.62	5.17	gi|130504059
3401	skeletal alpha-actin	*Sparus aurata*	316	36%	16	42.19	5.28	gi|6653228
11	myosin, light polypeptide 2, skeletal	*Danio rerio*	245	71%	15	16.64	4.39	gi|18859049
3404	beta-actin	*Misgurnus anguillicaudatus*	427	48%	20	42.04	5.29	gi|119943232
4705	Krt4 protein	*Danio rerio*	256	29%	21	53.98	5.34	gi|161612220
3703	Krt4 protein	*Danio rerio*	297	24%	18	53.98	5.34	gi|161612220
3406	beta actin	*Oncorhynchus mykiss*	606	50%	26	42.01	5.38	gi|8886013
1203	tropomyosin	*Thunnus thynnus*	195	32%	17	32.75	4.70	gi|38175083
1301	hypothetical protein LOC100124602	*Danio rerio*	68	20%	8	28.79	4.83	gi|156616350
7705	Uracil phosphoribosyltransferase homolog	*Danio rerio*	76	35%	11	28.79	6.37	gi|82185993
6302	actin, beta-like 2	*Danio rerio*	69	30%	10	41.98	5.18	gi|50344802

Table C.4 Continued

SSP	Protein Name	Species	Mascot Score	Sequence Coverage	Matched peptides	Mr (kDa)	pI	Accession#
6401	keratin 4	*Danio rerio*	118	20%	12	54.24	5.42	gi|18858947
4303	condensin-2 complex subunit D3	*Danio rerio*	66	12%	17	160.39	6.87	gi|41056171
3103	type II keratin E3-like protein	*Sparus aurata*	68	19%	8	38.60	4.89	gi|48476437
6101	proteasome alpha 2	*Paralichthys olivaceus*	147	39%	11	24.92	6.54	gi|81157903
202	Pyruvate kinase muscle isozyme	*Salmo salar*	133	30%	19	57.44	5.97	gi|224587654
1405	Adenylate kinase	*Osmerus mordax*	205	34%	12	21.34	6.19	gi|225707436
4408	beta actin	*Hippoglossus hippoglossus*	286	38%	15	37.36	5.46	gi|45237481
604	20S proteasome beta subunit	*Cirrhinus molitorella*	113	47%	13	26.13	5.60	gi|72537676
5503	enolase 1 isoform b	*Gillichthys mirabilis*	132	37%	17	43.54	5.90	gi|226441955
5102	Proteasome subunit alpha type-6	*Anoplopoma fimbria*	78	29%	9	27.38	6.45	gi|229367144
8204	receptor for activated protein kinase C	*Oreochromis mossambicus*	289	60%	21	35.09	7.60	gi|37498964
9202	fructose-bisphosphate aldolase A	*Epinephelus coioides*	151	29%	17	39.63	8.50	gi|295792244
6603	enolase 3-2	*Salmo salar*	114	29%	19	47.08	5.99	gi|213513724
5202	F-actin-capping protein subunit beta	*Anoplopoma fimbria*	158	38%	17	30.54	5.50	gi|229366390
9002	nucleoside diphosphate kinase	*Epinephelus coioides*	123	26%	7	16.55	6.84	gi|197725753

Table C.5 List of total identified proteins from Mascot database search of *Fundulus grandis* heart

SSP	Protein Name	Species	Mascot score	Sequence Coverage	Matched peptides	Mr (kDa)	pI	Accession#
4510	Enolase 1, alpha	*Danio rerio*	61	39%	15	47.39	6.16	gi|37590349
6602	methylmalonate-semialdehyde dehydrogenase acylating, mitochondrial	*Danio rerio*	79	22%	14	57.40	7.06	gi|50539808
8205	hydroxyacyl-coenzyme A dehydrogenase, mitochondrial	*Danio rerio*	66	27%	11	28.89	6.44	gi|51011113
4608	Enolase 1, alpha	*Danio rerio*	90	31%	17	47.39	6.16	gi|37590349
6806	aconitate hydratase, mitochondrial	*Danio rerio*	72	11%	16	87.50	6.61	gi|38707983
2602	TPA: desmin	*Takifugu rubripes*	78	36%	26	51.58	5.10	gi|33186832
6308	glyceraldehyde-3-phosphate dehydrogenase	*Astatotilapia burtoni*	204	23%	15	36.17	6.40	gi|51895785
8601	glutamate dehydrogenase 3	*Oncorhynchus mykiss*	82	32%	24	59.96	8.26	gi|21666614
6507	isocitrate dehydrogenase NADP, mitochondrial	*Danio rerio*	130	34%	22	47.28	6.57	gi|41054651
7304	glyceraldehyde 3-phosphate dehydrogenase	*Oncorhynchus mykiss*	149	43%	22	36.06	8.63	gi|15010816
6505	isocitrate dehydrogenase NADP, mitochondrial	*Danio rerio*	240	32%	26	47.28	6.57	gi|41054651
7004	manganese superoxide dismutase	*Epinephelus coioides*	67	23%	7	25.36	7.77	gi|56785773
5107	enoyl-CoA hydratase, mitochondrial	*Salmo salar*	76	17%	6	36.84	5.85	gi|213511865
6304	glyceraldehyde-3-phosphate dehydrogenase	*Astatotilapia burtoni*	131	32%	14	36.17	6.40	gi|51895785
7505	fumarate hydratase precursor	*Danio rerio*	63	19%	14	55.00	8.98	gi|41055718
7509	skeletal alpha-actin	*Carassius auratus*	95	39%	22	42.29	5.23	gi|762889
9404	ATP synthase subunit alpha, mitochondrial	*Danio rerio*	187	34%	24	59.82	9.23	gi|116325975
7401	fructose-bisphosphate aldolase C	*Oryzias latipes*	65	22%	11	36.04	6.36	gi|46849375
2613	TPA: desmin	*Takifugu rubripes*	156	45%	40	51.58	5.10	gi|33186832
7412	3-ketoacyl-CoA thiolase, mitochondrial	*Danio rerio*	66	28%	9	42.16	7.64	gi|47085765
4712	transferrin variant A	*Cyprinus carpio*	69	23%	18	75.60	5.75	gi|47225287
2601	warm-temperature-acclimation-related-65kDa-protein-like-protein	*Takifugu rubripes*	72	26%	11	50.07	5.47	gi|47076412
8202	heat shock cognate 71	*Rivulus marmoratus*	215	36%	35	70.71	5.23	gi|37925912
6811	aconitate hydratase, mitochondrial	*Danio rerio*	140	15%	22	87.50	6.61	gi|38707983
408	HSP70	*Dicentrarchus labrax*	232	33%	36	71.55	5.31	gi|38882982

Table C.5 Continued

SSP	Protein Name	Species	Mascot score	Sequence Coverage	Matched peptides	Mr (kDa)	pI	Accession#
3706	warm temperature-acclimated 65kDa protein	*Fundulus heteroclitus*	107	59%	11	7.88	7.08	gi|52430344
6504	beta-enolase	*Danio rerio*	278	49%	30	47.42	5.99	gi|47551317
4509	cytochrome b-c1 complex subunit 1, mitochondrial	*Danio rerio*	83	18%	16	52.71	6.28	gi|41387118
6406	creatine kinase brain isoform	*Chaenocephalus aceratus*	182	26%	17	42.60	5.89	gi|31322101
4506	ubiquinol-cytochrome c reductase core I protein	*Oncorhynchus mykiss*	93	17%	17	52.71	6.28	gi|18496665
8217	mitochondrial ATP synthase alpha-subunit	*Cyprinus carpio*	199	21%	17	59.70	9.33	gi|14009437
4602	Pkm2 protein	*Danio rerio*	155	31%	28	58.59	6.36	gi|45501385
5511	Enolase 1, alpha	*Danio rerio*	302	43%	27	47.39	6.16	gi|37590349
7404	medium-chain specific acyl-CoA dehydrogenase, mitochondrial isoform 1	*Danio rerio*	103	23%	12	39.80	6.08	gi|47085823
3611	transferrin variant A	*Cyprinus carpio*	77	17%	19	75.60	5.75	gi|18034630
6401	phosphoglycerate kinase 1	*Danio rerio*	114	21%	13	45.12	6.47	gi|47087077
1610	heat shock 60 kD protein 1	*Danio rerio*	102	40%	25	61.39	5.56	gi|31044489
5503	Enolase 1, alpha	*Danio rerio*	235	31%	15	47.04	6.16	gi|37590349
3702	mitochondrial uncoupling protein 3	*Danio rerio*	63	41%	14	26.90	9.62	gi|54261747
2401	fast myotomal muscle actin	*Salmo salar*	693	70%	43	4.23	5.22	gi|10953948
4719	putative transferrin	*Acanthopagrus schlegelii*	102	19%	20	76.15	6.38	gi|34329603
7515	sarcomeric mitochondrial creatine kinase-like	*Danio rerio*	160	21%	10	20.65	9.01	gi|292617951
2616	TPA: desmin	*Takifugu rubripes*	225	49%	44	51.58	5.10	gi|33186832
6511	isocitrate dehydrogenase NADP , mitochondrial	*Danio rerio*	437	41%	35	47.28	6.57	gi|41054651
7406	fructose-bisphosphate aldolase C	*Oryzias latipes*	201	41%	22	36.04	6.36	gi|46849375
7108	triosephosphate isomerase B	*Danio rerio*	583	65%	33	26.95	6.90	gi|47271422
3603	TPA: desmin	*Takifugu rubripes*	216	44%	42	51.58	5.10	gi|33186832
1301	putative dystrophin	*Takifugu rubripes*	72	19%	59	419.84	5.41	gi|30315803
6307	unnamed protein producmalate dehydrogenase, mitochondrial	*Danio rerio*	212	35%	18	35.97	8.56	gi|47085883
2501	skeletal alpha-actin	*Carassius auratus*	509	64%	35	42.27	5.22	gi|51340745

Table C.5 Continued

SSP	Protein Name	Species	Mascot score	Sequence Coverage	Matched peptides	Mr (kDa)	pI	Accession#
8404	aldolase A fructose-bisphosphate	*Danio rerio*	108	32%	18	40.23	8.45	gi|37595414
8302	glyceraldehyde-3-phosphate dehydrogenase	*Anguilla japonica*	251	42%	18	36.07	8.63	gi|21955965
7311	aldolase A fructose-bisphosphate	*Danio rerio*	411	26%	14	40.23	8.45	gi|37595414
2405	skeletal alpha-actin	*Carassius auratus*	378	69%	37	42.29	5.23	gi|762889
7303	lactate dehydrogenase B	*Fundulus heteroclitus*	461	58%	36	36.44	7.64	gi|388130
1411	skeletal alpha-actin	*Carassius auratus*	184	54%	33	42.29	5.23	gi|762889
1605	mitochondrial ATP synthase beta subunit-like	*Danio rerio*	480	59%	51	55.22	5.09	gi|66773080
1104	myosin, light chain 6, alkali, smooth muscle and non-muscle like	*Danio rerio*	169	45%	18	17.10	4.43	gi|54400408
306	cardiac tropomyosin	*Salmo trutta*	280	46%	41	32.75	4.63	gi|1045294
3301	beta tubulin	*Chionodraco astrospinosus*	86	25%	14	49.72	4.74	gi|10242186
8607	ATP synthase subunit alpha, mitochondrial	*Danio rerio*	130	28%	21	58.10	9.30	gi|116325975
209	C-type lectin	*Fundulus heteroclitus*		24%	8	23.92	5.41	gi|52430374
3205	unnamed protein product	*Tetraodon nigroviridis*	130	12%	8	37.16	8.49	gi|47214471
5513	skeletal alpha-actin	*Sparus aurata*	113	27%	13	41.84	5.28	gi|6653228
4403	heterogeneous nuclear ribonucleoprotein A/B isoform 1	*Mus musculus*	76	11%	10	34.79	5.21	gi|146260280
6105	heat shock cognate 71	*Rivulus marmoratus*	123	15%	11	70.48	5.23	gi|37925912
5607	Similar to isocitrate dehydrogenase 3 NAD+ alpha	*Danio rerio*	82	27%	12	39.96	7.04	gi|29124437
2203	prohibitin	*Danio rerio*	234	31%	13	29.67	5.28	gi|41152028
7604	dihydrolipoyl dehydrogenase, mitochondrial	*Danio rerio*	64	4%	4	49.69	6.68	gi|41393167
4104	keratin	*Takifugu rubripes*	112	22%	15	61.23	5.04	gi|59710087
6810	aconitate hydratase, mitochondrial	*Danio rerio*	150	12%	16	86.87	6.61	gi|38707983
8405	glutamate oxaloacetate transaminase 2	*Danio rerio*	69	10%	14	47.43	8.93	gi|41053395
8608	glutamate dehydrogenase 3	*Oncorhynchus mykiss*	104	19%	15	59.56	8.26	gi|21666614
4007	mitochondrial ATP synthase alpha subunit	*Danio rerio*	72	11%	5	39.51	9.18	gi|44969408
7101	triosephosphate isomerase B	*Danio rerio*	224	32%	12	26.66	6.90	gi|47271422
304	cardiac tropomyosin	*Salmo trutta*	97	23%	14	32.64	4.63	gi|1045294
8116	phosphoglycerate mutase 2 muscle	*Danio rerio*	100	27%	8	28.81	8.83	gi|41056123

Table C.5 Continued

SSP	Protein Name	Species	Mascot score	Sequence Coverage	Matched peptides	Mr (kDa)	pI	Accession#
2701	heat shock cognate 71	*Rivulus marmoratus*	94	21%	15	70.48	5.23	gi|37925912
8212	mitochondrial ATP synthase alpha-subunit	*Cyprinus carpio*	69	10%	9	59.53	9.33	gi|14009437
7205	glial fibrillary acidic protein; GFAP	*Cyprinus carpio*	111	35%	12	24.89	4.90	gi|435737
205	C-type lectin	*Fundulus heteroclitus*	69	21%	8	23.92	5.41	gi|52430374
7310	fructose-bisphosphate aldolase A	*Danio rerio*	72	17%	12	39.23	8.45	gi|41282154
7007	Adenylate kinase	*Salmo salar*	181	27%	10	21.41	7.66	gi|213512310
7312	glyceraldehyde 3-phosphate dehydrogenase	*Oncorhynchus mykiss*	98	12%	7	35.94	8.63	gi|15010816

Appendix D

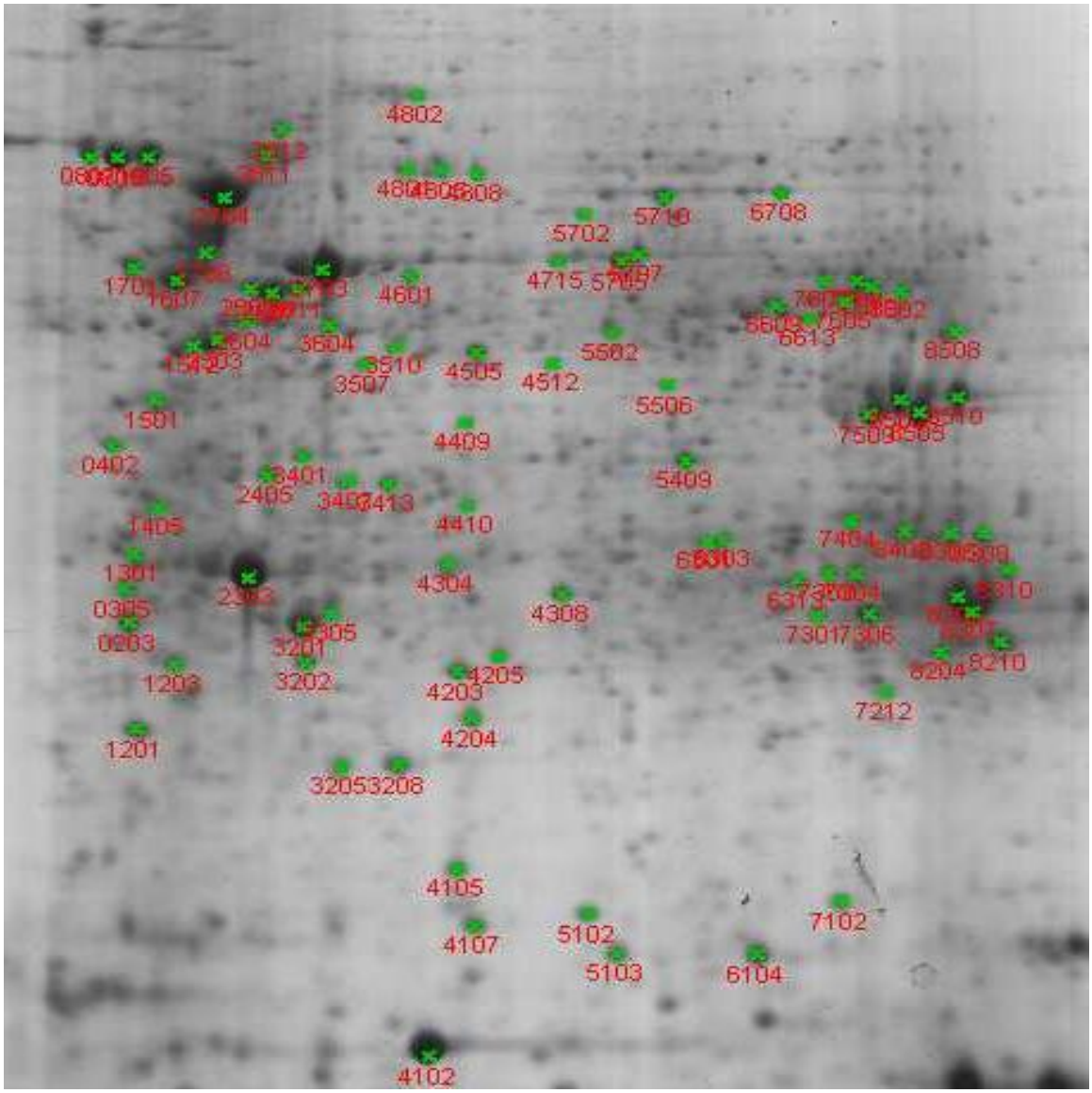

Figure D.1a Preparative gel image of liver with identified protein spots (1-96).

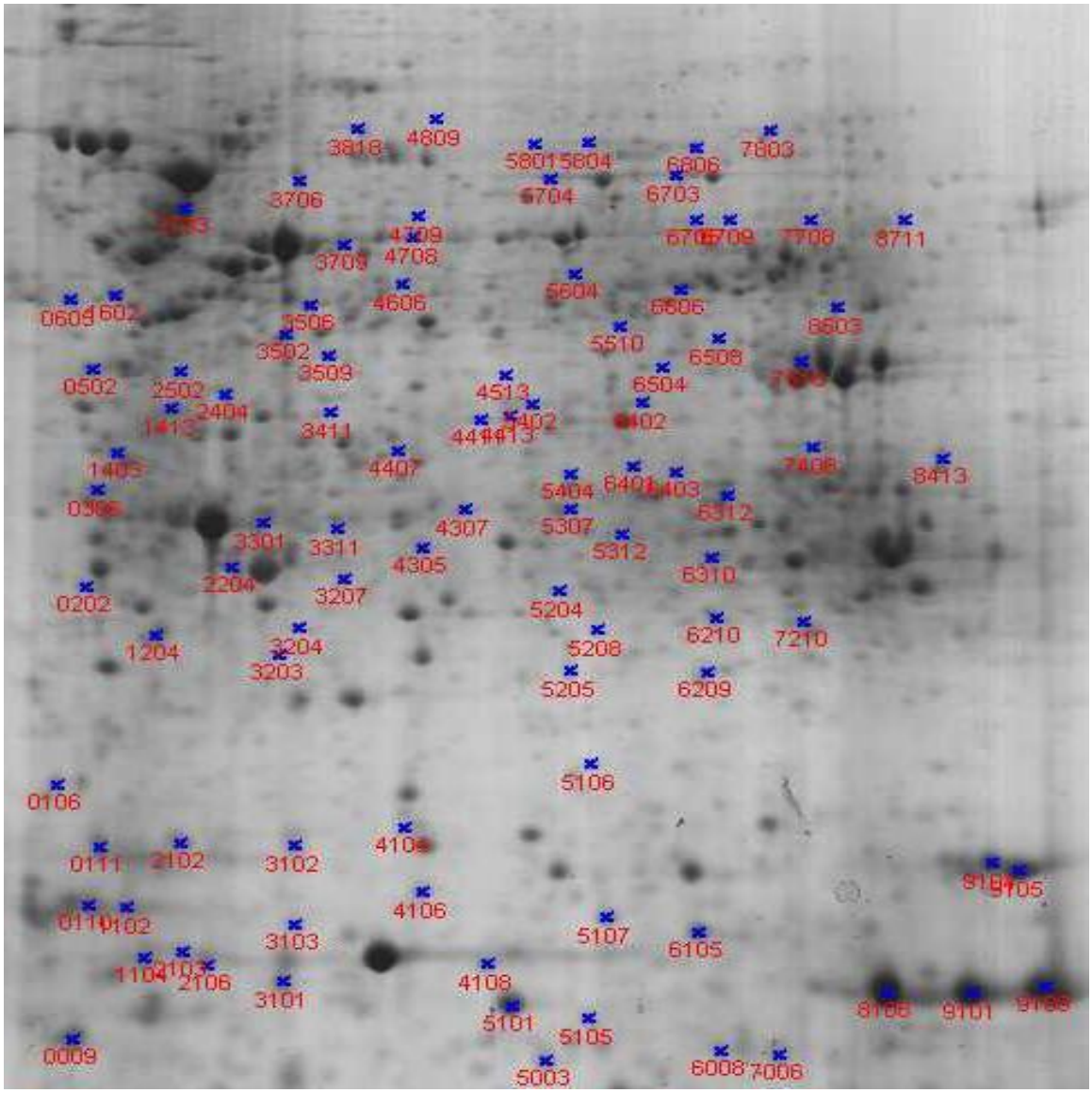

Figure D.1b Preparative gel image of liver with identified protein spots (97-192).

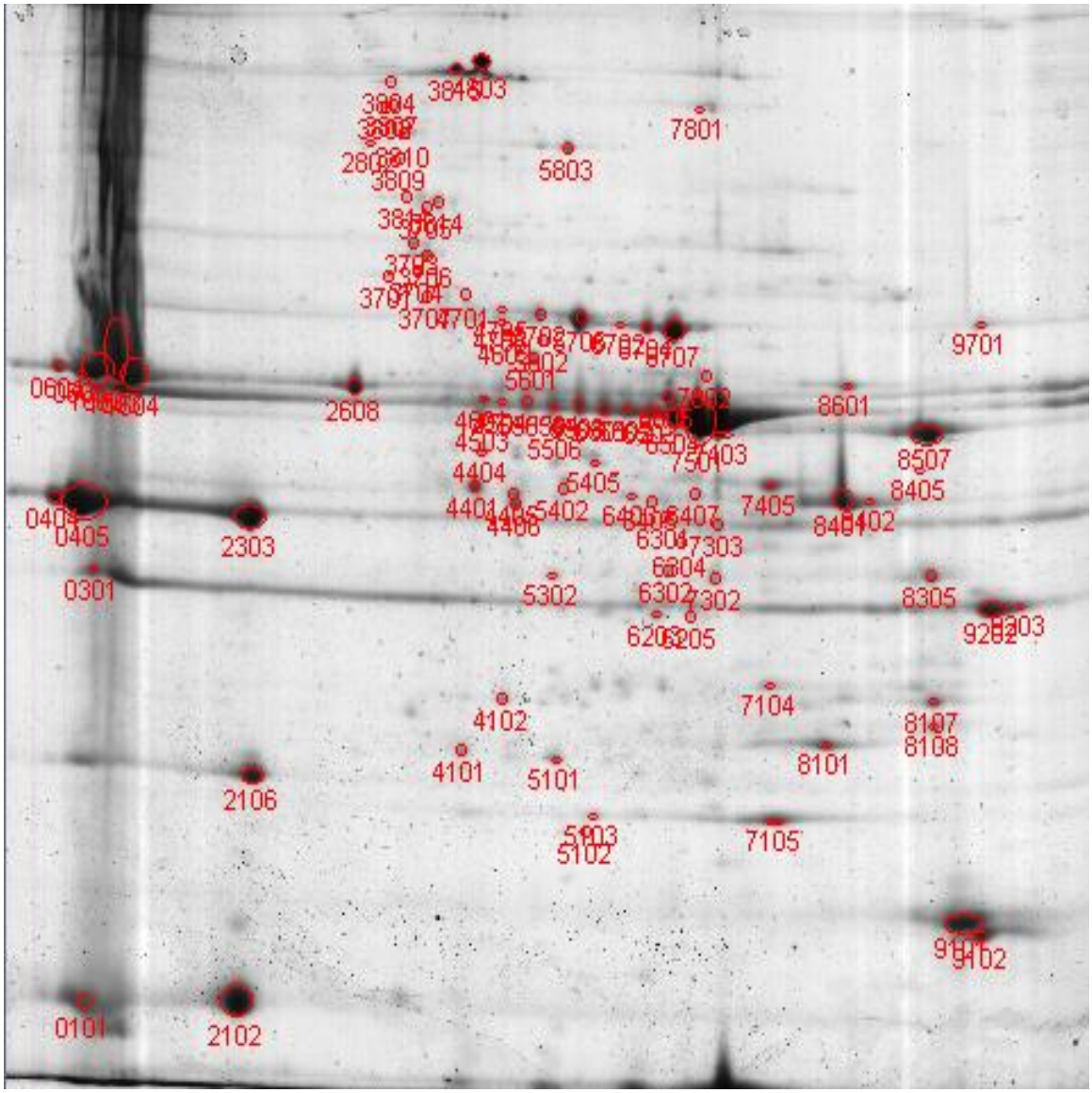

Figure D.2 Preparative gel image of skeletal muscle with identified protein spots (1-96).

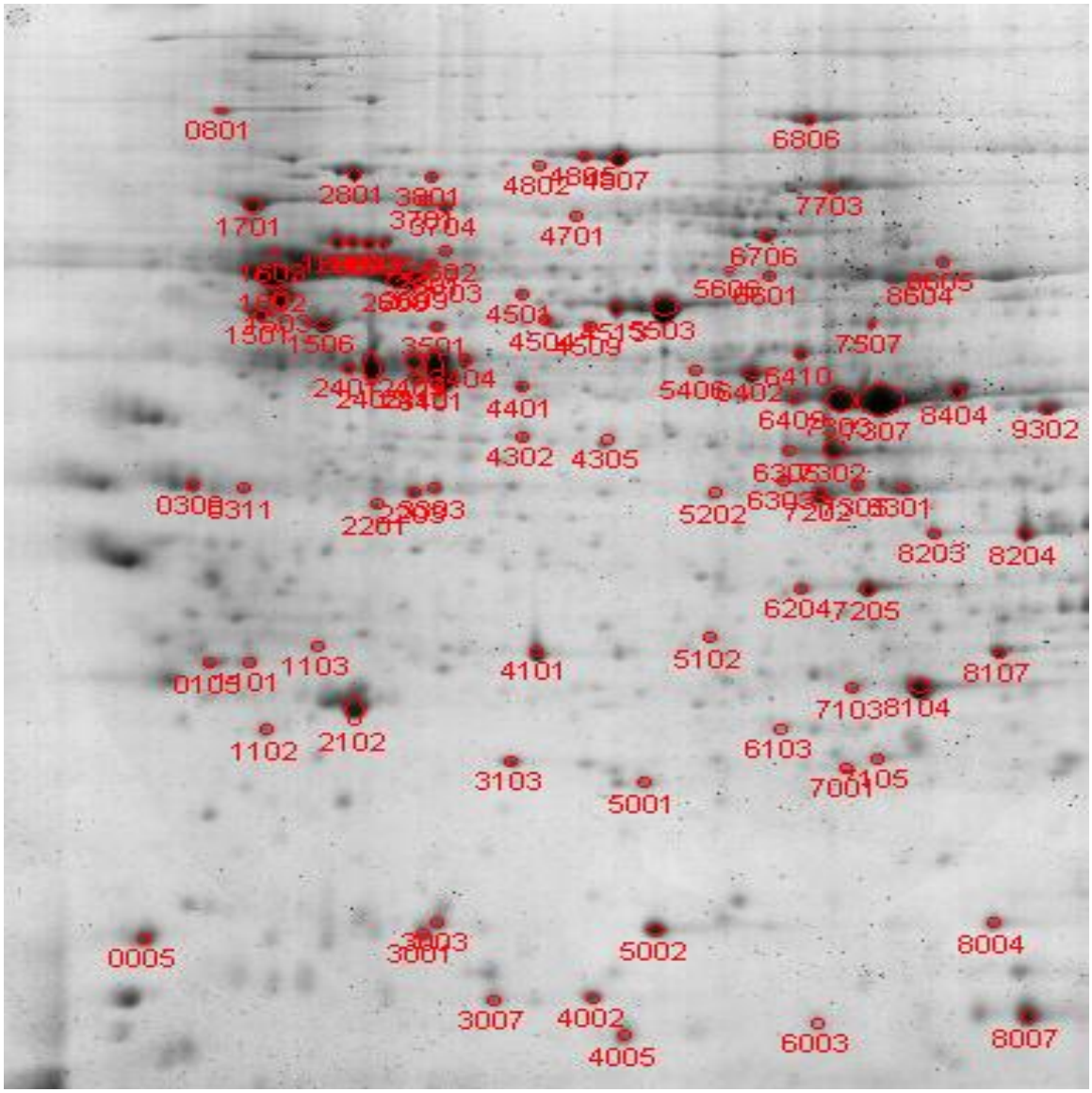

Figure D.3a Preparative gel image of brain with identified protein spots (1-96).

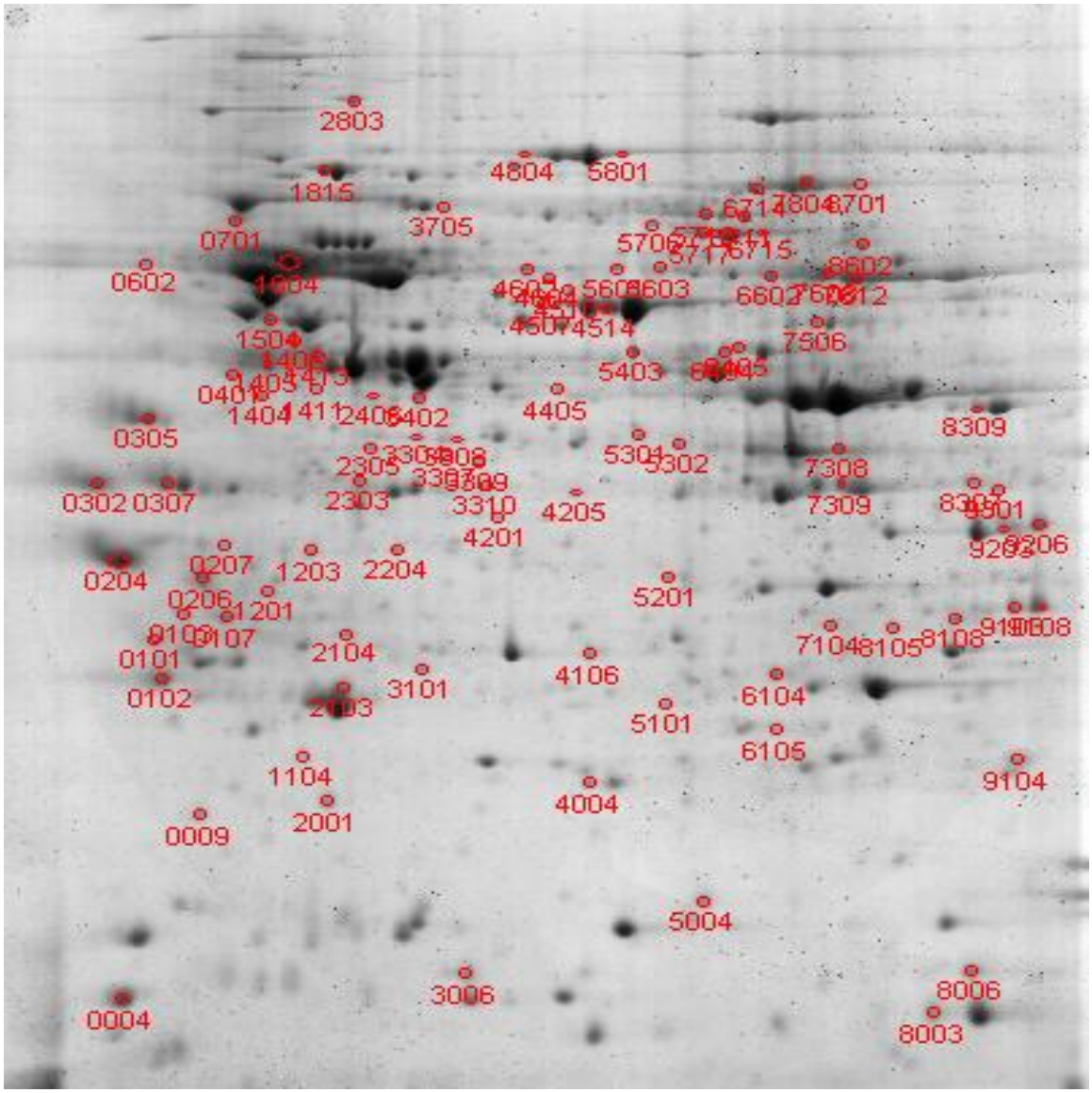

Figure D.3b Preparative gel image of brain with identified protein spots (97-192).

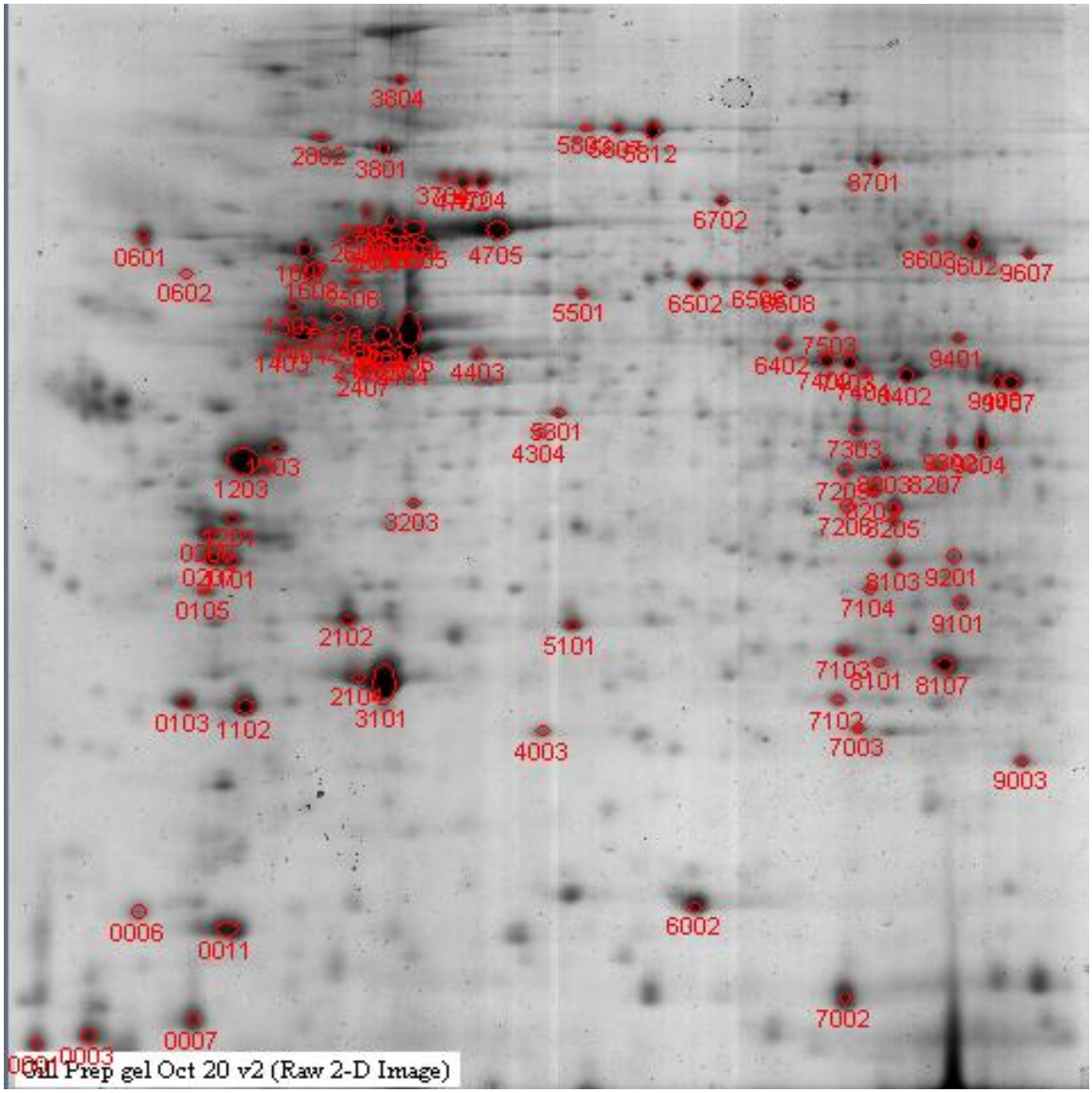

Figure D.4a Preparative gel image of gill with identified protein spots (1-96).

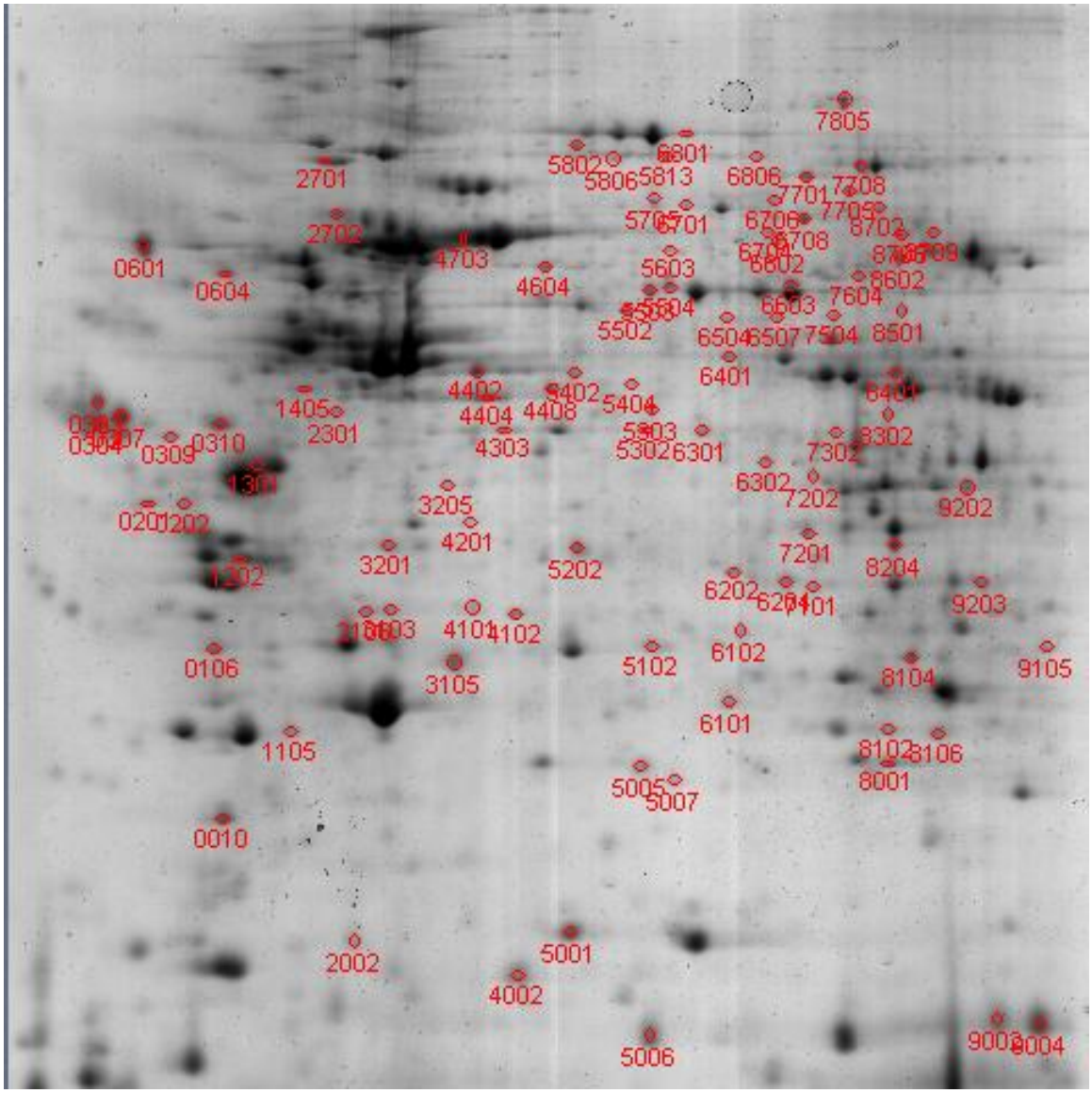

Figure D.4b Preparative gel image of gill with identified protein spots (97-192).

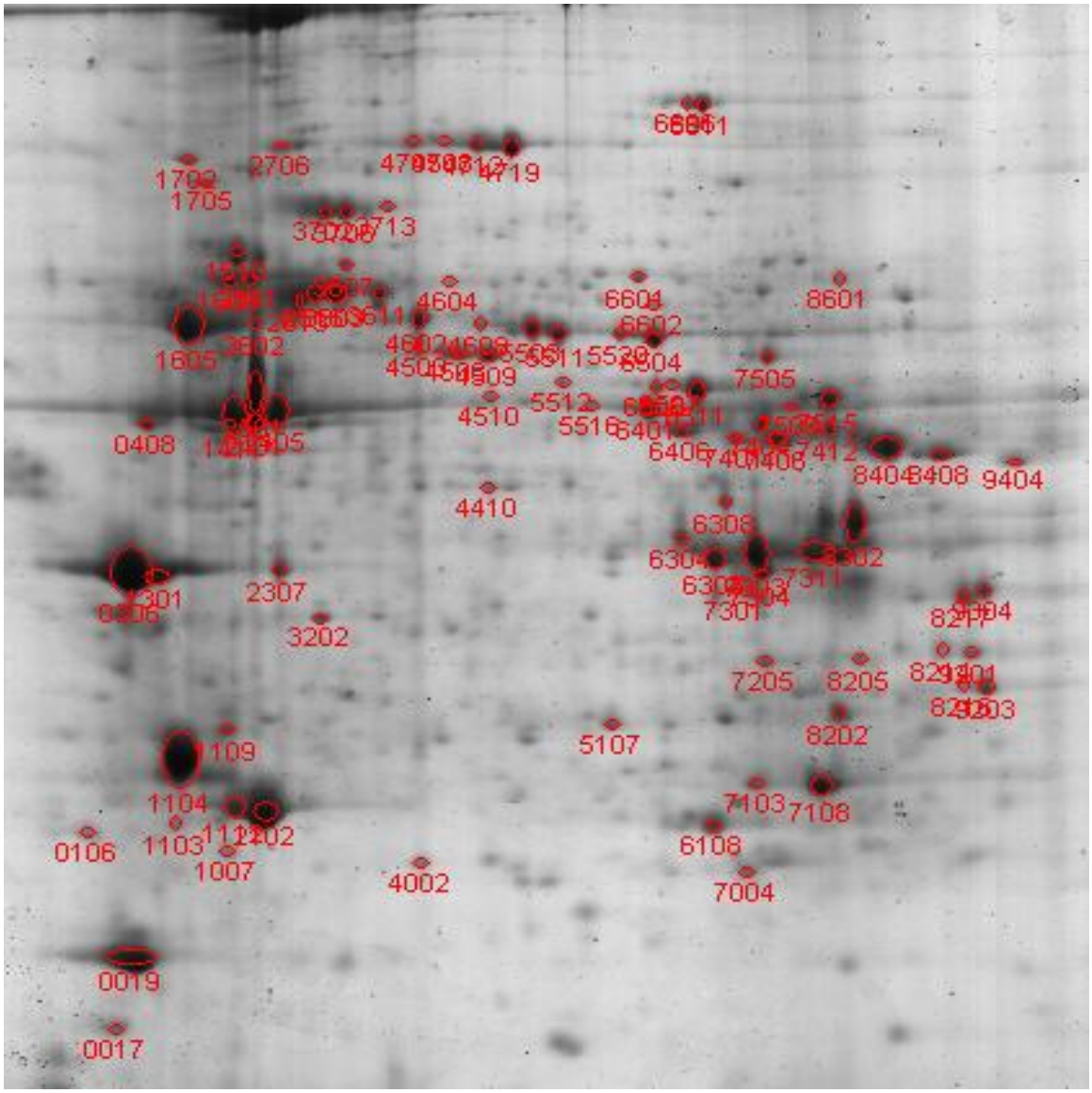

Figure D.5a Preparative gel image of heart with identified protein spots (1-96).

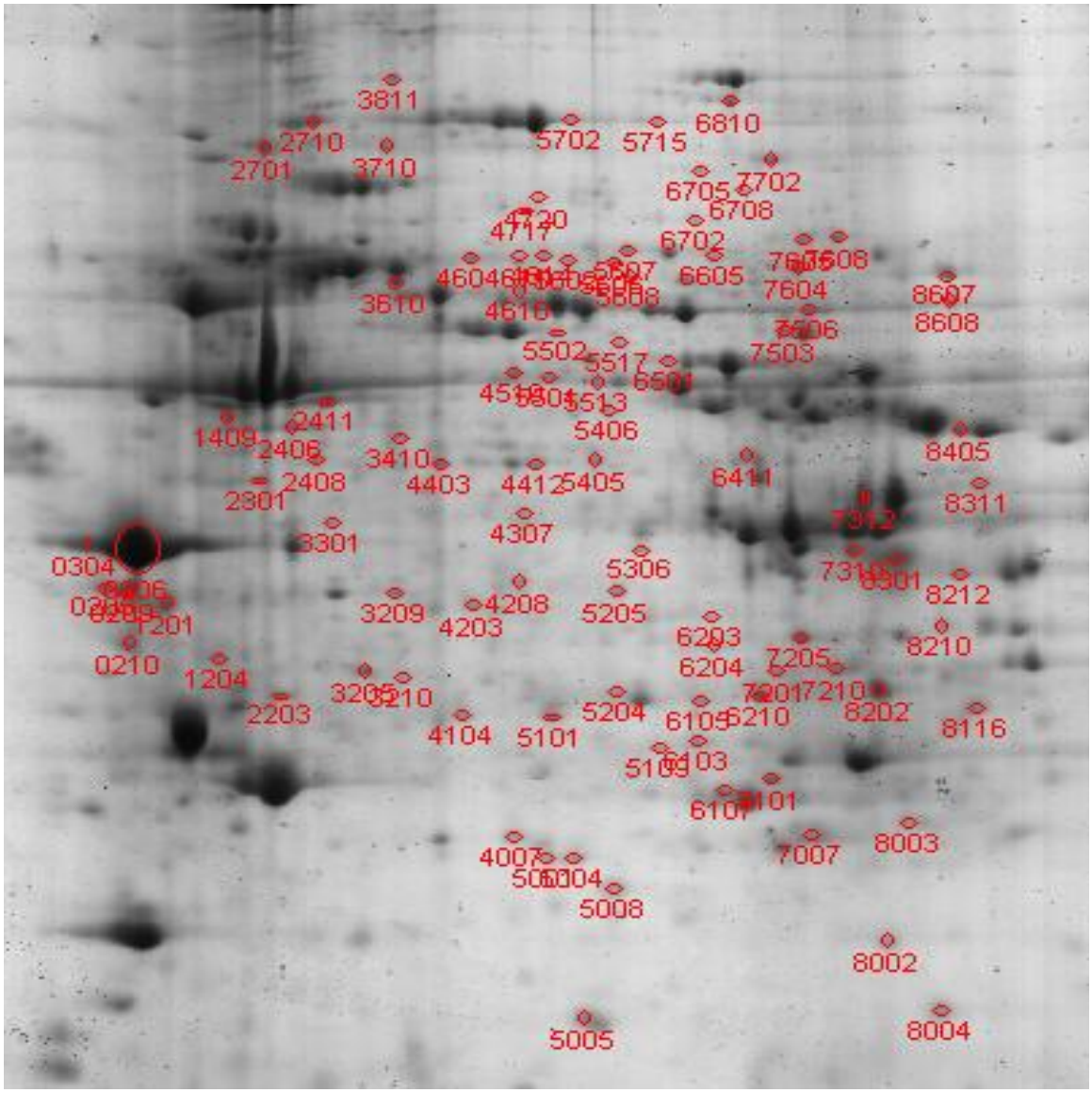

Figure D.5b Preparative gel image of heart with identified protein spots (97-192).

VITA

Naga Vijayalaxmi Abbaraju was born in Vijayawada, Andhra Pradesh, India. She obtained her Bachelor's degree in chemistry from Osmania University in 2001 and Master's degree in Analytical Chemistry from Pune University in 2003. Then she worked in a USFDA approved pharmaceutical company, Dr. Reddy's Laboratories for one year in India. To pursue PhD in Biochemistry, she joined the University of New Orleans chemistry graduate program Fall 2004 and became a member of Dr. Bernard B. Rees research group in Summer 2005.